Investigating the role of *cua-1* in maintaining copper homeostasis within a long-lived, insulin-signalling, *C. elegans* mutants

Katherine Elizabeth Ganio

Submitted in total fulfilment of the requirements of the degree of
Doctor of Philosophy

November 2017
Faculty of Medicine, Dentistry and Health Sciences
The University of Melbourne

ABSTRACT

Ageing is a complex process characterised by the accumulation of damage across the hierarchy of biological organisation (i.e. from molecules up to organs) and leads to the increased susceptibility to death or disease. Increased production or deregulation of reactive oxygen species (ROS) are in part, responsible for the pathological changes that occur throughout normal age and are observed in age-related diseases. Changes in biometals, specifically copper, play a key role in these pathologies because their crucial requirement for aerobic respiration leads to the production of significant amounts of ROS. The cellular and subcellular mechanisms by which homeostasis of copper is maintained throughout the ageing process and how these mechanisms may interact with one another as well as other cell signalling processes remains unclear.

Single gene mutations in an evolutionarily conserved insulin signalling pathway were found to extend healthy lifespan in *Caenorhabditis elegans* (*C. elegans*). While this discovery has built upon our understanding of how genes interact within pathways that regulate the rate of ageing within a whole organism model much of the subcellular processes involved in delayed ageing remain unresolved. More recently, the activity of the *C. elegans* ortholog of the mammalian P-type copper-transporting ATPase, *cua-1*, was shown to be a requirement for *daf-2* longevity suggesting a potential role of copper metabolism in delayed ageing.

Quantitation of total copper levels by inductively coupled plasma mass spectrometry (ICP-MS) throughout *daf-2* lifespan revealed these mutants have lower total copper levels across much of their lifespan compared to normal ageing populations. Decreased *cua-1* activity in *daf-2* mutants lead to a decreased in median lifespan and an overall decrease in total copper levels across lifespan to which both features could be restored to nearly physiological conditions through supplementation of sub-toxic levels of copper (II) salts. Further analysis using size-exclusion chromatography-inductively coupled plasma mass spectrometry (SEC-ICP-MS) of soluble native copper-binding proteins revealed an increase in copper associated to a specific low molecular weight protein. Using known metal binding affinities of the two *C. elegans* metallothionein (MTL) isoforms as well as two metallothionein deletion mutants (singly and in combination) it is suggested this peak is metallothionein.

All together these results indicate a specific pathway for copper metabolism that facilitates delayed ageing within *daf-2* mutants.

DECLARATION

This is to certify that:

i) the thesis comprises only my original work towards the PhD except where indicated in the preface

ii) due acknowledgement has been made in the text to all other material used

iii) the thesis is fewer than 100,000 words in length, inclusive of tables, bibliographies and appendices

Katherine Elizabeth Ganio
Florey Institute of Neuroscience and Mental Health
Faculty of Medicine, Dentistry and Health Sciences
The University of Melbourne
Parkville, Victoria 3010
Australia

PREFACE

I acknowledge that some experiments described in this thesis were carried out in collaboration with others:

- XFM analysis of individual *C. elegans* in Chapter 3 was performed by Dr. Simon James and Dr. Gawain McColl (The Florey Institute of Neuroscience and Mental Health)

ACKNOWLEDGEMENTS

There are a number of people whom I would like to thank for their involvement and support during my PhD. These people have been instrumental in the completion of this thesis:

Gawain McColl

I am and will always be very thankful to have had you as a supervisor. Your work ethic is admirable and I have grown tremendously during these past years from observing your integrity and diligence. I appreciate the independence you gave me on this project as well as the support and guidance whenever I needed it.

Blaine Roberts

I will never be able to truly express to you the gratitude I have for everything you have done for me. It will never be lost on me that the successes I've had and continue to have are thanks to the opportunities you gave me to build a strong foundation as a researcher. I am fortunate to have you as a mentor and friend.

Sharon LaFontaine

Sharon, thank you very much for your endless enthusiasm and support. I am grateful to have had you as a committee member and I very much appreciate that you always made yourself available to help.

James Camakaris

Thank you Jim for being a caring and supportive committee leader. Your help throughout the entire PhD process was greatly appreciated.

Dominic Hare

D, I would not have this PhD without you. Your mentorship is invaluable. You were always available with ideas, motivation and most importantly support. Any student should hope to have someone like you during their PhD.

The Molecular Gerontology Laboratory

Fransisca, Kirsten, Simon and Nicole, thank you for fostering a very enjoyable lab, for your advice, guidance and support with my research. The lunches, coffee breaks, inappropriate amounts of laughter and support were much appreciated.

George Ganio

How you put up with me during this time I will never know. You have given me the support and confidence I needed to finish this thesis. I am grateful for your positivity, humour and endless sacrifice for us. I love you and thank you for teaching me how to use Photoshop.

Irene Volitakis

Thank you very much for letting me be your ICP-MS shadow. I learned so much with your guidance and support and I am very appreciative of how accommodating you were with my research interests.

Friends/Family

Thank you to my endlessly supportive and loving friends and family. I love you all very much.

TABLE OF CONTENTS

LIST OF ABBREVIATIONS

ALS	Amyotrophic lateral sclerosis
ATP	Adenosine triphosphate
ATP7A	Mammalian P-type copper-transporting ATPase, Menkes' protein
ATP7B	Mammalian P-type copper-transporting ATPase, Wilson disease protein
Akt	Protein kinase B
Cp	Ceruloplasmin
CCO	Cytochrome c oxidase
CCS	Copper chaperone for superoxide dismutase
Ctr 1	Copper uptake protein 1
CUA-1	*C. elegans* P-type copper transporting ATPase homolog
CSF	Cerebrospinal fluid
C. elegans	*Caenorhabditis elegans*
Cu	Copper
Daf	Dauer formation
DNA	Deoxyribose nucleic acid
dsDNA	Double stranded deoxyribose nucleic acid
dsRNA	Double stranded ribonucleic acid
Fe	Iron
H_2O_2	Hydrogen peroxide
IGF-1	Insulin-like growth factor 1
IIS	Insulin/insulin-like growth factor 1 signalling
ICP-MS	Inductively coupled plasma-mass spectrometry
LA-ICP-MS	Laser ablation inductively coupled plasma-mass spectrometry
LC-ICP-MS	Liquid chromatography-inductively coupled plasma-mass spectrometry
MD	Menkes disease
Mn	Manganese
MNK	Menkes protein
mRNA	Messenger ribonucleic acid
MTL	*C. elegans* metallothionein

mRNA	Messenger RNA
NGM	Nematode growth media
O_2	Oxygen
O_2-·	Superoxide anion radical
OH·	Hydroxyl radical
OP50	*E. coli* strain
PD	Parkinson's disease
PI3K	Phosphoinositide 3-OH kinase
RNAi	Ribonucleic acid interference
ROS	Reactive oxygen species
SEC-ICP-MS	Size exclusion chromatography-inductively coupled plasma-mass spectrometry
SN	Substantia nigra
SOD	Superoxide dismutase
SOD1	Copper, zinc- superoxide dismutase
PI3K	Phosphoinositide-3-OH kinase
WD	Wilson's disease
WND	Wilson protein
XFM	X-ray fluorescence microscopy
Zn	Zinc

LIST OF FIGURES

LIST OF TABLES

CHAPTER 1 – Review of the literature

1.1 Ageing

One of the greatest scientific endeavours is resolving the underlying mechanisms responsible for ageing. Ageing is the progressive accumulation of cellular damage leading to the increased vulnerability to disease and death. The rate of age can be controlled by certain genes that are expressed across a range of taxa indicating these regulatory mechanisms of ageing may be conserved (1, 2). The ability to slow ageing through genetic interventions has raised the question, what influences do genes have on normal ageing? More specifically, are genes responsible for executing programmed ageing or does their activity or lack thereof merely influence longevity? However, ageing does not occur in a vacuum, as the molecules involved in cellular turnover and repair become the same molecules subject to the ageing process. The fidelity of these molecules are thus the determinants of longevity (3). Ageing is derived through characteristics such as maintaining physiological fitness and the efficiency by which cellular processes such as repair and turnover occur both of which can be modulated by gene activities (3). Ageing is a complex process that encompasses many changes occurring in parallel across different regions of the body and at different levels of biological organisation (*e.g.* tissues, proteins, organelles and cells), making it challenging to understand ageing at the cellular level.

Increased production or deregulation of reactive oxygen species (ROS) are in part, responsible for the pathological changes that occur throughout normal age and are observed in age-related diseases. Changes in biochemically functional metals, biometals, play a key role in these pathologies because their crucial requirement for aerobic respiration leads to the production of significant amounts of ROS. In addition to copper (Cu) and iron (Fe), other first row transition metals including zinc (Zn) and manganese (Mn) are required for a range of catalytic processes and maintaining protein structural integrity. Although extensively studied, the precise pathways by which these redox-active metals contribute to the process of ageing are yet to be fully resolved. A great deal of interest has focused on the role of Cu and Fe in ageing and age-related diseases, as their propensity to participate in electron transfer make them both essential and potentially toxic, depending on the chemical environment and concentration.

The key to resolving the mechanisms of ageing first requires an understanding of how changes to metal homeostasis and metabolism takes place at the molecular and genetic levels, and relating these finding to observations made at higher levels of organisation during the ageing process. Many of the pathophysiological changes that occur with ageing that are relevant to humans can be replicated in smaller model organisms, providing a useful tool for translational research into the molecular basis of senescence.

1.1.1 Oxidative stress in ageing

All aerobic organisms have a conflicted relationship with oxygen: it is both crucial for life and can be a potent cytotoxin. Aerobic respiration uses oxygen (O_2) to generate energy in the form of adenosine triphosphate (ATP) but this process provides a constant stream of reactive oxygen species (ROS) by-products and with it cumulative cellular oxidative stress (4). The oxidative stress or 'free radical theory of ageing' was established over a half of a century ago and continues to be the most robust hypothesis for the biochemical cause of ageing. The primary source of ROS is in mitochondria, where the process of transporting electrons produces superoxide, which can in turn produce other reactive species through interactions with detoxifying enzymes (5). Redox reactions within organelles release ROS into the cytoplasm (6, 7) that serve as secondary messengers (8), gene regulators and can also regulate insulin signalling (9). Metabolic rates change with age as does the production of ROS but the relationship between these two events and the targets of ROS are not fully resolved. When not properly regulated, ROS can react with almost all biomolecules within cells leading to impaired cellular function. Primary ROS-induced damage arises from lipid peroxidation, protein oxidation and mutations to DNA (10). Within the cell, hydroxyl radicals, hydrogen peroxide and superoxide anions undergo a series of reactions that result in the conversion of hydrogen peroxide into water (Figure 1.1A&B) (11). Subsequently, Harman proposed that metals participate in ROS formation in the cell *via* Haber-Weiss chemistry (4) specifically the net Haber-Weiss reaction that creates the hydroxyl radical requires a metal ion catalyst to occur in biological systems (Figure 1.1C). The major mechanism by which this reaction occurs was first proposed to be catalysed by Fe, making use of Fenton chemistry, although other transition metals are capable of catalysing this same reaction (12). Harman's theory has since been well supported by evidence demonstrating ROS produced *in vivo* (13) and through the

characterisation of a highly conserved superoxide anion scavenging enzyme, superoxide dismutase (SOD) (14).

(A) $2O_2^{-}\cdot + 2H^+ \rightarrow H_2O_2 + O_2$ (15)

(B) $O_2^- + H_2O_2 \rightarrow OH^- + \cdot OH + O_2$ (11)

(C) $M^{n+} + H_2O_2 \rightarrow OH^- + \cdot OH + M^{(n+1)+}$ (16)

Figure 1.1 Haber-Weiss and Fenton reactions

(A) The ability of the superoxide anion radical (O2-·) to participate in biological processes has been implicated by the protective activity of superoxide dismutase against cellular injury. (B) Superoxide can interact with hydrogen peroxide to form the highly reactive hydroxyl radical a reaction that was discovered to occur in biological systems with the help of metal ion catalysts (C), particularly Fe.

Nitric oxide acts as an intracellular messenger in key biological processes including cellular signalling, vasodilation and immune response (17, 18). Nitric oxide, a reactive nitrogen species, is produced by nitric oxide synthases and has a single unpaired electron allowing it to function as an electron donor or accepter. Nitric oxide is known to combine with superoxide to produce peroxynitrite. The decomposition of peroxynitrite results in the formation of a strong oxidant that can act similarly to the hydroxyl radical (19) and via nitration can disrupt the normal functioning of certain amino acids. The increased risk of oxidative damage to an array of molecules is an inevitable consequence of ageing (20-23), to which organisms have developed multiple redundant systems to detoxify and remove ROS from cells, collectively known as antioxidants. Chronic and acute oxidative stress have been implicated in several degenerative diseases affecting a wide range of physiological functions including, neurological disorders, atherosclerosis, diabetes, inflammatory diseases, cancer, pulmonary and haematological diseases (24). Antioxidants functioning to scavenge ROS require redox-active metal ions to serve as catalytic and structural cofactors. Alas, these same metal cofactors that are required for antioxidant activity when not properly regulated can participate in the formation of ROS. Strict homeostatic control of these metals is crucial because an abundance or deficiency may result in serious consequences for all aerobic organisms. Specifically, excess Cu can generate ROS, and in conditions of Cu depletion detoxifying enzymes may not become catalytically active, potentially resulting in an accumulation

of ROS. The complexity of the actions of ROS in the cell are furthered as H_2O_2 can easily travel between organelles and the cytoplasm and is essential for a range of cellular functions including gene regulation, cell signalling, protein activation/deactivation and cellular differentiation (25-27). The diversity of processes ROS are involved in makes it difficult to arrive at a conclusive answer as to the amount of ROS and at what point during normal ageing ROS production crosses the threshold to become damaging. Hypotheses of ageing speculate that such damage occurs from the imbalance between ROS production and antioxidant defences, and that reducing this imbalance would mitigate damage and extend lifespan. It would therefore seem that enhancing antioxidant activity would maintain lower levels of ROS and slow the accrual of structural damage to macromolecules and prolong longevity. However, despite numerous efforts, altering antioxidant defences have failed to extend durability beyond species-specific maximum lifespan; in some cases increased antioxidant activity has in fact shortened lifespan and ultimately these studies revealed low amounts of oxidative damage (28-30). This suggests that a steady state of ROS exists in young, healthy organisms and that ROS production and ultimate health implications involve a huge amount of variation from environmental and genetic influences, including interlinked processes and feedback systems.

1.1.2 Studying ageing in a model organism

Significant insights into the genetic and biochemical pathways that influence ageing have been made in studies using the nematode round worm *Caenorhabditis elegans*, an approximately 1 mm long round worm that is a staple of contemporary genetic sciences. Use of *C. elegans* as a scientific resource began in the mid-1970s, when it was used a tool for studying the function and development of the nervous system (31). This model organism has since been extensively used in a range of scientific fields including genetics, proteomics, toxicology and neurobiology, with popularity stemming from their numerous experimental advantages. Such advantages include ease of laboratory culturing due to their small size, simple husbandry, amendable living conditions and short life cycle with well-characterised developmental stages. Sizable numbers of genetically identical offspring produced by gravid hermaphroditic adults facilitates the capacity of genetic malleability (32). The *C. elegans* nervous system is comparatively simple (each adult hermaphrodite has 302 neurons) and can be easily visualised by way of their transparent cuticle (33). Furthermore, *C. elegans* often experience toxicity predictive of outcomes observed in higher

eukaryotes. In addition to toxicity outcomes, similarity at the genetic and physiological level observed in higher eukaryotes (*e.g.,* mice and humans) has been observed in *C. elegans* (34). The growing evidence supporting these observations is not surprising given that homologues for 60-80% of human genes have been identified in the *C. elegans* genome (35).

Large-scale genetic screens using *C. elegans* have helped to elucidate specific gene activities capable of modulating biological outcomes (36). These screens have, in addition to identifying genes that were previously unknown to be involved in modulating lifespan, also built upon our understanding of how genes interact within pathways that regulate the rate of ageing within a whole organism model (37). A unique capability of *C. elegans* is their capacity to experience decreased gene expression *via* a bacterial food source that express double-stranded RNA (dsRNA) targeting genes of interest (38) is an extremely useful research tool. This technique, in conjunction with highly sensitive analytical techniques, has been used to study the bioinorganic chemistry of ageing in *C. elegans*, which, as a whole multicellular organism, provide unprecedented insight into the complex biology of a functioning system (39-41).

1.1.3 Genetic factors influencing ageing

Ageing, conceptualised as the progression of deterioration can be driven by two forces: (1) gene-regulated efficiency of physiological systems to maintain homeostasis and/or (2) severe or accumulating events that impact the ability of an organism to maintain homeostasis. The ageing process is believed to occur as a result of evolutionary responses that optimise the allocation of metabolic resources across growth, reproduction and maintenance events. When environmental circumstances change during an organism's life, the ability to vary metabolic allocations in response to changing circumstances has evolved (42). Specifically, restricted access to food is a well-established influencer of the rate of ageing in various model organisms (43). For example, responding to altered environmental circumstances is seen in a larval, long-lived, stress-resistant stage of arrested development in *C. elegans*. The discovery of the influence of genetic factors on lifespan and ageing is, however, more recent (44, 45). A great deal of progress towards this goal has been through the discovery and further study of genetic interventions that modulate lifespan.

Nutrient signalling pathways are evolutionarily conserved, well-characterised pathways of which genetic interventions can regulate lifespan (46, 47). Genetic interventions in nutrient signalling pathways represent a well-characterised modality for extending healthy lifespan in model organisms (48). The most robustly conserved and widely studied example of which is the insulin/insulin-like growth factor 1 (IGF-1) signalling (IIS) pathway wherein single gene mutations can significantly extend lifespan. The IIS pathway can extend lifespan in multiple species through genetic or pharmacological inhibition as well as dietary restriction (1, 49, 50). Model organisms containing IIS pathway mutations share characteristics associated with longevity including reduced insulin signalling, increased sensitivity to insulin, reduced oxidative damage to macromolecules and increased stress resistance; all of which support the theory that the fundamental mechanisms of the modulation of ageing are evolutionarily conserved (51). When the activity of specific genes within the IIS pathways are decreased, an improvement in health by the delayed onset of some age-related pathologies has been observed (52-58). Reduced IGF-1 signalling protected against the toxic effects of protein aggregates associated with neurodegeneration in *C. elegans* and mice (54, 55, 59). Additionally, genetic inhibition of the IIS pathway suppressed tumour growth in these model organisms (53, 60). The mechanisms responsible for mediating these beneficial effects as well as the downstream targets that aid in mediating these effects still remain largely unknown. Possible targets include genes that encode detoxification enzymes as these are upregulated following reduced IIS (61). Insulin and IGF-1 belong to a family of hormones/growth factors that regulate metabolism, growth and cell differentiation and survival of a majority of tissues in mammals (62). These effects are mediated by the IGF receptors that are expressed on the surface of cells. IGF-1 is a tetrameric protein consisting of two alpha and two beta subunits functioning as allosteric enzymes, in that the alpha subunit can inhibit the activity of the beta subunit. When insulin binds to the alpha subunit the kinase activity of the beta subunit is reduced followed by transphosphorylation of the beta subunit catalysing a conformational change and re-establishing kinase activity. The reduced activity of the IIS pathway that extends lifespan requires the activity of the forkhead transcription factor, FoxO (63). This family of transcription factors regulates several hundred genes that control an array of functions including stress response, protein turnover and antimicrobial resistance (64). FoxO proteins regulate activation of genes involved in glucose metabolism. FoxO family proteins have

been shown to extend lifespan in *Drosophila melanogaster* (65, 66) and recent studies suggest they have similar capabilities in humans (67).

Lifespan modulation resulting from genetic mutations was first reported using *C. elegans* (68). More specifically, extending lifespan through genetic interventions of components of the IIS pathway were first reported using *C. elegans* (69-71). In *C. elegans* the mammalian IGF-1 receptor is encoded by *daf-2* (71, 72) which shows 35% homology to the human insulin receptor and 34% to the human IGF-I receptor (73). As part of an elaborate endocrine system, *daf-2* regulates longevity, metabolism and development in *C. elegans* and null mutations cause constitutive arrest at the dauer larval stage whereas loss-of-function mutants have modulated metabolic rates (74, 75) and have increased propensity to live longer than reproductive adults (71). Under normal conditions, DAF-2 binds an insulin-like substrate(s) that initiates a cascade of events, one of which includes activation of *age-1*, a gene encoding the homolog of the mammalian phosphoinositide-3-OH kinase (PI3K) (76). Mutants with loss of function of *age-1* have been reported to experience a lifespan extension of up to 65%, demonstrate increased resistance to oxidative stress and increased antioxidant activity (SOD and catalase), with both traits occurring in an age dependent fashion (77, 78). *Age-1* activates the Akt homologs *akt-1* and *akt-2*, genes encoding protein kinase B, which is a serine/threonine kinase that blocks the function of DAF-16 by preventing its translocation to the nucleus (76). The longevity effects of IIS gene mutations are dependent on the activity of *daf-16*, the nematode ortholog to the mammalian forkhead transcription factors, FoxO (79, 80). Loss of *daf-16* activity suppresses the phenotypes of *daf-2* and *age-1*, suggesting that the IIS pathway regulates ageing through gene expression and the determinants of ageing likely exist among transcriptional targets of DAF-16 (70, 79). As *daf-16* activity is required for longevity in *daf-2*/*age-1* mutants, great effort has been devoted to identifying the genes that act downstream of *daf-16* and the effects of gene expression in *daf-2* as well as *daf-16* mutants.

Insulin signalling can be enhanced or suppressed depending on the amount of cellular ROS generated (9). Several models of IIS mutants exhibit resistance to ROS (78, 81, 82). Antioxidant expression levels are increased in *daf-2* mutants (82, 83), resulting in lower levels of free radicals, increased resistance to stress stimuli and less macromolecular damage; all traits credited to longevity (84, 85). While ROS is capable of stimulating the signalling cascade, so can redox-active

transition metal ions including Cu(II) (86). Copper ions are well known to elicit insulin-like effects in a variety of cells and tissues. In human hepatoma cells, Cu(II) exerted an insulin-mimetic effect on the PI3K/Akt pathway, resulting in the phosphorylation and nuclear exclusion of the FoxO transcription factor (87). Similarly, in rat hepatocytes and rat renal cortex, gluconeogenesis was diminished when exposed to Cu(II) (88, 89). Glycogen levels in the liver of rats exposed to Cu salts doubled compared to those under control conditions (90). The PI3K/Akt signalling cascade is anti-apoptotic and cytoprotective, and is also involved in regulating gene expression and insulin signalling that can be activated by Cu(II). Activation of Akt by Cu(II) is independent of ROS formation as incubation of human cervix carcinoma cells with Cu(II) was shown to stimulate Akt phosphorylation *before* detectable levels of ROS were generated. Interestingly, exposure of these cells to (Fe)(II) caused formation of ROS without the detection of Akt phosphorylation (91, 92). Therefore, a change in the activity of the IIS pathway resulting in the long-lived phenotype of mutant organisms could be the result of the insulin-like effects from a Cu imbalance (93), and along with increased insulin resistance this suggests that mechanisms influencing ageing may be evolutionarily conserved (51, 94).

Manipulation of genes involved in ROS detoxification has helped to clarify the mechanisms by which ROS facilitates ageing. *C. elegans* have been extensively utilised to understand the how ROS functions as a causative factor in ageing by genetic manipulation modulating endogenous antioxidant defences. An increase in expression levels of *C. elegans* antioxidant enzymes including *ctl-1*, catalase and Cu, Zn-SOD1, *sod-1* and Mn, Fe-SOD, *sod-3*, occurs in *daf-2* mutants, facilitating their increased resistance to oxidative stress (82, 83). A key component to *daf-2* longevity is the lower levels of free radicals, highlighting the central role of oxidative stress in regulation of ageing mechanisms (84, 95). A mutation that affects mitochondrial complex II, abnormal methyl viologen sensitivity, *mev-1*, increases ROS production and mutants show elevated levels of oxidative damage and are short-lived (96). The *age-1* mutant allele displaying the greatest increase in lifespan did not exhibit increased resistance to oxidative stress from the production of H_2O_2 an observation potentially decoupling the effects of *age-1* resistance to oxidative stress from its longevity (97). These *age-1* mutants confer resistance to other forms of stress including heat and metal exposure, indicating that multiple forms of stress and damage, in addition to oxidative stress, may contribute to ageing. Insulin signalling, mitochondrial respiration and caloric intake

represent the three known processes in *C. elegans* that can be modulated to result in increased longevity and stress resistant populations (70, 98, 99).

1.1.3.1 Investigating the mechanisms responsible for daf-2 longevity

The discovery and subsequent characterisation of longevity-conferring mutants of the IIS pathway has significantly improved our understanding of the pathways involved in ageing. Numerous genes involved in *C. elegans* have been identified using large-scale RNA interference (RNAi) screens. RNAi is a cellular defence mechanism that uses double-stranded RNA (dsRNA) to degrade RNA is a sequence-specific manner (100). Introduction of the dsRNA into *C. elegans* can occur through microinjection or through feeding bacteria expressing dsRNA that targets specific genes. Since its discovery nearly 30 years ago (101), extensive work has been done to determine the mechanisms by which *daf-2* confers longevity (1, 45). In addition to RNAi screens, transcriptional analyses and mass spectrometry-based proteomic screens have shown that ageing and metabolism are more directly related than previously believed (102). Recently, an RNAi library of thousands of genes were screened to determine what gene activities were required to confer longevity in the *daf-2* mutant (103). Among their findings, the ortholog of the mammalian Cu-transporting ATPases, ATP7A/B, *cua-1*, activity was necessary to confer *daf-2* longevity. Furthermore, they found that *cua-1*'s activity had the second greatest impact on *daf-2* longevity, just behind that of *daf-16*. Since this discovery no further investigation into the possible role CUA-1 has in *daf-2* longevity has been reported in the literature. However, as indicated in previous sections Cu has been shown to interact with the IIS pathway effecting processes associated with ageing. Further probing into the relationship between CUA-1 and *daf-2* may lead to a better understanding of the processes responsible for modulating lifespan. In the biology of ageing, the greatest challenge is, and remains, identifying the mechanisms underlying the increased lifespan observed in these model organisms.

1.1.4 Metals in ageing and disease

Metal ions are crucial for numerous processes such as respiration, immune function and enzymatic reactions. An estimated one third of the human proteome and half of all enzymes require metal ion cofactors for catalytic activity or structural support (104) and represent a majority of reactivity within a cell. In addition, many biological processes require metals to

coordinate receptor-ligand interactions. Given their unique chemical properties and capacity to form ROS metal trafficking must be tightly regulated. Altered metal homeostasis is implicated in a range of severe debilitating and often fatal disorders including various types of cancers, genetic disorders, cardiovascular disease, diabetes and neurodegenerative diseases (105, 106). Within cells transition metals can exist as free ions, associated to biomolecules or small molecules such as amino acids or glutathione.

Endogenously redox-active metals (*e.g.* Fe, Cu and Mn) and non-redox active (*e.g.* zinc and magnesium) can generate ROS when their homeostasis is disturbed (107). The age-associated accumulation of oxidative damage from ROS have been directly implicated in several forms of cancer (108). These observations sparked investigation into the speciation and metabolism of metals in cancer onset and progression. Depleting cells of Cu has been shown to indirectly inhibit tumour development in a broad range of cancers (109) although the underlying mechanism of tumour sensitivity to Cu remains unknown. Many neurological disorders are associated with changes in metal concentrations in the central nervous system (110). These observations are of significance as the brain consumes 20% of the body's oxygen required for energy production respiration despite accounting for only 2% of the average human body mass. The higher metabolic rate of activity is seen in numerous metal-regulated cellular functions. It is not surprising then the brain contains significantly higher concentrations of redox-active metal ions compared to other regions of the body (111, 112). In the ageing human brain, a loss of Cu homeostasis is believed to be involved in the onset and progression of age-associated neurodegenerative diseases including Alzheimer's disease, amyotrophic lateral sclerosis, Parkinson's disease, Huntington's disease and prion disease (113, 114).

The most common form of motor neuron disease, amyotrophic lateral sclerosis (ALS) is a fatal neurodegenerative disease. Approximately 10% of ALS cases occur *via* genetic causes. The most common gene mutations identified in familial forms of ALS occur in *sod-1*, a gene encoding Cu, Zn-SOD1, in which the translated protein has been found in deposits within ALS tissue. Although how such genes and/or proteins are involved in disease onset and progression is still not completely understood, considerable effort has gone into exploring the role of Cu in ALS pathogenesis as markers of oxidative damage have been observed in disease tissue as well as cerebrospinal fluid

(CSF), urine and plasma (115). Increased levels of Cu, Fe and Zn in ALS CSF are proposed to give rise to ROS-mediate oxidative stress leading to motor neuron loss (116, 117). Copper levels are elevated in the spinal cord of $SOD1_{G93A}$ transgenic mice. The ALS phenotype of these transgenic mice was ameliorated upon lowering of spinal cord Cu *via* chelation. Disturbances in Cu outside of the active site of SOD1 may lead to disease as mutations disrupting Cu binding to the active site of SOD1 still had an age-associated increase in spinal cord Cu aside from SOD1 tissue fractions (118). Elevated levels of serum ferritin in ALS subjects, compared to controls, indicate that Fe metabolism is also disrupted during disease supporting the continuing conundrum as to whether such markers are the cause of or an effect of increases in oxidative stress associated with many neurodegenerative diseases.

Changes in metal levels within specific regions of the brain can be used to mark the onset and progression of Parkinson's disease (PD). Oxidative stress that is mediated by disturbances in metals has been observed in the substantia nigra (SN) region of the brain in PD patients (119, 120). These observations coupled with the established importance of specific metals in the brain have fuelled interest in the role of biometals and PD. Although the role of Cu in PD remains largely unknown evidence continues to grow supporting the involvement of regional disturbances in brain Cu homeostasis and Cu-associated proteins in PD related cell death. In a healthy brain the SN requires higher levels of Cu compared to other regions so a reduction in total Cu within this tissue may be implicated in the PD-associated neuronal death. Total Cu levels within this region of PD brain tissue are 34-51% lower than healthy controls (121) and further, regional Cu deficiency was observed at the single cell level within neurons (122) in the SN of PD and Incidental Lew body diseases cases suggesting that these changes occur prior to disease diagnosis (121). The overall deficiency in SN Cu levels decreases the activity of ceruloplasmin (Cp) within the SN of PD patients and analysis of these regions in PD patients revealed an increase in Fe and subsequent oxidative stress (121). The pathology of PD is characterised by the formation of Lewy bodies, intracellular inclusion bodies containing alpha-synuclein whose interaction with Cu increases its propensity to aggregate. These studies demonstrate that changes in Cu homeostasis effects the function of Cu and Fe-binding proteins. Functional changes of such metalloproteins can affect Fe levels and this cascade of events act in conjunction to increase oxidative stress.

Dyshomeostasis of metals with age has been well characterised in numerous models of neurodegenerative disease. Targeting metal disturbances has become a primary therapeutic target for disease intervention however most of these therapies are only able to act to alleviate symptoms of disease rather than acting to prevent disease onset. In conjunction with changes in the spatial heterogeneity of metal ions within the cell, metal ion 'signals' have been observed in which specific cellular events can mobile metals from cellular labile pools (123). The extent of activities metals ions are involved with, in conjunction with their cellular distribution, exacerbates the many possible ways in which they may influence ageing and age-associated diseases.

1.2 Copper in biological systems

Life on earth originated in anoxia environment about 10^9 years ago. However, the gradual oxygenation of the earth's atmosphere 500-600 million years ago saw the evolution of multicellular organisms utilising oxygen for respiration. The increased prevalence of aerobic respiration lead to increased Cu-binding proteins and levels of bioavailable Cu in multicellular organisms due to limited Fe availability as a result of the evolution of O_2 in the atmosphere. All aerobic and many anaerobic organisms require Cu. As a first row transition metal, Cu belongs to a small number of elements that can exist in multiple oxidation states, Cu is predominantly found in two oxidation states Cu(I) and Cu(II). The electron affinity of Cu(II) makes it the most effective bioavailable divalent cation for binding organic molecules, and Cu(I) exhibits the same trait for monovalent cations (124). These features of Cu have facilitated its involvement in a range of crucial biochemical roles including cellular respiration, free-radical defence, Fe metabolism, neurotransmitter synthesis and neuronal myelination (125-127). Copper must be tightly regulated because excessive or unbound cytosolic (labile) metal has the potential to be toxic (128-131). As discussed in previous sections, disturbances in Cu homeostasis has been widely reported as this a common feature of numerous disorders while also being associated with normal ageing (132).

The importance of Cu homeostasis is underscored by the genetic disorders leading to compromised Cu transport in the brain (Menkes disease) and liver (Wilson's disease) (133, 134). Wilson's disease (WD) is an autosomal recessive disorder causing Cu deposition in various tissues (135). Death from severe neurological complications can occur if left untreated. The discovery of

the involvement of the P-type Cu-transporting ATPase, ATP7B, in WD pathogenesis (136) provided greater understanding the role of Cu in the liver and nervous system. The ATP7B gene is expressed in the liver, kidney and placenta and is responsible for Cu delivery to Cp and Cu export. Genomic mutations that impair ATP7B-mediated excretion of Cu lead to accumulation of Cu in the liver and WD. ROS formed from excess Cu is believed to be the cause of the damage seen in WD hepatocytes. Menkes disease (MD) is an X-linked syndrome that causes Cu deficiency due to reduced uptake of Cu across the small intestine and defective distribution within the body (137). The link between MD and Cu was first reported by David Danks based off his observed abnormalities in children with MD and the effects of Cu deficiency in animals. Copper deficiency in the brains of Menkes patients along with the severe neurologic abnormalities demonstrates the involvement of ATP7A in transporting Cu across the blood-brain barrier (138). Although MD causes overall Cu deficiency, as certain tissues display defective Cu efflux diagnosis of MD is done through the identification of impaired Cu efflux from cultured cells of patients (139).

Appropriate mechanisms for Cu uptake and efflux in addition to cellular sensors to ensure Cu is being trafficked to its appropriate cofactors to drive essential biochemical processes all the while preventing its accumulation to toxic concentrations is crucial for organismal survival (130). Although Cu is less prevalent than Fe or Zn it has specific properties that are crucial for redox reactions and is employed by most enzymes for the purpose of electron transfer reactions (*e.g.* oxidation reactions and energy generation in mitochondria). Despite the well-established understanding of the biology of transition metals, the cellular and subcellular mechanisms by which homeostasis of these metals (including Cu) is maintained and how these mechanisms may interact with one another as well as other cell signalling processes remains unclear.

1.2.1 Copper-iron relationships in biology

The close relationship between Cu and Fe in biological systems has been recognised for over 100 years (140, 141). While investigating treatments for anemia patients in the 19th century the discovery of Cu's involvement in haemoglobin formation marked a major event in the biological relationship between Cu and Fe (142). The extent to which the interactions between Cu and Fe facilitate various molecular mechanisms has only more recently begun to be understood (143, 144). Copper can influence Fe transport as seen in cases of severe Cu deficiency causing Fe

accumulation in tissues (145). Iron is an essential nutrient for all life, with the exception of two genera of bacteria (*Lactobacillus* and *Bacillus*), that facilitates a vast range of physiological processes. Like Cu, Fe can exist in multiple charge states facilitating its utilisation as a cofactor for the activity of many essential enzymes involved in oxygen transport including the heme molecule. As with Cu, Fe can be toxic in excess. Labile pools of these metals, specifically Fe(II) and Cu(I) have the capacity to catalyse Fenton and Fenton-like reactions causing the dismutation of H_2O_2 to form hydroxyl radicals. These characteristic see Fe and Cu participating in many similar biological reactions including electron transfers and oxygenase activities (144). Just as evolutionarily conserved mechanisms exist across taxa to maintain Cu homeostasis so exists similar mechanism to maintain strict homeostatic control of Fe as its dyshomeostasis can lead to the generation of oxidative stress that is associated with serve pathological consequences including neurodegenerative (146, 147) and cardiovascular diseases (148, 149), diabetes (150) and some types of cancer (151, 152). Such damage is presumed to be due to the ability of cuprous Cu and ferrous Fe to catalyse the dismutation of hydrogen peroxide into hydroxyl via the Haber-Weiss and Fenton reactions. As with Cu, disturbances in Fe metabolism have been reported in numerous models of ageing (95, 153, 154). Efforts to further understand the roles of Cp, the major Cu-binding protein in blood, have provided further examples of the Fe and Cu interrelationship. Ceruloplasmin plays an essential role in Fe metabolism (155) with Cp deficiency shown to induce Fe deficiency causing ataxia, reduced mitochondrial function and lowered levels of red blood cells. All of these symptoms have been replicated in models of Cu deficiency (156).

1.2.2 Mammalian copper metabolism and homeostasis

Although the size of the Cu proteome is small, representing less than 1% of the total proteome in eukaryotes (157), its potential deleterious effects (redox damage to DNA, protein and lipids (158) and displacement of native metal ions effecting protein folding and function) combined with its essential physiological activities (central nervous system functions, connective tissue formation and antioxidant to name a few) require Cu ions to be tightly regulated. Much of what is known about the systems of cellular Cu transport have come from studies utilising yeast and mammalian cells that showed these systems are highly conserved (159, 160)

Eukaryotes require Cu import to the cytosol to serve as structural and catalytic cofactors for cytoplasmic cuproproteins, mitochondrial cytochrome c oxidase (CCO) and Cp. The first Cu transport protein associated with the plasma membrane, Ctr1, was identified in yeast, *Saccharomyces cerevisiae* (161). Genes encoding Ctr1 orthologs have since been identified in higher model organisms due to the high sequence homology across taxa. Ctr1 is a trimeric integral membrane protein that forms a permeation pathway specific for Cu entry into the cell. Ctr1 localises to the plasma membrane and intracellular vesicles in mammals to accumulate Cu (162). Copper import via Ctr1 requires Cu(II) to be reduced to Cu(I) a reaction believed to be accomplished by metalloreductases (163). Copper enters the cell by coordination of Cu(I) to the methionine-rich motifs located in the N-terminus extracellular domain of the Cu transporter 1 (Ctr1)(Figure 1.2)(164). Under conditions of Cu excess or depletion Ctr1 transcription can be down-regulated or up-regulated, respectively, in both yeast and humans (165, 166). Furthermore, to decrease Cu uptake under conditions of high extracellular Cu Ctr1 localises to vesicles (167). Two Ctr1's have been identified in human and mouse genomes (Ctr1 and Ctr2) with Ctr1 knockouts displaying severe defects in Cu delivery to all characterized intracellular Cu-containing proteins (164, 168). In studies using cultured cells Ctr2 can act as a low-affinity Cu(I) importer but its primary function at a whole-organism level remains unknown. The importance of Ctr1 is supported by the neonatal lethality of Ctr1 ablation in mouse intestinal epithelial cells (169). An alternative, Ctr1 independent Cu importing system was demonstrated in Ctr1-deletion mouse embryonic cells (170). The divalent metal transporter 1 (Dmt1) has been shown to facilitate both Cu(II) (171) and Cu(I) (172) entry into the cell.

Once Cu crosses the plasma membrane it can be trafficked by three independent delivery pathways depending on cellular requirements, (1) the secretory pathway, (2) Cu, Zn-SOD (SOD1) or (3) CCO in the mitochondria (131, 173, 174)(Figure 1.2). Copper chaperones were identified as ubiquitous proteins responsible for the management of cellular Cu to prevent any free or labile Cu(I) from generating radicals through Fenton-like chemistry by transporting Cu within the cytoplasm to the site of utilisation by cuproprotein (175). Studies utilising species ranging from prokaryotes to bacteria through to humans have identified these proteins and a well-characterised mechanism for Cu trafficking has been established (Figure 1.2). Copper is chaperoned by one of three known Cu chaperones (1) the Cu chaperone for SOD1 (CCS) which

delivers Cu to SOD1, (2) Cox17 that is responsible for delivery of Cu to CCO in the mitochondria and (3) Atox1 which delivers Cu to specific cuproenzymes and other Cu-binding molecules as well as to the nucleus and trans-Golgi network (176).

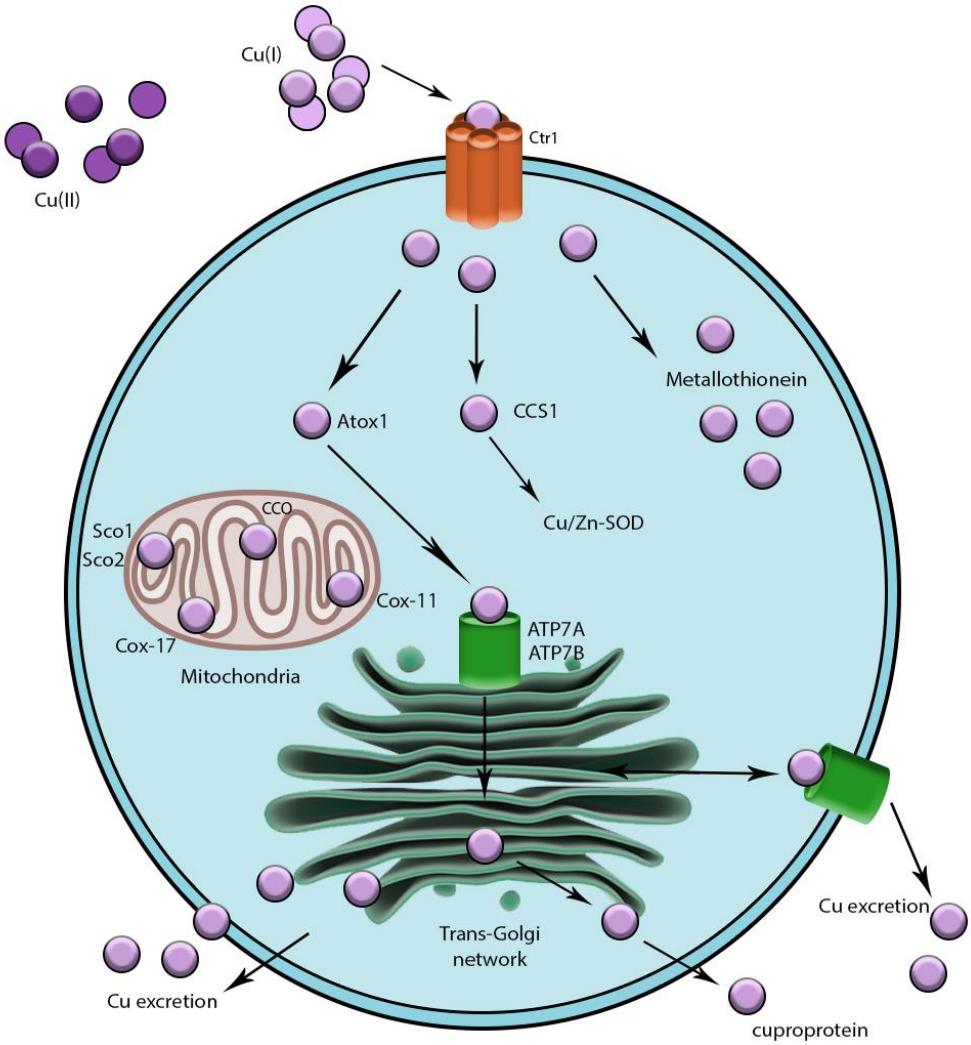

Figure 1.2. **Mammalian Cu distribution pathways**

Reduced Cu ions are primarily transported into the cell via Ctr1. Once inside the cytosol, Cu is delivered to one of three pathways: (1) the secretory pathway via Atox1 and ATP7A/B, (2) Cu, Zn-SOD1 via CCS1 or (3) cytochrome c oxidase inside the mitochondria via Cox17.

Many Cu-binding proteins pass through the secretory pathway en route to the plasma membrane or to be secreted outside the cell. Two types of proteins are involved in the delivery of Cu to the secretory pathway, Atox1 Cu chaperone and the Cu-transporting ATPases ATP7A/B. The yeast homolog of Atox1, Atx1 was first discovered by its ability to suppress ROS toxicity in yeast mutants lacking SOD1. Shortly after its discovery it was shown to chaperone Cu. Interestingly, in the same study, Atx1-mediated Cu delivery to the integral membrane Fe importer, Fet3p was shown to be a requirement for its activity (177). The mammalian homolog, Atox1 coordinates one atom of Cu and directly interacts, when Cu is bound, to ATP7A/B at the trans-Golgi network (178). Atox1 is essential for delivery of Cu to the secretory pathway in the trans-Golgi network. The ATP7A/B Cu-transporters contain six metal binding domains at the N-terminus (Figure 1.4) each capable of binding one Cu atom *in vitro* (179, 180). These transporters undergo Cu-mediated changes in intracellular trafficking. Delivery of Cu to secreted cuproproteins is facilitated by both transporters at the trans-Golgi network under conditions of low Cu. When cellular Cu is elevated ATP7A re-localises to the plasma membrane to efflux Cu outside the cell (181). A di-leucine motif near the C-terminal of ATP7A allows its endocytosis back to the trans-Golgi independent of protein synthesis (182). Excretion of excess intracellular Cu can be facilitated by ATP7B upon relocalisation from the trans-Golgi to intracellular vesicles (183).

The first line of cellular defence against oxidative insult is provided by SOD1. SOD1 is a highly conserved homo dimeric enzyme mainly localised in the cytosol with a small fraction in the intermembrane space of the mitochondria (184) and some evidence of SOD1 localised to the nuclei, lysosomes and peroxisomes (185). Copper is an essential structural and catalytic cofactor for SOD1's antioxidant activity that scavenges the superoxide anion. Copper is trafficked to SOD1 by the Cu chaperone CCS. Mitochondrial Cu, Zn-SOD1 localisation serves to mitigate the superoxide by-products of ATP production (186). Disturbances in the metallation status of SOD1 leading to misfolding and aggregation has been implicated in some forms of ALS (187).

The production of ATP in the mitochondria requires oxygen. In order for oxygen to be utilised in this process, CCO is required to reduce oxygen and in order to reduce oxygen Cu must be bound to CCO. The Cu binding sites of CCO are encoded within the mitochondria genome requiring CCO

metallation to occur within the mitochondria. The mechanism by which Cu is trafficked from the cytoplasm to the mitochondria for incorporation into CCO is unknown.

In addition to Cu chaperones, Cu can be associated with another class of Cu-binding protein, metallothionein (Figure 2). Metallothioneins are highly conserved, low molecular weight, metalloproteins with a significant number of cysteine residues whose primary biological function remains unresolved. Growing evidence suggests metallothioneins do not have a single function but are a rather versatile protein with many functions (188). Observed functions of metallothioneins include metabolism and homeostasis of metals including Zn and Cu (189) and detoxification of ROS (190). Ten metallothionein isoforms have been identified in mammals supporting the theory of their diverse physiological functions. The isoforms are grouped into four subdivisions (MT-I thru MT-IV) MT-I and MT-II are expressed in nearly all tissue, MT-III is expressed in the brain and MT-IV is found in stratified epithelial cells (191) and their expression is upregulated in Alzheimer's disease (192), amyotrophic lateral sclerosis, multiple sclerosis and in cases of neuroinflammation and oxidative stress induced by acute and chronic brain injury (193). Although a diverse range of functions have been uncovered, metallothionein appears to be non-essential for survival as mice lacking functioning metallothionein genes retained normal reproduction capacity and survival (194).

The gene family *cut*, (*cut*A-F), is believed to be involved in Cu import, storage, transport and export. Only *cut*C is conserved across taxa. Human CutC is distributed throughout the cytoplasm and was shown to bind Cu(I) and is believed to function as an enzyme containing a Cu cofactor to alleviate Cu stress rather than as a Cu transporter (195). However, the biological function of CutC in mammalian cells is still unresolved.

1.2.3 C. elegans copper metabolism

Recent *in vivo* and cell culture studies have identified a majority of the cellular Cu regulatory mechanisms in *C. elegans.* As with other eukaryotes, *C. elegans* show significant similarity with mammalian Cu trafficking systems. Intestinal copper uptake at the apical surface remains unresolved but may occur via one or more of the nine orthologs of the high affinity Cu(I) importer family of proteins, Ctr1 (SLC31A) identified in *C. elegans* based on sequence identity (K12C11.3,

K12C11.6, K12C11.7, F58G6.3, F58G6.7, F58G6.9, F31E8.4, F27C1.2 and Y58A7A.1)(Figure 1.3). Once inside the cell, Cu can be acquired by the three characterised Cu chaperones (1) Cox-17 (2) Cox-11or (3) Cuc-*1*, the proposed ortholog of Atox1.

C. elegans have five genes encoding SODs identified by sequence homology, (*sod-1* through *sod-5*) three of which are Cu, Zn-SOD (*sod-1*, *sod-5* and *sod-4*) with the bulk of SOD activity provided by *sod-1* and *sod-2* (196). Cytosolic Cu, Zn-SOD is predicted to be encoded by *sod-1* (78); *sod-2* and *sod-3* encode Mn, Fe-SOD that are predicted to be localised to the mitochondria (197) and *sod-4* and *sod-5* are predicted to be extracellular Cu, Zn-SOD (198). Activation of Cu, Zn-SOD occurs via a CCS-independent pathway suggested to involve glutathione (199). In contrast to the outcomes in yeast, flies and mice, deletion of Cu, Zn-SOD genes was found to have no effect on lifespan despite increased sensitivity to oxidative stress (200). Furthermore, multiple *sod* deletion mutants displayed increases in lifespan. These results suggest that regulation of lifespan may not be as simple as increased sensitivity to oxidative stress.

Copper delivery to secretory vesicles is achieved by the Cu chaperone CUC-1, a functional *C. elegans* homologue of *Saccharomyces cerevisiae* Atx1p (201). Expression of *cuc-1* and *cua-1*, which encodes the single Cu-ATPase, was seen in intestinal cells of adult *C. elegans* suggesting a similar Cu trafficking pathway to mammalian Atox1 and ATP7A/B.

C. elegans have two isoforms of metallothionein, MTL-1 and MTL-2. The two isoforms are predicted to have distinct functions *in vivo* as their expression profiles are quite different and interestingly their protein sequences differ from one another more than the vertebrate isoforms. MTL-1 active in the lower pharyngeal bulb and MTL-2 induced in intestinal cells in the presence of cadmium (202). Using electrospray ionisation mass spectrometry and circular dichroism spectroscopy the metal binding properties of the two isoforms showed a clear metal preference of MTL-1 towards Zn(II) and MTL-2 towards cadmium (Cd)(II) (203).

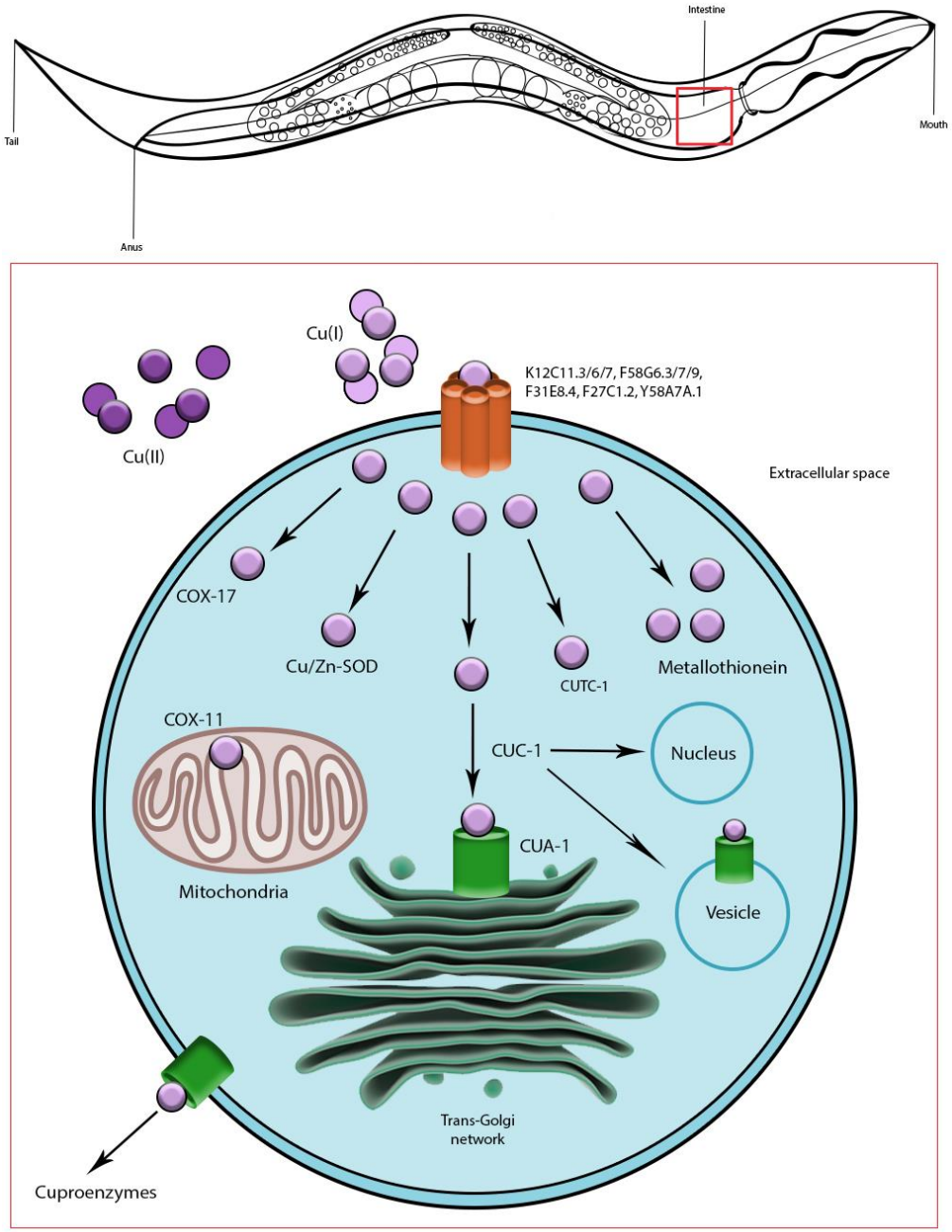

Figure 1.3. Proposed model of *C. elegans* cellular Cu trafficking.

Model of *C. elegans* Cu trafficking where reduced ions are believed to be imported by an uncharacterised CTR1-like (based on sequence identify) ortholog. Once inside the cell Cu is acquired by the Cu chaperone CUC-1 that is believed to transport Cu to CUA-1 in the trans-Golgi network. COX-17 is involved in trafficking to the mitochondria for incorporation into COX-11. The mechanism by which Cu, Zn-SOD acquires Cu is unknown. Based on sequence similarity, CUA-1 is believed to be involved in excretion of Cu from the cell and into cuproproteins. Metallothioneins and CUTC-1 are proposed to chelate available, labile, Cu..

The role of the putative Cu chaperone, CUTC-1 was investigated at the genetic level in *C. elegans*. Wild type and *cutc-1* knockdown via RNAi populations were exposed to excess Cu resulted in a global but statistically indistinguishable increase in whole body Cu. Brood size, growth and bagging rates were affected in *cutc-1* knockdown populations suggesting a role for *cutc-1* in protection from excess Cu (204).

Despite the understanding of Cu biochemistry and transport, relatively little is known of how changes in Cu homeostasis result in disease. One of the major impediments to gaining a greater understanding of Cu homeostasis has been the difficulty in quantifying Cu at physiological levels in its native state.

1.2.4 Copper-transporting ATPase

Cu ATPases are part of a large family of integral transmembrane proteins present in all phyla that are responsible for controlling the flux of ions and molecules across lipid membranes (205). In eukaryotes, Cu homeostasis is largely regulated by the P-type Cu-ATPases (ATP7A and ATP7B) (206, 207)(Figure 4). Invertebrates utilize one Cu-transporting P(1B)-type ATPase whereas vertebrates have two genes encoding ATP7A (Menkes protein, MNK) and ATP7B (Wilson protein, WND). The primary function of P-type-ATPases is to maintain strict homeostatic control of transition metals and to supply these metals for transmembrane or periplasmic assembly of essential metalloenzymes. The four core components of these ATPases as revealed by crystal structures and sequence analysis are: a membrane spanning domain, M-domain, that contains the ion binding sites, cytoplasmic actuator (A-domain) responsible for dephosphorylation, phosphorylation (P-domain) responsible for auto-phosphorylation and dephosphorylation and nucleotide-binding domains (N-domain) responsible for auto-phosphorylation. Translocation of metals across the lipid bilayer requires the energy of ATP hydrolysis therefore the ATP-binding domain of Cu-ATPases is highly conserved. Just as Cu-ATPase does, so do all P-type ATPases contain the conserved ATP-binding sequence motif G-D-G-V-N-D in the P-domain along with the phosphorylation region D-K-T-G-T (182, 208). The sequence of events starts with Cu and ATP binding to the cytosolic portion of ATPase, Cu is transferred to the transmembrane part of the transporter, the ATP undergoes hydrolysis and phosphorylation at which point Cu is released into the extracellular

space triggering dephosphorylation and the sequence resets. The primary roles of the Cu-ATPases differ across kingdoms as determined by their intracellular localisation. In eukaryotes, Cu homeostasis is maintained by Cu-ATPase mediate delivery of intracellular Cu to cuproenzymes in the secretory pathway and effluxing excess Cu and transporting it across various types of cellular membranes in order to prevent toxic accumulation (209). Intracellular Cu levels regulate Cu-ATPase activity and localisation (210). The fate of Cu is determined by the intracellular localisation of Cu-ATPases. Under normal conditions of physiological Cu levels the Cu-ATPases are localised to the trans-Golgi network where Cu can be utilised for the biosynthesis of cuproenzymes, in the secretory pathway. When intracellular Cu levels are increased ATP7B localizes to post-Golgi vesicles to facilitate Cu excretion (210, 211). Additionally, the location of ATP7B can be determined by Cu-mediated phosphorylation. ATP7B becomes hyperphosphorylated and traffics Cu to vesicles in conditions of elevated Cu whereas basal levels results in dephosphorylation of ATP7B enabling its trans-Golgi Cu-trafficking (212). Cu-ATPases do not bind free Cu ions, rather Cu is transferred from metallochaperones both of which contain the GMXCXXC motif that binds Cu(I) via the two sulfurs from the cysteine residues (179, 180). Copper is then transferred across the membrane by the Cu-ATPase and transferred to acceptor molecules. The affinity for Cu in the Cu-ATPases does not significantly differ from that of the metallochaperone, instead the metal binding domain of the Cu-ATPase retains Cu better which favours a metal donor-metal acceptor transfer of Cu rather than equilibrium (213). It remains unresolved if and how the activity of Cu-ATPase Cu-donors and acceptors can modulate the activity of Cu-ATPases.

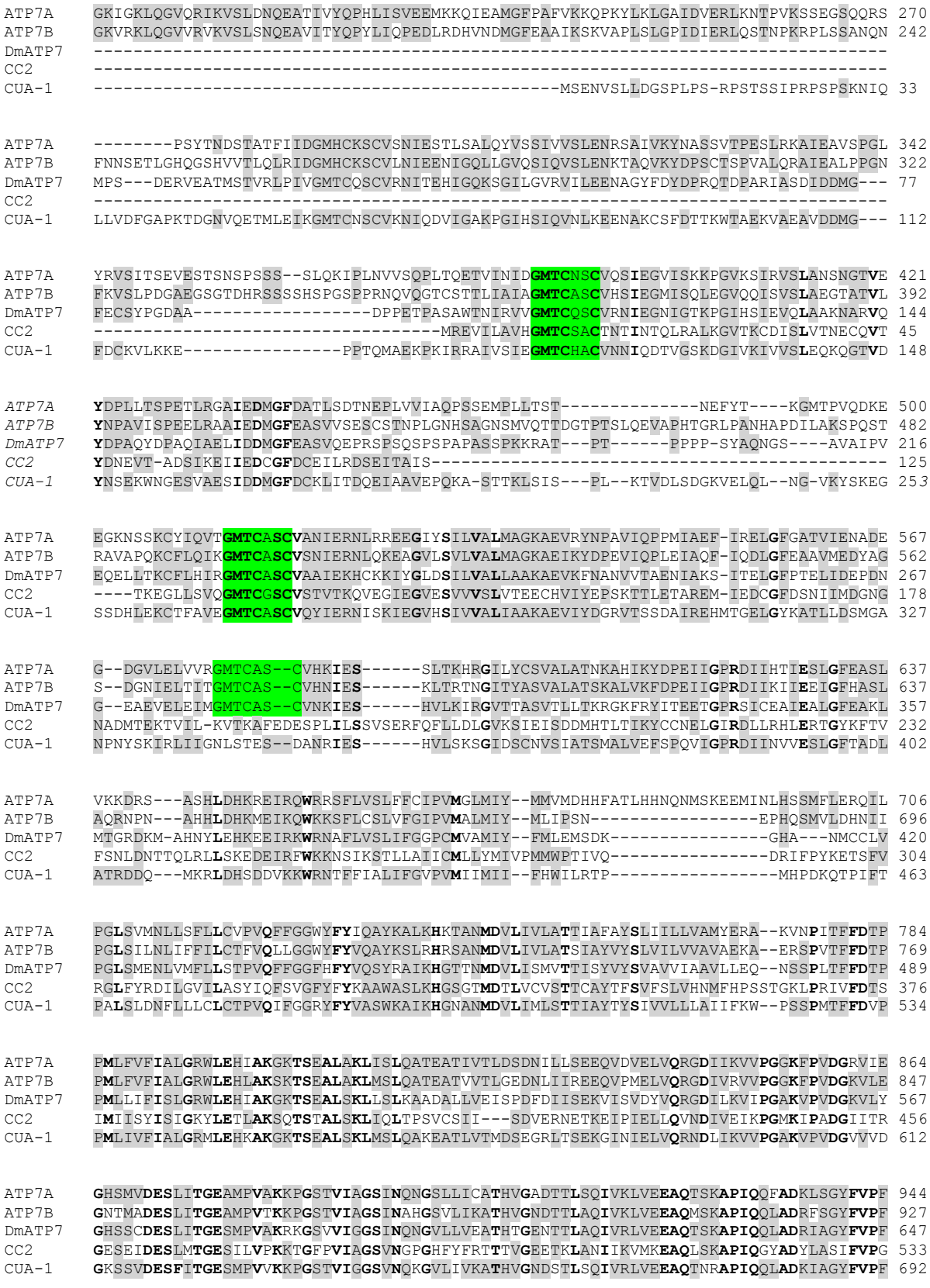
ATP7A GKIGKLQGVQRIKVSLDNQEATIVYQPHLISVEEMKKQIEAMGFPAFVKKQPKYLKLGAIDVERLKNTPVKSSEGSQQRS 270
ATP7B GKVRKLQGVVRVKVSLSNQEAVITYQPYLIQPEDLRDHVNDMGFEAAIKSKVAPLSLGPIDIERLQSTNPKRPLSSANQN 242
DmATP7
CC2
CUA-1 MSENVSLLDGSPLPS-RPSTSSIPRPSPSKNIQ 33
ATP7A --------PSYTNDSTATFIIDGMHCKSCVSNIESTLSALQYVSSIVVSLENRSAIVKYNASSVTPESLRKAIEAVSPGL 342
ATP7B FNNSETLGHQGSHVVTLQLRIDGMHCKSCVLNIEENIGQLLGVQSIQVSLENKTAQVKYDPSCTSPVALQRAIEALPPGN 322
DmATP7 MPS---DERVEATMSTVRLPIVGMTCQSCVRNITEHIGQKSGILGVRVILEENAGYFDYDPRQTDPARIASDIDDMG--- 77
CC2
CUA-1 LLVDFGAPKTDGNVQETMLEIKGMTCNSCVKNIQDVIGAKPGIHSIQVNLKEENAKCSFDTTKWTAEKVAEAVDDMG--- 112
ATP7A YRVSITSEVESTSNSPSSS--SLQKIPLNVVSQPLTQETVINIDGMTCNSCVQSIEGVISKKPGVKSIRVSLANSNGTVE 421
ATP7B FKVSLPDGAEGSGTDHRSSSSHSPGSPPRNQVQGTCSTTLIAIAGMTCASCVHSIEGMISQLEGVQQISVSLAEGTATVL 392
DmATP7 FECSYPGDAA----------DPPETPASAWTNIRVVGMTCQSCVRNIEGNIGTKPGIHSIEVQLAAKNARVQ 144
CC2 ----------MREVILAVHGMTCSACTNTINTQLRALKGVTKCDISLVTNECQVT 45
CUA-1 FDCKVLKKE----------PPTQMAEKPKIRRAIVSIEGMTCHACVNNIQDTVGSKDGIVKIVVSLEQKQGTVD 148
ATP7A YDPLLTSPETLRGAIEDMGFDATLSDTNEPLVVIAQPSSEMPLLTST----------NEFYT----KGMTPVQDKE 500
ATP7B YNPAVISPEELRAAIEDMGFEASVVSESCSTNPLGNHSAGNSMVQTTDGTPTSLQEVAPHTGRLPANHAPDILAKSPQST 482
DmATP7 YDPAQYDPAQIAELIDDMGFEASVQEPRSPSQSPSPAPASSPKKRAT---PT------PPPP-SYAQNGS----AVAIPV 216
CC2 YDNEVT-ADSIKEIIEDCGFDCEILRDSEITAIS---------- 125
CUA-1 YNSEKWNGESVAESIDDMGFDCKLITDQEIAAVEPQKA-STTKLSIS---PL--KTVDLSDGKVELQL--NG-VKYSKEG 253
ATP7A EGKNSSKCYIQVTGMTCASCVANIERNLRREEGIYSILVALMAGKAEVRYNPAVIQPPMIAEF-IRELGFGATVIENADE 567
ATP7B RAVAPQKCFLQIKGMTCASCVSNIERNLQKEAGVLSVLVALMAGKAEIKYDPEVIQPLEIAQF-IQDLGFEAAVMEDYAG 562
DmATP7 EQELLTKCFLHIRGMTCASCVAAIEKHCKKIYGLDSILVALLAAKAEVKFNANVVTAENIAKS-ITELGFPTELIDEPDN 267
CC2 ----TKEGLLSVQGMTCGSCVSTVTKQVEGIEGVESVVVSLVTEECHVIYEPSKTTLETAREM-IEDCGFDSNIIMDGNG 178
CUA-1 SSDHLEKCTFAVEGMTCASCVQYIERNISKIEGVHSIVVALIAAKAEVIYDGRVTSSDAIREHMTGELGYKATLLDSMGA 327
ATP7A G--DGVLELVVRGMTCAS--CVHKIES------SLTKHRGILYCSVALATNKAHIKYDPEIIGPRDIIHTIESLGFEASL 637
ATP7B S--DGNIELTITGMTCAS--CVHNIES------KLTRTNGITYASVALATSKALVKFDPEIIGPRDIIKIIEEIGFHASL 637
DmATP7 G--EAEVELEIMGMTCAS--CVNKIES------HVLKIRGVTTASVTLLTKRGKFRYITEETGPRSICEAIEAALGFEAKL 357
CC2 NADMTEKTVIL-KVTKAFEDESPLILSSVSERFQFLLDLGVKSIEISDDMHTLTIKYCCNELGIRDLLRHLERTGYKFTV 232
CUA-1 NPNYSKIRLIIGNLSTES--DANRIES------HVLSKSGIDSCNVSIATSMALVEFSPQVIGPRDIINVVESLGFTADL 402
ATP7A VKKDRS---ASHLDHKREIRQWRRSFLVSLFFCIPVMGLMIY--MMVMDHHFATLHHNQNMSKEEMINLHSSMFLERQIL 706
ATP7B AQRNPN---AHHLDHKMEIKQWKKSFLCSLVFGIPVMALMIY--MLIPSN----------EPHQSMVLDHNII 696
DmATP7 MTGRDKM-AHNYLEHKEEIRKWRNAFLVSLIFGGPCMVAMIY--FMLEMSDK----------GHA---NMCCLV 420
CC2 FSNLDNTTQLRLLSKEDEIRFWKKNSIKSTLLAIICMLLYMIVPMMWPTIVQ----------DRIFPYKETSFV 304
CUA-1 ATRDDQ---MKRLDHSDDVKKWRNTFFIALIFGVPVMIIMII--FHWILRTP----------MHPDKQTPIFT 463
ATP7A PGLSVMNLLSFLLCVPVQFFGGWYFYIQAYKALKHKTANMDVLIVLATTIAFAYSLIILLVAMYERA--KVNPITFFDTP 784
ATP7B PGLSILNLIFFILCTFVQLLGGWYFYVQAYKSLRHRSANMDVLIVLATSIAYVYSLVILVVAVAEKA--ERSPVTFFDTP 769
DmATP7 PGLSMENLVMFLLSTPVQFFGGFHFYVQSYRAIKHGTTNMDVLISMVTTISYVYSVAVVIAAVLLEQ--NSSPLTFFDTP 489
CC2 RGLFYRDILGVILASYIQFSVGFYFYKAAWASLKHGSGTMDTLVCVSTTCAYTFSVFSLVHNMFHPSSTGKLPRIVFDTS 376
CUA-1 PALSLDNFLLLCLCTPVQIFGGRYFYVASWKAIKHGNANMDVLIMLSTTIAYTYSIVVLLLAIIFKW--PSSPMTFFDVP 534
ATP7A PMLFVFIALGRWLEHIAKGKTSEALAKLISLQATEATIVTLDSDNILLSEEQVDVELVQRGDIIKVVPGGKFPVDGRVIE 864
ATP7B PMLFVFIALGRWLEHLAKSKTSEALAKLMSLQATEATVVTLGEDNLIIREEQVPMELVQRGDIVRVVPGGKFPVDGKVLE 847
DmATP7 PMLLIFISLGRWLEHIAKGKTSEALSKLLSLKAADALLVEISPDFDIISEKVISVDYVQRGDILKVIPGAKVPVDGKVLY 567
CC2 IMIISYISIGKYLETLAKSQTSTALSKLIQLTPSVCSII---SDVERNETKEIPIELLQVNDIVEIKPGMKIPADGIITR 456
CUA-1 PMLIVFIALGRMLEHKAKGKTSEALSKLMSLQAKEATLVTMDSEGRLTSEKGINIELVQRNDLIKVVPGAKVPVDGVVVD 612
ATP7A GHSMVDESLITGEAMPVAKKPGSTVIAGSINQNGSLLICATHVGADTTLSQIVKLVEEAQTSKAPIQQFADKLSGYFVPF 944
ATP7B GNTMADESLITGEAMPVTKKPGSTVIAGSINAHGSVLIKATHVGNDTTLAQIVKLVEEAQMSKAPIQQLADRFSGYFVPF 927
DmATP7 GHSSCDESLITGESMPVAKRKGSVVIGGSINQNGVLLVEATHTGENTTLAQIVRLVEEAQTSKAPIQQLADRIAGYFVPF 647
CC2 GESEIDESLMTGESILVPKKTGFPVIAGSVNGPGHFYFRTTTVGEETKLANIIKVMKEAQLSKAPIQGYADYLASIFVPG 533
CUA-1 GKSSVDESFITGESMPVVKKPGSTVIGGSVNQKGVLIVKATHVGNDSTLSQIVRLVEEAQTNRAPIQQLADKIAGYFVPF 692

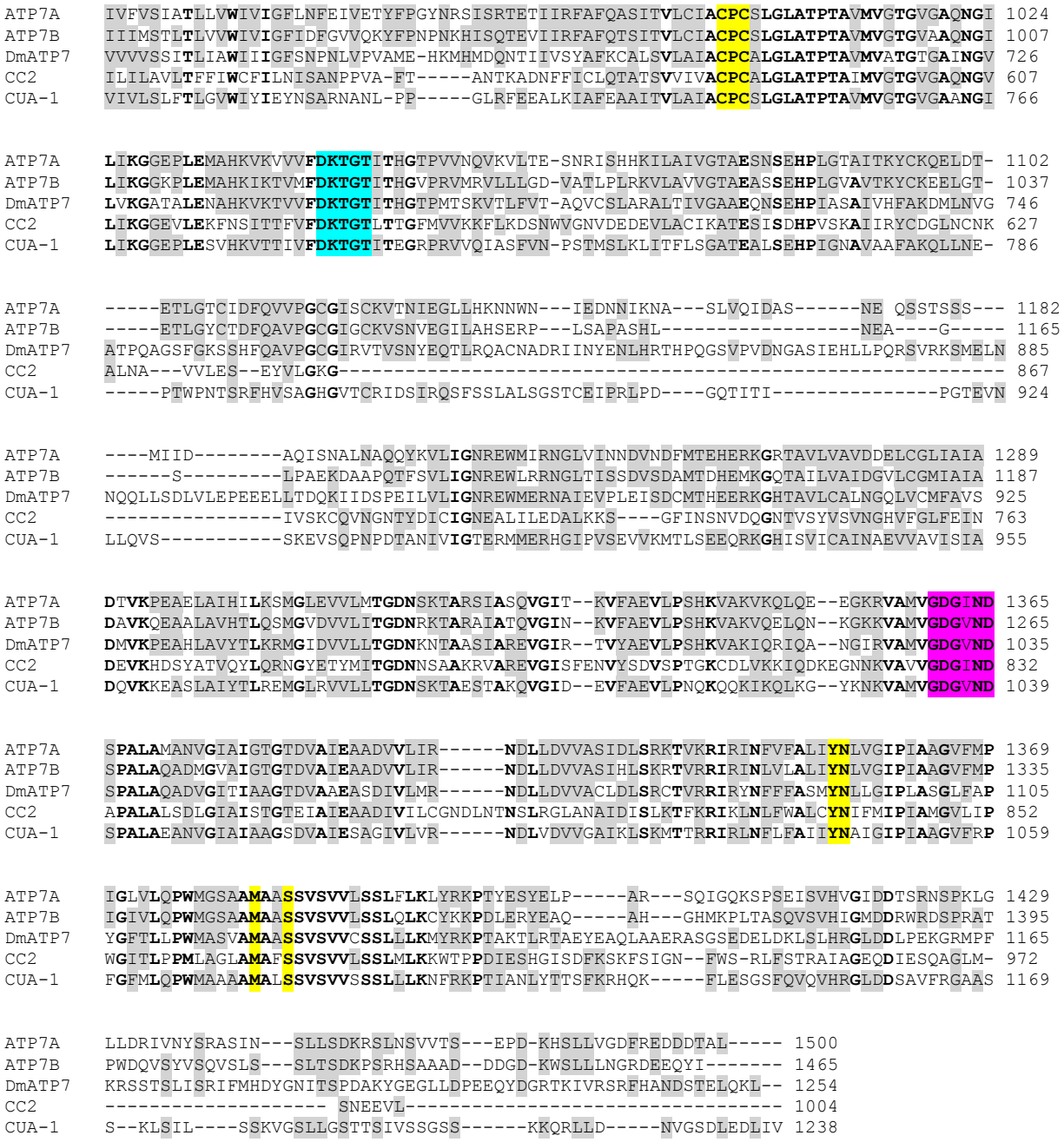

Figure 1.4. Sequence alignment of five representative P-type Cu-ATPases

From the top, the sequences of human ATP7A, and ATP7B, *Drosophilia melanogaster* DmATP7, *Saccharomyces cerevisiae* CC2 and *C. elegans* CUA-1. Identical residues are bolded and conserved residues within two or more sequences are in grey. The conserved regions are as follows: phosphorylation domain in blue, ATP-binding site in pink, N-terminal metal binding sites in green and residues predicted to be involved in Cu coordination within the membrane in yellow. Sequences were aligned using CLUSTAL (214).

The functional domains of Cu-ATPases have been extensive studied and are well characterised in eukaryotes. The commonalities and differences among Cu-ATPase homologs have helped to increase understanding of the specific mechanisms of Cu transport for each gene. Smaller, simpler organisms such as yeast, insects and nematodes have one gene encoding the P-type Cu-ATPase raising the question as to the potential overlap in function the single gene has with its mammalian homologues. The *Drosophila* Cu-ATPase ortholog, ATP7, shows high sequence similarity to ATP7A and ATP7B (Figure 1.4) which has been extensively studied and demonstrates clear evidence of Cu efflux activity (215). The *C. elegans* Cu-ATPase homologue, *cua*-1, was identified by rescuing Cu delivery to the multi-Cu oxidase, Fet3 in *Saccharomyces cerevisiae ccc2* (ATP7A/B homologue) loss of function mutants (216). Recently, CUA-1 was reported to be responsible for maintaining systemic Cu homeostasis via intestinal efflux of Cu coordinated by extraintestinal levels (217).

Given the following observations: (1) *cua-1* is responsible for maintaining Cu homeostasis in *C. elegans* (2) *cua-1* activity is required for *daf-2* longevity and (3) excess Cu stimulates activity in components of the IIS pathway; the stage has been set for the utilisation of *C. elegans* as a whole-animal model organism to investigate the underlying mechanisms of *cua-1* activity in regulating longevity within the *daf-2* mutant.

1.2.5 Measuring copper in biological matrices

Despite their physiological importance, the metalloproteomes of simple and complex organisms remain largely undefined. The ability to image and quantify Cu in its physiological state is an analytical challenge due to its ubiquity as a trace element in the cell and maintaining its native state. The sensitivity of techniques available to quantitate biometals continues to improve thus enhancing our understanding of metal distribution and concentration. The most common technique for the detection of multiple elements over a wide linear range of concentrations is inductively coupled plasma mass spectrometry (ICP-MS) (218). This technique measures metals concentrations in whole samples and therefore cannot be used to assess spatial distribution of metals. When determining the appropriate technique advantages and limitations, in regard to sample preparation, in order to maintain native metal coordination, quantitative capacity and accessibility to the instrumentation must be taken into

consideration. For the purpose of quantification, when an analyte is present in low levels the limits of detection of the analytical technique used must be low enough to reliably report the concentration of the particular analyte. Quantification of Cu in various biological matrices is routinely done using the same principle that the motion of a charged particle in a vacuum will be detected in accordance to its unique mass-to-charge ratio (m/z). Analysis of metalloproteins using chromatographic separation requires sample preparation techniques that ensure their native state is kept intact to avoid disrupting the ionic interactions between the metal cofactor and protein.

Characterizing subtle changes in low abundance elements, such as Cu, *in vivo* is the best approach to understanding the complex mechanistic relationship between Cu dyshomeostasis and ageing. Detectors with improved sensitivity for the purpose of X-ray fluorescence microscopy (XFM) allow for *in vivo* quantitative imaging of metal distribution with improvements on data acquisition time requirements for trace elements including Cu. Quantification, special distribution and even protein-association of trace elements can be determine in *C. elegans* by XFM (95, 219). Quantitative measurements of Cu have not been reported likely due to the optimised analytical parameters required due to its low abundance in the nematode.

Laser-ablation-inductively coupled plasma-mass spectrometry (LA-ICP-MS) is an attractive analytical tool for understanding metal biochemistry as it can couple the bulk analysis from ICP with spatial distribution of metals within various matrices with high sensitivity. However, quantification of trace elements using this technique requires matrix-matched reference materials that are not available currently for use with *C. elegans*.

Quantification of biometals in small multicellular organisms using ICP-MS has typically required large sample sizes to overcome analytical limits of quantitation (220-222). Obtaining such large numbers of *C. elegans* can be challenging when utilising a slow-growing or reproductively challenged mutant. Furthermore, treatments or interventions can exacerbate these traits and executing certain interventions can supersede the ability to culture large populations. To overcome these obstacles analytical methods are continually advancing to

reduce the sample size necessary to achieve sensitive proteomic and trace element analyses (223, 224).

A strong body of evidence discussed in this chapter implicates disrupted Cu homeostasis is a key component of processes of ageing and age-associated disease. Whether Cu dyshomeostasis is a cause of ageing pathology or merely an artefact of the process remains unresolved. Previous findings indicating an important role the activity of *cua-1* has on *daf-2* mutant longevity suggests Cu homeostasis may be a determinant of lifespan. A more thorough understanding of how *cua-1* activity regulates Cu metabolism in a long-lived model is required in order to continue to resolve the mechanisms of *daf-2* longevity. Based off the literature reviewed above this thesis will test the hypothesis that maintaining longevity in a *daf-2* mutant requires *cua-1*-mediated Cu homeostasis. In order to test the hypothesis a quantitative method for measuring trace biometals in individuals will be developed in order to quantify changes in total Cu levels in long-lived ageing populations with compromised *cua-1* activity. The potential effects the knockdown of *cua-1* activity has on the Cu-binding status of other soluble cuproenzymes will be investigated. These results could provide insight into the pathways by which CUA-1 mediates Cu levels to facilitate longevity in insulin-signalling mutant *C. elegans*. These findings could have implications into how these underlying mechanisms are regulated in more complex organisms given the high degree of conservation of the IIS and Cu trafficking pathways.

CHAPTER 2 – Materials and methods

2.1 Safety and ethics

All experiments in this thesis were carried out in a personal containment level II laboratory accredited by the Office of the Gene Technology Regulator. No ethics requirements were necessary for any experiments in this thesis.

2.2 Strains and culturing

All *C. elegans* strains were obtained from the Caenorhabditis Genetics Center (CGC, which is funded by NIH Office of Research Infrastructure Programs (P40 OD010440)) and maintained at 20 °C on Nematode Growth Media (NGM) plates unless otherwise indicated (31). All reagents used for the purpose of the thesis were made using Milli-Q H_2O (Merck Millipore, US) unless otherwise stated. *C. elegans* strains used in this work included N2 (Bristol), wild-type; CB1370 [*daf-2*(*e1370*)]; ZS1 [*mtl-1*(*tm1770*); *mtl-2*(*gk125*)](225); *mtl-1*(*tm1770*); *mtl-2*(*gk125*)(*mtl* strains were generously donated by Prof. Sturzenbaum at Kings College, UK); DR1309 [*daf-16*(m26); *daf-2*(*e1370*)] (226); GA187 [*sod-1*(*tm776*)]; GA416 [*sod-4*(*gk101*)]; GA503 [*sod-5*(*tm1146*)] and *cuc-1*(*tm1427*) generously donated by the Mitani Lab (Tokyo, Japan) through the National BioResource Project (Japan).

NGM was autoclave-sterilised and cooled to 60 °C at which point the following sterile, filtered reagents are added: 5 mg/mL cholesterol (dissolved in 100% undenatured ethanol) (Sigma-Aldrich, US), 1 mM calcium chloride ($CaCl_2$) (Univar, US), 1 mM magnesium sulfate ($MgSO_4$) (Univar, US), 25 mM potassium phosphate (KPO_4) (10.83% w/v potassium phosphate monobasic (KH_2PO_4) (AnalaR, US), 3.56% w/v potassium phosphate dibasic (K_2HPO_4)(Sigma-Aldrich) (31) immediately prior to pouring into sterile plastic petri dishes . The general food source is the *E. coli* strain, OP50, a uracil auxotroph as its growth is limited on NGM plates. A culture of OP50 from a glycerol stock is used to streak Luria broth (LB) agar (1% w/v tryptone, 0.5% w/v yeast, 0.5% w/v NaCl, 1.5% w/v agar, autoclave sterilised) plates (227) placed at 37 °C overnight. From these plates, under sterile conditions, a single colony is picked from the plate and used to inoculate LB medium (1% w/v tryptone, 0.5% w/v yeast, 0.5% w/v NaCl, autoclave sterilise) which is allowed to grow for 12 hr at 37 °C at 225 rpm prior to seeding NGM plates. Approximately 24 hr after pouring NGM plates are seeded with a lawn of the OP50 as food (228).

Culturing large populations, mass culture, is often facilitated by adding a larger percentage of peptone than typically used in the NGM protocol and therefore all mass culturing is done on 8P agar media (0.3% w/v NaCl, 2% w/v peptone, 2.5% w/v agar, autoclave sterilise) (229) that contain the same concentration of additives as NGM. To provide an adequate food source for large populations, concentrated OP50 was grown by inoculating 5 L of LB medium with 0.5 mL overnight culture started from a single colony, centrifuged and resuspended in 15 mL of S-BASAL (0.585% w/v NaCl, 0.1% w/v K_2HPO_4, 0.6% w/v KH_2PO_4, autoclave sterilise) and pipetted onto 8P plates as needed.

2.2.1 Developmentally synchronous cultures

Two different methods were used to obtain developmentally synchronous cultures depending on the assay end point. When comparing individuals within a population it is necessary to control for variables that can impact synchronicity in order to ensure any changes in the variable of interest is due to the intervention administered. These variables include duration of egg-lay, temperature of plates during egg-lay and throughout development and accuracy of NGM additives. When culturing *C. elegans*, populations can be considered synchronous according to developmental stage or age (typically reported as days old past embryogenesis). In some cases, when comparing genotypes that develop at different rates it can be advantageous to obtain synchrony according to developmental stage rather than age. Populations can be developmentally synchronous or age synchronous. For all lifespan and elemental analyses by ICP-MS synchronous populations were obtained by transferring gravid adults to new NGM plates seeded with OP50, adults were allowed to lay eggs for 3 hr and were then removed leaving only embryos behind to be used for subsequent assays.

For mass spectrometry analyses large scale culturing was required in order to obtain optimal population sizes. These populations were obtained by hypochlorite treatment of gravid adults (Fabian & Johnson 1994). Gravid adults were washed from NGM plates with Milli-Q H_2O, collected in a 15 mL falcon tube, allowed to gravity settle, supernatant was aspirated off and 2 volumes of hypochlorite solution (1M sodium hydroxide (NaOH), household bleach (5% v/v sodium hypochlorite)) was added to the tube. After approx. 3 min, adult carcasses had disintegrated

leaving only eggs behind, solution was diluted with 3 volumes of Milli-Q H_2O, centrifuged for 30 sec at 2500 rpm at room temperature and supernatant aspirated. Eggs were washed three times with fresh Milli-Q H_2O, then transferred into a sterile glass lidded watchglass (10 cm diameter) containing fresh S-BASAL to facilitate hatching of embryos at 20 °C for 8 hr at which point larva can be plated.

2.3 Life span analyses

All populations were cultured at 20 °C for three days until reaching larval development stage 4 (L4). Day one of life span assays commenced once populations of L4 worms were then transferred onto new NGM plates and maintained at 20 °C. Populations were examined every day for the first two weeks of the assay and then every two days for the remainder of the assay. When necessary, populations were transferred to new NGM plates to avoid starvation or larval crowding. Death events were noted as failure to respond to touch with a platinum wire and those lost or dead due to internal larval hatching were recorded as censored data. The assay was considered complete once the final individual on the final plate was scored as dead or censored. All life span analyses were performed at 20 °C unless otherwise stated. All lifespan assays were conducted using OP50 *E. coli* as the food source unless otherwise stated.

2.4 Copper treatment

A stock solution of Cu(II) chloride ($CuCl_2$) was made by dissolving $CuCl_2$ (AnalaR, US) in Milli-Q H_2O to a concentration of 150 mM. This solution was used to carry out all subsequent Cu treatment assays. As required to achieve the desired concentration of exogenous Cu, $CuCl_2$ was pipetted into the multant NGM immediately following the addition of the additives immediately prior to pouring plates.

The final concentration of Cu in NGM was verified by taking NGM samples approximating 1 cm cubed with and without Cu supplementation for elemental analysis by ICP-MS. Samples of NGM were weighed, dried in a centrifuge under vacuum, digested overnight in 50 µL of concentrated (65%) nitric acid (HNO_3) (Merck, US), then diluted using 1% HNO_3 to a final volume of 1 mL.

2.5 RNA interference

All RNAi plasmids used in the thesis were obtained as frozen glycerol stocks from the Ahringer *C. elegans* RNAi library (230)(University of Cambridge, UK). Fragments for the genes of interest for RNAi were obtained by polymerase chain reaction (PCR) and cloned into the empty RNAi feeding vector L4440 (pPD129.36) (38). This plasmid was transformed into the bacterial strain HT115 (DE3). The specific plasmids used in this thesis are as follows: (1) the empty feeding vector L4440 to serve as a control (2) R13H8.1 *daf-16*(RNAi) (primers 5'-AGTACAGCAATTCCCAAATGAAA-3' and 5'-AATTGGATTTCGAAGAAGTGGAT-3') and (3) Y76A2A.2 *cua-1*(RNAi) primers (5'-GTGTGATGAGAGTGAGATGACGA-3' and 5'-AAAAAGAAGCATCACTTGCAATC-3').

Under sterile conditions, a sample from each glycerol stock was streaked on an LB agar plate containing 50 mg/mL ampicillin and grown at 37 °C overnight. From the plate, single colonies of *E. coli* containing plasmids were used to inoculate a 250 mL flask containing 50 mL of autoclave sterilised LB medium containing 50 mg/mL ampicillin that was then placed at 37 °C shaking incubator at 225 rpm for 10 – 12 hr until a cell density of OD_{600} = 0.8 was achieved. The cells were then directly applied onto agar plates containing 1 mM Isopropyl-ß-D-thiogalactopyranoside (IPTG) (231) as the gene of interest is in-between two IPTG-inducible T7 promoters (38). Worms were added to plates individually; or many worms were added by washing development plates with S-BASAL and transferring using glass transfer pipette directly onto new plates.

2.6 Dauer formation assay

Developmentally synchronous adult wild-type and *daf-2*(*e1370*) were left to lay eggs at 20 °C for 3 hr on RNAi plates. Following egg lay, gravid adults were removed and plates were shifted to 27 °C for 3 days. The number of adults and dauer larvae on each plate were counted. Scoring of dauer larvae was confirmed by testing their resistance to excess 1% (w/v) sodium dodecyl sulfate (SDS) exposure for 30 min.

2.7 Inductively coupled plasma mass spectrometry

2.7.1 Sample preparation

Samples were prepared for elemental analysis using inductively coupled plasma mass spectrometry as indicated in previous methods (224). Briefly, developmentally synchronous populations were picked individually from plates and the desired number of individuals was transferred into 1.7 mL microcentrifuge tube (TechnoPlas) containing 200 µL of S-BASAL. Samples were washed 3X with fresh S-BASAL followed by three washes with fresh Milli-Q H_2O to get rid of any bacteria inside the gut as well as any stuck to the individuals. Samples were then flash frozen, lyophilized using a vacuum freeze dryer and digested in 20 µL of 65% HNO_3 at room temperature. Matrix blanks were prepared in conjunction by aliquoting equivalent volumes of 65% HNO_3 to separate 1.7 mL tubes to measure possible elemental contamination from the nitric acid. Digested samples and matrix blanks were diluted to 200 µL final volume using 1% HNO_3 prior to analysis. In addition to matrix blanks, method blanks were prepared for analysis by aliquoting 200 µL of 1% HNO_3 to separate 1.7 mL microfuge tubes to measure possible contamination in the 1% nitric acid.

2.7.2 Elemental analysis by ICP-MS

Total metal content of a range of elements (including Mn, Fe, Cu and Zn) were determined by ICP-MS (7700s series, Agilent Technologies, Santa Clara, CA, USA) analysis using routine multi-element operating conditions and a helium reaction gas cell (He gas flow at 4.3 mL min^{-1}) in spectrum mode. Samples were introduced to the ICP-MS by a Micromist nebulizer, the plasma flow rate was set at 15 L min^{-1} and the RF power at 1.5 kW. Certified multi-element ICP-MS standard calibration solutions (Accustandard, New Haven, CT, USA) were used to calibrate the instrument with 0, 0.5, 1, 3, 5, 10, 50, 100 and 500 ppb standards. An internal standard containing 200 ppb of Yttrium (Y 89) (Accustandard) was used as an internal control and introduced to the ICP-MS using an internal standard line connected to a peri-pump. Metal concentrations were calculated as µg metal per individual.

2.8 Liquid chromatography – inductively coupled plasma mass spectrometry

2.8.1 Sample preparation

Developmentally synchronous populations were collected from 8P plates by washing with S-BASAL, filtering out all embryos and bacteria using a 0.4 µm mesh filter (Falcon, U.S.A.) and collecting the flow-through into 15 mL conical-based, screw top centrifuge tubes. The sample remaining in the filter was collected and further washed 3X with fresh S-BASAL followed by three washes with fresh MilliQ-H_2O. Following the final wash, samples were flash frozen in liquid N_2 and stored at -80 °C until homogenisation for mass spectrometry analysis.

Frozen *C. elegans* pellets were weighed and placed in 1.7 mL tubes on wet ice. Two times the sample volume of 1X Tris-buffered saline (TBS)(pH 7.5) containing 1X EDTA protease inhibitors (Roche), dissolved in MilliQ-H2O, was added to each sample (e.g. if the pellet volume was 500 µL, 1000 µL of buffer was added). The lysate was homogenized by hand using a cell homogenizer (isobiotech, Germany) kept at 4 °C on wet ice and centrifuged for 15 min at 15,000 x g at 4 °C to separate the soluble and insoluble fractions. The supernatant was collected and the protein concentration for each sample was determined by absorbance at 280 nm using a micro volume spectrophotometer (Nanodrop, ThermoScientific).

2.8.2 Analysis of metalloprotein profile by LC-ICP-MS

Soluble proteins were size-excluded followed by in-line elemental analysis by ICP-MS and analysed according to their metal status using size-exclusion chromatography-inductively coupled plasma mass (SEC-ICP-MS). The HPLC (1290, Agilent Technologies) was equipped with binary pumps, in-line degasser, temperature controlled auto-sampler that was maintained at 4 °C for the duration of the method, column compartment and variable wavelength detector. Sample volumes containing 200 µg of protein were injected onto the column. This amount was kept consistent for each experiment. The proteins in the sample were separated over a BioSEC 5 4.6 mm x 50 mm, 150 Å, 3 um size exclusion column (Agilent Technologies) with 200 mM ammonium nitrate (NH_4NO_3) (Sigma Aldrich,) pH 7.5 (using ammonium hydroxide) with 10 µg per L ^{133}Cesium (Cs) (Choice Analytical, Lot # 1209403) and 121 Antinomy (Sb) (Choice Analytical, Lot # 1208035), both dissolved in 2% (v/v) HNO_3 + 5% (v/v) tartaric acid, spiked internal standard at a flow rate

of 0.4 mL min^{-1}. The column temperature was maintained at 25 °C and absorbance monitored at 280 nm. After passing through the UV wavelength detector, samples are introduced directly into a micro mist nebulizer for ICP-MS analysis. The ICP-MS was set up for bulk analysis (Section 2.3.2) with the exception of the acquisition mode set to TRA. Bovine Cu, Zn-SOD1 was used as a molecular weight standard for each experiment as it was used to determine the elution of SOD1 from the column.

2.9 Statistical Analysis

All statistical analyses and associated figures were performed and created using Prism v6.0d (Graphpad, USA).

2.9.1 Lifespan assays

Kaplan-Maier survival curves were generated for all life span assays. All survival curves represent the combination of three independently conducted lifespan assays. Survival curves and mean survival times were compared via non-parametric log rank tests (Mantel-Cox).

2.9.2 Elemental analysis via ICP-MS

Differences in mean elemental content over time for an individual strain were analysed using a one-way ANOVA with a Tukey's multiple comparisons post hoc test. Differences over time and between treatments for an individual strain were analysed by two-way ANOVA and multiple comparisons between groups were tested using Tukey's multiple comparisons post hoc test. When differences between only two groups were compared, an unpaired Student's t-test was performed.

2.9.3 Metalloprotein analysis via LC-ICP-MS

For each data set, chromatograms were baseline corrected by subtracting the mean signal intensity (counts per second) of the first 60 recorded data points from each sample for all elements measured. Each chromatogram represents the mean signal intensity calculated from three independent replicate samples.

Chapter 3 – Quantifying biometals at the individual level using inductively coupled plasma mass spectrometry

The results for this chapter are presented in the published form, following an expanded introduction and rationale.

3.1 Introduction and Rationale

Metabolism and homeostasis of metal ions is a key component of numerous physiological as well as disease processes. Continuous improvements in the sensitivity of analytical techniques as well as in the integration of these techniques into the biosciences have greatly facilitated the detection of metals furthering the understanding of the cellular and subcellular mechanisms by which these metals are changing. As previously discussed in detail (Chapter 1) changes in biometals are well established to be a feature of ageing and age-associated diseases. Quantifying changes in such metals is paramount to understanding how these changes contribute to age and disease. The aim of this chapter was to develop a method to determine the minimum sample size necessary to quantify metals at an individual level using *C. elegans* via inductively coupled plasma mass spectrometry that can easily be adopted for use with other small model organisms.

Previous studies have used varying numbers (40 – many thousands) of individuals to quantify biometals in *C. elegans* (95, 220, 222, 232). When using these methods with large populations multiple factors, within the sample preparation, can arise that may influence the accuracy and precision metal quantification at the individual level. Therefore, the first part of the aim of this chapter was to develop a technique in which the minimum number of individuals is necessary to quantify biologically significant metals. The method we have published includes detailed sample preparation, instrument parameters and analysis settings necessary for specific metals of interest. From this method we can determine the variation for these metals between individuals within genetically identical and developmentally synchronous populations. Measurements of Fe, Zn and Mn in genetically and developmentally synchronous populations obtained using XFM were used to compare with the results obtained by ICP-MS. XFM offers very high sensitivity for quantitative imaging (submicron-resolution) of most metals in biological samples (233). We observed good agreement between these two analytical

techniques supporting our technique for assessing biometal content in small populations of *C. elegans*.

3.2 Published Manuscript

Analyst

PAPER

View Article Online
View Journal

CrossMark click for updates

Cite this: DOI: 10.1039/c5an02544c

Accurate biometal quantification per individual *Caenorhabditis elegans*†

Katherine Ganio,[a] Simon A. James,[a] Dominic J. Hare,[a,b] Blaine R. Roberts[a] and Gawain McColl*[a]

Received 11th December 2015,
Accepted 19th January 2016

DOI: 10.1039/c5an02544c

www.rsc.org/analyst

In the life sciences, small model-organisms are an established research platform. Due to the economy of culturing and maintenance animals such as the roundworm *Caenorhabditis elegans*, and the fly *Drosophila melanogaster*, have been instrumental for investigating key genetic pathways, early development, neuronal function, as well as disease pathogenesis and toxicology. Small model organisms have also found utility in the study of inorganic biochemistry, where the role of metal ion cofactors are investigated for numerous fundamental cellular processes. The metabolism and homeostasis of metal ions is also central to many aspects of biology and disease. Accurate quantification of endogenous metal ion content is an important determinant for many biological questions. There is currently no standardised method for quantifying biometal content in individual *C. elegans* or estimating the variation between individuals within clonal populations. Here, we have determined that ten or more adults are required to quantify physiologically important metals *via* inductively coupled plasma mass spectrometry (ICP-MS). The accuracy and precision of this method was then compared to synchrotron-based X-ray fluorescence microscopy (XFM) to determine the variation between isogenic, developmentally synchronous *C. elegans* adults.

Introduction

Accurate analytical tools for studying metals are important for a range of biological investigations, including fundamental inorganic biochemistry,[1] toxicology[2] and disease mechanisms.[3] The roundworm *Caenorhabditis elegans* is a classic, versatile model organism that has been applied to the study of metals in biology. For example, the ecotoxicity of metal and metal oxide engineered nanoparticle exposure have been investigated in this organism.[4–6] *C. elegans* can be raised in tightly controlled experimental conditions, facilitating analysis of metal and metal–ligand complex uptake, localisation and metabolism, and the resulting effects on life history traits.[7–9]

A growing number of diseases have been correlated with the loss of homeostasis or change in the metabolism of endogenous metal ions in cells and tissues.[10,11] The underlying mechanisms by which metals may contribute to the onset of disease are areas of intense investigation due to better integration of contemporary analytical techniques into the biosciences. Metal cofactors are essential for the structural and catalytic activity of nearly one-third of the human proteome.[12] For example, cytochromes use an iron (Fe)-containing heme group and numerous antioxidants rely upon a redox-active metal center. In addition, metal ions including manganese (Mn), Fe, copper (Cu) and zinc (Zn) can have specific deleterious effects when in overabundance or insufficiency.

To determine the concentration of metals per individual or between populations of small multicellular organisms, like *C. elegans* that weigh less than 1 μg, requires sensitive analytical techniques.[13] Quantification of specific metals in *C. elegans* by inductively coupled plasma-mass spectrometry (ICP-MS) has been reported using forty to hundreds of thousands of individuals per assay.[14–16] Collecting samples that consist of more than several hundred can present practical challenges, and include concerns that large populations may not be as developmentally synchronous as those cultured using standard smaller scale methods. These issues may confound the biological variation of metals and additionally prevent metal levels from being reported as concentration per individual. It is therefore adventitious to develop an analytical protocol that does not require culturing on an overly large scale. In addition, there is no standardised method of sample preparation for the purpose of elemental analysis per individual specimen. A validated approach that is capable of accurate

[a]*The Florey Institute of Neuroscience and Mental Health, The University of Melbourne, 30 Royal Parade, Parkville, Victoria 3052, Australia. E-mail: gawain.mccoll@florey.edu.au; Tel: +61 3 903 56608*
[b]*Elemental Bio-imaging Facility, University of Technology Sydney, Broadway, New South Wales, Australia*
† Electronic supplementary information (ESI) available: ESI table and figure. See DOI: 10.1039/c5an02544c

and precise quantification of metals using smaller sample number would overcome these limitations, and may also be amenable for further development into high-throughput screens, for which *C. elegans* are well suited.

Experimental

Chemicals and reagents

Ultra-pure water (18.2 MΩ; Milli-Q H_2O; Merk Millipore, Australia) was used for the dilution of all reagents and standards. Analytical grade 65% (v/v) nitric acid (HNO_3; Merck) was used to digest samples and was diluted to 1% as the standard diluent. The instrument was calibrated for manganese (Mn), iron (Fe), copper (Cu) and zinc (Zn) using mixed 0, 0.5, 1, 3, 5, 10, 50, 100 and 500 parts per billion (ppb) standard calibration solutions in standard diluent from commercially-available ICP-MS-CAL2-1, ICP-MS-CAL3-1 and ICP-MS-CAL4-1 certified reference standards (AccuStandard, USA). A reference element solution containing 200 μg L^{-1} yttrium (Y) (ICP-MS-Internal Standard Solution-1, Accustandard) was introduced by a T-piece positioned after the peristaltic pump and was used to normalise all measurements. The tuning solution for instrument optimisation contained 1 μg L^{-1} of cerium (Ce), cobalt (Co), lithium (Li), thallium (Tl) and Y in 2% (v/v) HNO_3 (Agilent Technologies, Australia). All standards were stored in polyethylene bottles washed using 1% HNO_3 in MilliQ-H_2O, prior to use. Seronorm™ Trace Elements Serum L-1 and L-2 (Sero, Norway, lot #0903106) were used to externally assess analytical performance.

Caenorhabditis elegans strains

Wild type *C. elegans* (strain N2) were obtained from the Caenorhabditis Genetics Center and were maintained on standard nematode growth media (NGM) at 20 °C using established protocols.[17]

Sample preparation for ICP-MS

Ten independent biological replicates of groups consisting of 10, 25, 50, 100 and 200 individual *C. elegans* were analysed. This was repeated and the data pooled to give a total of 20 independent replicates for each sample size. Gravid wild type hermaphrodites were allowed to lay eggs for 3 hours at 20 °C in order to obtain developmentally synchronous young adults (4 day old post egg lay). Young adults were counted and removed from NGM plates and then transferred into 1.5 mL polypropylene microfuge tubes (TechnoPlas, Australia) containing 200 μL S-basal (5.85 g L^{-1} NaCl; 1 g L^{-1} KH_2PO_4; 6 g L^{-1} K_2HPO_4). The microfuge tubes were gently inverted for 30 minutes to flush the gut of bacterial feed. Samples were then washed three times with 200 μL S-basal, followed by three washes in 200 μL ultra-pure water to remove any remaining bacteria. Aspiration between washes was performed using a stereomicroscope to avoid sample loss. Following the washes samples were then flash frozen in liquid N_2 and lyophilized overnight. Following lyophilisation, samples were digested in 20 μL of 65% HNO_3 for 12 hours at room temperature and diluted 1 : 10 to a final volume of 200 μL using 1% HNO_3. Ten digest blanks were prepared for each experiment, giving 20 blanks in total, to determine the limit of detection and limit of quantification for the elements measured, as well as, correcting for any contamination that may occur during the digestion process.

Inductively coupled plasma-mass spectrometry

All measurements were performed on an Agilent Technologies 7700× ICP-MS with a MicroMist nebulizer (Glass Expansion, Australia). Torch positioning, sample depth adjustment and lens optimization were set according to manufacturer recommendations while the other instrumental parameters (ESI Table 1†) were optimized during a batch-specific user tune prior to each experimental run. Helium collision gas at 3 mL min^{-1} was used to minimise polyatomic interferences. Samples were introduced directly from 1.5 mL polypropylene tubes *via* an integrated automation system (IAS) autosampler (Agilent) using a peristaltic pump. Tubing length consisted of 400 mm of 0.15 mm I.D. polypropylene tubing and 0.25 mm I.D. Tygon PeriPump tubing, with approximately 150 μL of sample needed for each measurement. Sample uptake time comprised of 52 s with a stabilisation time of 40 s and integration time of 0.1 s for each of the element isotopes monitored and internal standard.

Sample preparation for hydrated XFM

A cohort of developmentally synchronous *C. elegans* adults (4 day old post egg lay; generated as described above) were washed four times in 500 μL S-basal[17] to remove excess bacteria, anesthetised in S-basal kept at 4 °C with 0.2% (w/v) sodium azide (NaN_3). Once completely immobilised, samples were transferred to an agarose (2%, w/v) pad approximately 10 μm thick with 0.2% (w/v) NaN_3, affixed to a 2 μm thick silicon nitride window (Silson, UK), covered with 4 μm thick Ultralene film (Volga Instruments, India) to prevent evaporate loss and immediately mounted for XFM.

X-ray fluorescence microscopy

The distribution of metals was mapped at the XFM beamline at the Australian Synchrotron. A beam of 15.6 keV was focused to a spot of 2 μm (full-width at half-maximum) using a Kirkpatrick-Baez mirror pair.[18] The X-ray energy was chosen to induce K-shell ionisation of elements with atomic numbers below 37 as well as for separating the relatively intense elastic and inelastic scatter peaks from the fluorescence lines of lighter elements. Scanning of the specimen occurred continuously through the focus with a virtual pixel size of 0.8 μm in both the horizontal and vertical while X-ray fluorescence (XRF) was collected with the Maia detector system. An elemental map of 3200 × 1600 pixels (5.12 Mpixels) was collected using a dwell time of approximately 3.13 ms per pixel. Manganese and platinum (Micromatter, Canada) reference metal foils were used to calibrate XRF intensity to elemental areal density using a fundamental parameter approach. Analysis of the X-ray

fluorescence spectra, including corrections for self-absorption, scatter from the air path and the efficiency of the detector were performed using GeoPIXE v7.2f (CSIRO, Australia).

Statistical tests

The limit of detection (LOD) and limit of quantification (LOQ) were calculated according to Boumans[19] (three times and ten times the standard deviation of the background signal, respectively). Variation of the mean metal concentration between sample groups was determined *via* a one-way ANOVA with Tukey's *post hoc* multiple comparisons test in Prism v6.0d (GraphPad, USA). Outliers were detected and removed using a method that combines robust regression with outlier detection, ROUT,[20] with a false discovery rate, Q, set to 1% using Prism v6.0d. In total, four outliers were removed from the ICP-MS data set; two from the Cu analysis group containing 100 individuals per measure and one from the group containing 200 individuals per measure as well as one from the Zn analysis group containing 100 individuals per measure (Fig. 1).

Results and discussion

Analytical sensitivity of ICP-MS

Here we describe a method that determines the minimum number of adult *C. elegans* per assay (*i.e.* minimum sample size) necessary to accurately quantify endogenous metals by ICP-MS, which can be easily adopted for use with other small model organisms. The accuracy and precision of this method was compared and contrasted with synchrotron-based X-ray fluorescence microscopy (XFM), an alternative analytical technique that we have previously used to produce quantitative micrometer resolution maps of metals in biological specimens.[21,22] We observed good agreement between these two analytical techniques, supporting our approach for assessing low-level biometal content in small populations of *C. elegans*.

To account for the small size of adult *C. elegans* and low abundance of Cu,[23] samples were digested and subsequently diluted with minimal amounts of solvent to avoid diluting analyte concentrations beyond the ICP-MS detection limits (final volume = 200 μL). The experimental limits of detection and quantitation calculated from the standard deviation of the mean for each element in the digest blanks and the background equivalent concentration are presented in ESI Table 2.† The background equivalent concentrations are calculated using the background signal for a given element, using the analyte specific intensity of the background and as a result are usually greater than detection limits.[24] Several factors can influence the detection limits of a given assay including elemental abundance in the 0 parts per billion (ppb) calibration standard, the linearity of the calibration curve, flow rate of the carrier gas, integration time for each element, as well as, polyatomic interference for certain elements. Some elements are more ubiquitous in a non-clean-room environment. Iron and zinc have a higher background intensity that is reflected in the background equivalent concentration for the given analyte.

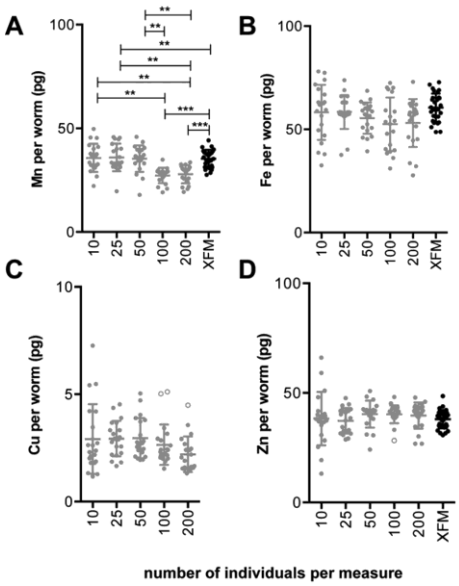

Fig. 1 Comparison of ICP-MS and XFM estimates of Mn, Fe, Cu and Zn content per individual adult *wild-type C. elegans* (ICP-MS data: n = 20 replicates per measure, for XFM data: n = 29 replicates, Tukey's multiple comparisons test; $^{**}p < 0.01$, $^{***}p < 0.001$). The ICP-MS data represents a combination of two independent analyses. (A) The average Mn content per worm measured by ICP-MS differed between sample groups. Sample groups containing 100 and 200 individuals had lower Mn per individual compared to other sample groups ($p < 0.01$) including XFM measurements ($p < 0.001$). (C) Note that Cu was below the limit of quantification for the XFM measurement parameters used in this study. (B–D) No significant difference for average Fe, Cu or Zn content per individual between groups measured *via* ICP-MS or between those and XFM measurements. Bar represents mean ± standard deviation. For mean, SD and coefficient of variation for each sample group refer to Table 2. Data excluded from analysis indicated as open circles.

ICP-MS data was pooled from two independent measurements. All samples included in the analysis yielded values above the limits of detection and the limits of quantification for all elements of interest and all outliers were removed. To verify the accuracy of the calibration standards triplicate measurements of two Seronorm standards were generated. All values were within acceptable range, as established by the standards manufacturer (Sero), with recoveries within 15% of the certified values for both standards (Table 1).

Quantification of metal content per individual

Our method suggests as few as 10 individuals per measure can be used to accurately quantify Mn, Fe, Cu and Zn *via* ICP-MS

Table 1 Secondary instrument calibration verification standards. All values reported as mean μg L^{-1} with estimates ± one standard deviation from triplicate measures

Element	Seronorm standard	Expected value	Measured value	% Recovery
Mn	L-1	15.00	14.57 ± 0.38	94.3 ± 2.5
	L-2	19.90	19.07 ± 0.26	95.8 ± 1.3
Fe	L-1	1390	1383 ± 7	99.5 ± 0.5
	L-2	2030	2024 ± 13	99.7 ± 0.7
Cu	L-1	1691	1688 ± 16	99.9 ± 0.9
	L-2	2887	2826 ± 14	97.9 ± 0.5
Zn	L-1	1738	1597 ± 1	91.9 ± 0.1
	L-2	2520	2204 ± 4	87.5 ± 0.2

(Fig. 1). With the exception of Mn increasing the number of individuals sampled did not result in significant change in the average metal content. Across all elements, the coefficient of variation (as a percentage) ranged from 7.56 to 55.6% (Table 2), with the largest variance seen in Cu levels of measures using 10 adults. Copper is present in very low abundance in these nematodes (approximately 2 pg per individual) a level near the limit of detection of the ICP-MS. The difficulty of measuring such a low abundance is reflected by the high variation between estimates. Increased precision when measuring metals of relative low abundance may require increased number of biological replicates. For Mn and Zn the precision of estimates improved using samples comprising more than 10 individuals (Table 2). In contrast, the coefficient of variation for Fe and Cu estimates improved less with increasing sample size, and ranged from 22.92% and 55.61% (Fe and Cu, respectively, n = 10 individuals per measure) to 21.80% and 31.04% (n = 200 individuals per measure; Table 2). Overall similar levels of variation about the mean were comparable to estimates for the dagger nematode, *Xiphinema vuittenezi*, for Mn, Fe, Cu and Zn quantification *via* ICP-MS.[25] Variation of element levels within sample groups may arise from biological, instrumental or procedural sources. Despite optimisation of sample preparation and instrumental settings, natural variation even between genetically identical and co-cultured individuals may still occur. The source of such variation may include small stochastic differences in development, reproductive status and nutritional status.

The number of elements that can be analysed during each run is limited by the sample volume and abundance of the elements of interest, which may then require further optimisation of the quantitative parameters. However, our method can be applied to a wide range of elements restricted only by abundance and sensitivity of the instrument used. The background levels will also limit detection of less abundant elements. If the sample matrix contains significant background a higher number of individuals per sample or optimisation of the method parameters of the ICP-MS specific to that element may be required.

Comparison of analytical techniques

A complementary technique for accurate quantification of metals in biological systems is X-ray fluorescence microscopy (XFM), providing spatial maps of elements *in situ*, often with minimal disruption of the sample during perperation.[13] A population of wild type adults was imaged using XFM (Fig. 2) to quantify Mn, Fe and Zn (Table 2, only whole imaged animals were used, see ESI Fig. 1† for masks used). The means were compared to those determined *via* ICP-MS. Estimates of

Table 2 Quantification of metals in adult wild type *C. elegans* from ICP-MS and XFM. Concentration reported as mean pg per individual ± standard deviation with n = replicates and percent coefficient of variation reported for each sample group

No. of individuals per measure	Mn	Fe	Cu	Zn
ICP-MS				
10	35.83 ± 6.79	58.26 ± 13.36	2.92 ± 1.62	38.27 ± 12.17
	n = 20	n = 20	n = 20	n = 20
	18.95	22.92	55.61	31.80
25	35.42 ± 6.69	49.82 ± 11.22	2.93 ± 0.82	37.25 ± 5.83
	n = 20	n = 20	n = 20	n = 20
	18.57	22.53	28.04	15.64
50	36.05 ± 6.42	55.53 ± 7.61	2.95 ± 0.93	40.27 ± 6.16
	n = 20	n = 20	n = 20	n = 20
	18.13	13.70	31.55	15.29
100	27.31 ± 3.71	52.51 ± 12.95	2.38 ± 0.47	40.82 ± 3.09
	n = 20	n = 20	n = 18	n = 19
	13.58	24.67	19.73	7.56
200	27.92 ± 4.36	53.13 ± 11.58	2.09 ± 0.65	39.63 ± 5.99
	n = 20	n = 20	n = 19	n = 20
	15.62	21.80	31.04	15.10
XFM				
	35.47 ± 4.22	60.56 ± 6.85	No data	37.95 ± 4.16
	n = 29	n = 29		n = 29
	11.90	11.30		10.95

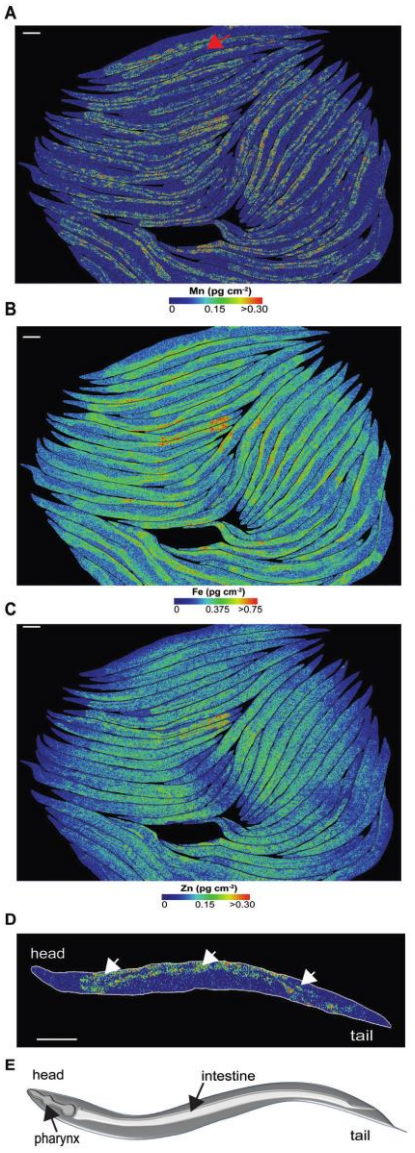

Fig. 2 X-ray fluorescence micrographs of adult *C. elegans*. (A) Distribution and quantification (see color scale bars) of Mn in wild type, hermaphrodite, *C. elegans* with the red arrow indicating individual enlarged for D. (B, C) Iron and Zn distribution and quantification. (D) Enlarged representative map of Mn, showing enriched distribution within the intestinal cells, that surround the intestinal lumen. (E) Simplified schematic indicating major anatomical features of an adult hermaphrodite *C. elegans* (scale bar = 100 μm).

Mn, Fe and Zn determined *via* ICP-MS were within 86.7 to 108.3% of those determined using XFM. However, significant disparity was observed for Mn in assays of 100 and 200 individuals per ICP-MS measure (27.31 ± 3.71 and 27.92 ± 4.36 pg per individual, respectively) that were lower than that for XFM (35.47 ± 4.22 pg per individual, $p < 0.001$). Previous comparison between XFM and inductively couple plasma-optical emission spectrometry (ICP-OES) showed variation of up to 11% in highly uniform, reference materials.[26]

However, a direct comparison of XFM and laser ablation-ICPMS analysis of brain tissue, a complex biological matrix, showed a range of 70.8 to 164% variation for Fe, Cu and Zn content.[27] Despite *C. elegans* also being a complex biological matrix, our methods provided good agreement between these different quantitative techniques.

The low abundance of Cu in *C. elegans* determined by ICP-MS could not be compared to XFM as a quantitative map for Cu distribution was not obtained within the available scan times. A measurement scheme with improved sensitivity, for example, achieved by increasing the dwell time, may be required to quantify the trace amounts of Cu fluorescence. Spatial distribution of Cu in *C. elegans* has been previously reported, but only following high Cu supplementation.[28]

Conclusions

In conclusion, the present work reports a comparison of biometals quantification using XFM and ICP-MS in order to determine minimum sample size necessary to accurately quantify these metals using ICP-MS as well as determining the variation between individuals within genetically identical and developmentally synchronous populations. To elucidate the role transition elements have in biology it is imperative to be able to accurately measure their abundance. Our method allows for the quantification of low abundance elements using the minimum sample size and can be adapted for the analysis of other trace elements. By comparing the values obtaining using ICP-MS with the most robust method available to quantify metals at the individual level, XFM, we have demonstrated that our method is a suitable alternative to XFM, when spatial resolution is not required. This method can be adapted to other small model organisms to understand the essential role metals have in biology.

Acknowledgements

We gratefully acknowledge support from the Australian Research Council (DP130100357 and LP140100095) and the Victorian Government's Operational Infrastructure Support Program. We also thank Barbara Cardoso, Irene Volitakis, Neuroproteomics facility (Florey Institute) and the Australian Synchrotron for technical assistance. Part of this research was undertaken on the XFM beamline at the Australian Synchrotron (XFM9373). The nematode strain used in this study was

provided by the CGC, which is funded by NIH Office of Research Infrastructure Programs (P40 OD010440).

Notes and references

1 S. J. Lippard, *Nat. Chem. Biol.*, 2006, **2**, 504–507.
2 N. Cedergreen, *PLoS One*, 2014, **9**, e96580.
3 K. J. Barnham and A. I. Bush, *Chem. Soc. Rev.*, 2014, **43**, 6727–6749.
4 J.-Y. Roh, S. J. Sim, J. Yi, K. Park, K. H. Chung, D.-Y. Ryu and J. Choi, *Environ. Sci. Technol.*, 2009, **43**, 3933–3940.
5 H. Ma, P. M. Bertsch, T. C. Glenn, N. J. Kabengi and P. L. Williams, *Environ. Toxicol. Chem.*, 2009, **28**, 1324–1330.
6 H. Wang, R. L. Wick and B. Xing, *Environ. Pollut.*, 2009, **157**, 1171–1177.
7 D. Barsyte, D. A. Lovejoy and G. J. Lithgow, *FASEB J.*, 2001, **15**, 627–634.
8 A. N. Minniti, D. L. Rebolledo, P. M. Grez, R. Fadic, R. Aldunate, I. Volitakis, R. A. Cherny, C. Opazo, C. Masters and A. I. Bush, *Mol. Neurodegener.*, 2009, **4**, 2.
9 B. Crone, M. Aschner, T. Schwerdtle, U. Karst and J. Bornhorst, *Metallomics*, 2015, **7**, 1189–1195.
10 R. McRae, P. Bagchi, S. Sumalekshmy and C. J. Fahrni, *Chem. Rev.*, 2009, **109**, 4780–4827.
11 S. J. Stohs and D. Bagchi, *Free Radicals Biol. Med.*, 1995, **18**, 321–336.
12 A. Lothian, D. J. Hare, R. Grimm, T. M. Ryan, C. L. Masters and B. R. Roberts, *Front. Aging Neurosci.*, 2013, **5**, 35.
13 D. J. Hare, E. J. New, M. D. de Jonge and G. McColl, *Chem. Soc. Rev.*, 2015, **44**, 5941–5958.
14 G. McColl, D. W. Killilea, A. E. Hubbard, M. C. Vantipalli, S. Melov and G. J. Lithgow, *J. Biol. Chem.*, 2008, **283**, 350–357.
15 I. M. Klang, B. Schilling, D. J. Sorensen, A. K. Sahu, P. Kapahi, J. K. Andersen, P. Swoboda, D. W. Killilea, B. W. Gibson and G. J. Lithgow, *Aging*, 2014, **6**, 975–991.
16 Y.-T. Lin, H. Hoang, S. I. Hsieh, N. Rangel, A. L. Foster, J. N. Sampayo, G. J. Lithgow and C. Srinivasan, *Free Radicals Biol. Med.*, 2006, **40**, 1185–1193.
17 S. Brenner, *Genetics*, 1974, **77**, 71–94.
18 D. Paterson, M. D. de Jonge, D. L. Howard, W. Lewis, J. McKinlay, A. Starritt, M. Kusel, C. G. Ryan, R. Kirkham, G. Moorhead and D. P. Siddons, *AIP Conf. Proc.*, 2011, **1365**, 219–222.
19 P. W. J. M. Boumans, R. J. McKenna and M. Bosveld, *Spectrochim. Acta, Part B*, 1981, **36**, 1031–1058.
20 F. R. Hampel, E. M. Ronchetti, P. J. Rousseeuw and W. A. Stahel, *Robust Statistics: the Approach Based on Influence Functions*, John Wiley and Sons, New York, 1986.
21 D. J. Hare, M. W. M. Jones, V. C. Wimmer, N. L. Jenkins, M. D. de Jonge, A. I. Bush and G. McColl, *Metallomics*, 2016, DOI: 10.1039/C5MT00288E.
22 S. A. James, B. R. Roberts, D. J. Hare, M. D. de Jonge, I. E. Birchall, N. L. Jenkins, R. A. Cherny, A. I. Bush and G. McColl, *Chem. Sci.*, 2015, **6**, 2952–2962.
23 S. A. James, M. D. de Jonge, D. L. Howard, A. I. Bush, D. Paterson and G. McColl, *Metallomics*, 2013, **5**, 627.
24 R. Thomas, *Practical guide to ICP-MS: a tutorial for beginners*, CRC press, 2nd edn, 2013.
25 Z. Sávoly, P. Nagy, K. Havancsák and G. Záray, *Microchem. J.*, 2012, **105**, 83–87.
26 S. A. James, D. E. Myers, M. D. de Jonge, S. Vogt, C. G. Ryan, B. A. Sexton, P. Hoobin, D. Paterson, D. L. Howard, S. C. Mayo, M. Altissimo, G. F. Moorhead and S. W. Wilkins, *Anal. Bioanal. Chem.*, 2011, **401**, 853–864.
27 K. M. Davies, D. J. Hare, S. Bohic, S. A. James, J. L. Billings, D. I. Finkelstein, P. A. Doble and K. L. Double, *Anal. Chem.*, 2015, **87**, 6639–6645.
28 B. P. Jackson, P. L. Williams, A. Lanzirotti and P. M. Bertsch, *Environ. Sci. Technol.*, 2005, **39**, 5.

Chapter 4 – Investigating the role of copper in long-lived mutants

4.1 Introduction

Copper is an essential cofactor in an extensive range of biological processes largely due to its ability to primarily exist in two oxidation states. This unique biochemical property of Cu has established it as an essential nutrient for all aerobic, as well as many anaerobic organisms (reviewed in Chapter 1). It is the same characteristics of Cu that can potentially have toxic effects to cells when regulatory mechanisms are not properly maintained. Despite how much is known about the biochemical properties of Cu and its cellular trafficking, the subcellular mechanisms by which Cu dyshomeostasis can lead to pathologies of ageing remain largely unknown. Resolving the genetic and molecular mechanisms capable of modulating Cu metabolism can influence ageing may facilitate translation of such mechanisms to targeted interventions for both normal and pathological features of ageing.

Single gene mutations that cause a loss of function of *daf-2* are a well-established model of delayed ageing in *C. elegans* (101) (Figure 4.1). When *daf-2* activity is lost insulin/insulin-like ligands are unable to bind to insulin receptors on the cell-surface thus preventing a cascade of phosphorylation events causing the transcription factor, DAF-16, to remain active in the nucleus resulting in delayed ageing (234). A large number of genes are regulated downstream of the insulin signalling pathway by *daf-16* (235) and since the discovery of *daf-2* mutants, great effort has gone into identifying gene activities that can modulate lifespan.

Investigation into the role of *cua-1* in *daf-2* longevity was prompted by its identification from a genome wide screen of *daf-2* gene activities necessary to confer longevity. Sequence alignment of *cua-1* with mammalian ATP7A and ATP7B (Figure 1.4) shows slightly more similarity to ATP7B (59% coverage compared to 43% coverage for ATP7A) indicating *cua-1* may primarily function to supply Cu to cuproproteins as well as efflux excess Cu (211). Suppression of the single Cu ATPase encoding gene in the *Drosophilia melanogaster* genome, *DmATP7*, resulted in an approximate4-fold increase in total Cu was observed (236). Copper efflux activity by *cua-1* was demonstrated in yeast as *cua-1* could rescue a yeast strain lacking the *ccc2* gene, the yeast

ortholog of *cua-1* (216). From this, a possible mechanism by which *cua-1* activity could influence the rate of ageing in *daf-2* is through a unique regulation of intracellular Cu efflux.

Copper can act as an insulin mimetic and stimulate components of the insulin-signalling pathway (88-90). Mammalian cells exposed to Cu(II) salts (3-100 μM) activated the family of phosphoinositide 3'-kinases (PI3K) (87, 237, 238) stimulating the insulin/IGF-1 signalling (IIS) pathway resulting in the phosphorylation and subsequent inactivation and nuclear exclusion of the FoxO transcription factor. This effect was mimicked in *C. elegans* as Cu exposure activated the PI3K ortholog, *age-1*, and similarly resulted in the nuclear exclusion of *daf-16*, the ortholog of the FoxO transcription factor (87). However, as this assay was done in a wild type background the sensitivity of IIS mutants to Cu exposure, and any potential subsequent effects on lifespan, may be different. Furthermore, populations were exposed to high concentrations of Cu(II) salts (0.1 and 1 mM) that are not typically representative of physiological conditions for short period of time (24 hr) and only young adults (< 2 days of age at 20 °C) showed consistent nuclear exclusion. The potential effects of changes in Cu within insulin signalling mutants should be investigated by implementing long-term exposure to concentrations of Cu closer to physiological levels. This could help to identify the underlying mechanisms downstream of *daf-16*, by which Cu dyshomeostasis effects longevity in these mutants.

Given what is known about Cu's relationship with the IIS pathway, *daf-2* mutant longevity is hypothesised to be due to its unique ability to metabolise Cu via *cua-1* activity. In efforts to resolve the underlying mechanisms of *cua-1*'s role in *daf-2* longevity it is imperative to understand how *cua-1* activity affects Cu levels in *daf-2* mutants. Follow-up from the genome-wide RNAi screen that identified the requirement of *cua-1* activity to confer *daf-2* longevity (103) is necessary to determine how *cua-1* activity is capable of regulating *daf-2* longevity. A great deal is known about the structure and function of Cu- ATPases in other organisms (yeast, flies, mice and mammals) however the function of *cua-1* in Cu metabolism within *C. elegans* is still largely unresolved.

4.2 Results and Discussion

4.2.1 Effects of daf-2 activity on lifespan

Under standard culturing conditions the median lifespans for wild type and *daf-2*(*e1370*) mutant populations are 39 days and 11 days, respectively (Figure 4.1).

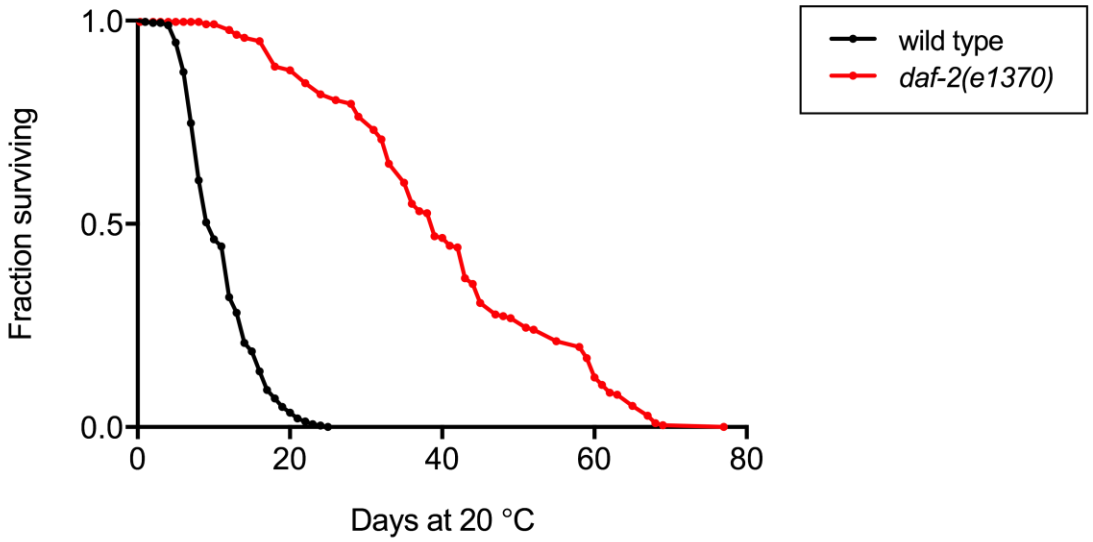

Figure 4.1 Lifespan analysis of *daf-2*(*e1370*) mutants

A single gene mutation, resulting in the loss of function of the *C. elegans* ortholog of the mammalian insulin/insulin-like receptor, *daf-2*, significantly increases lifespan (39 day median lifespan) compared to wild type (11 day median lifespan); log-rank test, $p < 0.0001$; n (wild type) = 360, n (*daf-2*(*e1370*)) = 360, pooled data from 3 independent experiments.

The *C. elegans* genome contains 37 insulin like ligands, most of which are expressed in neurons but are also found in the intestine, muscle, epidermis and germ-line (239). As the only member of the insulin receptor family in the *C. elegans* genome, *daf-2* displays 35% sequence homology to the human insulin receptor, 34% to the human insulin-like growth factor-I (IGF-1) and 33% to the human insulin receptor-related receptor (240-242). The insulin receptor is a member of the receptor tyrosine kinase family. The activity of the conserved tyrosine kinase region of the receptor is essential for insulin signalling transduction (243, 244) and is the region containing the *daf-2*(*e1370*) mutation that substitutes a proline for serine residue (P1465S) and results in

the greatest increase in lifespan from a single gene mutation compared to other mutant *daf-2* alleles (71).

Reduced insulin signalling in *daf-2* mutants is believed to protect against ageing by up regulating stress resistance mechanisms including those protecting against oxidative stress. From these observations the correlation between superoxide dismutase expression (a family of key antioxidant enzymes) and lifespan has been extensively investigated. *C. elegans* have five SODs, two cytosolic Cu, Zn-SODs encoded by *sod-1* and *sod-5*, one extracellular Cu, Zn-SOD encoded by *sod-4* and two mitochondrial Mn, Fe-SODs encoded by *sod-2* and *sod-3*. Deletion of *sod-5*, did not impact *daf-2* mutant lifespan whereas deletion of *sod-1*, of which nearly 80 % of total SOD activity comes from, and *sod-4* caused a significant decrease (196). Interestingly, overexpression of *sod-1* only slightly increased lifespan suggesting the role of *sod* activity in modulating longevity through antioxidant activity may only be a small component of their longevity assurance.

Aside from changes in expression levels of antioxidant genes under conditions of stress, biometal homeostasis of *daf-2* mutants as a possible mechanism of longevity is largely unexplored. The loss of Fe homeostasis has been previously reported in ageing *daf*-2 mutants with a trend of total Fe accumulation with age observed in both wild type and *daf-2* mutant populations (95). At all time-points measured however, Fe accumulation was much greater in wild types than age-matched *daf-2* cohorts. This finding suggests that the assurance of *daf-2* longevity may be due to its ability to delay or suppress the accumulation of redox-producing metals such as Fe or Cu. Quantification of Cu in *daf-2* mutants throughout lifespan hasn't been previously reported.

4.2.2 Total copper levels throughout daf-2 mutant lifespan

The accumulation of Cu in *daf-2* mutants at multiple time points during lifespan was measured using ICP-MS. Total Cu levels increased throughout lifespan in both wild type and *daf-2* (Figure 4.2, Table A4.1).

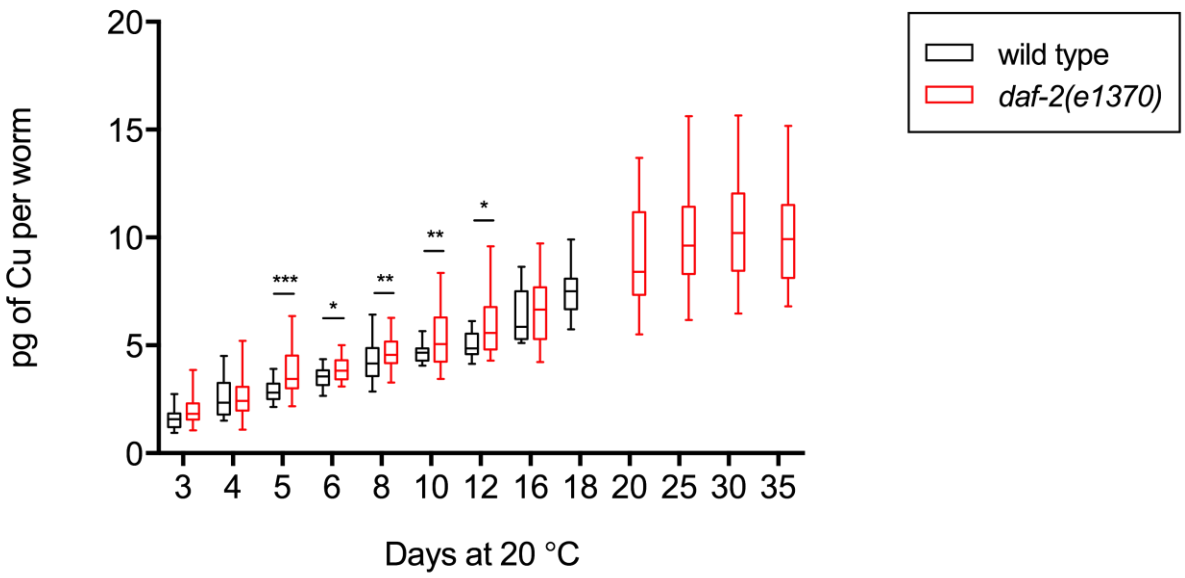

Figure 4.2 Quantification of total Cu in individual wild type and *daf-2* mutant *C. elegans* by ICP-MS at intervals across lifespan

An increase in total Cu is observed for wild type and *daf-2* throughout lifespan. Copper levels in *daf-2* mutants were significantly higher in 5, 6, 8, 10 and 12-day old age matched individuals compared wild type. Two-tailed unpaired Student's t-test; * $p < 0.05$, ** $p < 0.01$ and *** $p < 0.001$; mean ± SD; *n* individuals per measurement per genotype = 25; *n* replicate measurements per time-point per genotype = 10.

Significantly higher levels of Cu were observed in *daf-2* individuals compared to wild types for most of the time points across wild type lifespan. At 5, 6, 8, 10 and 12 days of age *daf-2* had higher levels of total Cu than wild type ($p < 0.01$). Although the strains were aged-matched at the time of collection, *daf-2* age slower, becoming gravid 2-3 days after wild type and *daf-2* mutants experience protracted reproduction periods (98) and were observed to be reproductive days and even weeks longer than wild type when maintained at 20 °C. These developmental differences could explain the difference in total Cu levels between the genotypes as some Cu-binding proteins, including Cu-ATPases, have different expression levels according to developmental stage, reproductive and hormone activity in other eukaryotes (209). Specifically, at 5 days of age, under standard culturing conditions wild type are typically at the peak of their reproductive maturity while *daf-2* are just beginning to become gravid, egg-laying adults. At 12 days of age wild type were no longer gravid while some *daf-2* populations were fertile for several more days. Furthermore, differences in total Cu between wild type and

daf-2 mutants especially during reproduction may be due to increased lipogenesis in *daf-2* mutants. Increased fat storage via unresolved regulatory mechanisms by *daf-16* can occur in *daf-2* mutants (245). Reduced brood size could also be a contributing factor to elevated Cu levels in *daf-2* longevity as resources necessary for progeny production are no longer available for cellular maintenance and repair. Interestingly, the ablation of the entire gonad and germ cells in wild type did not have an effect on their lifespan (101) whereas ablation of one of the germ line precursor cells increased lifespan in both wild type and *daf-2* mutant background (246) suggesting that signalling from the germ line is capable of shortening life span. Reduced fecundity and thus reduced allocation of resources for reproduction, could also be contributing to the reduced fat metabolism of *daf-2* mutants (239, 247). Along with lifespan, IGF1 activity can determine mammalian body size (248, 249). Isocitrate lyase and malate synthase, two phosphatases of the glyoxylate pathway which drives anabolic metabolism at the expense of fat are reduced in *daf-2* mutants relative to wild type (250). Increased fat storage could account for the higher levels of total Cu observed during these time points.

Accumulation of Fe, Zn and Mn was observed in ageing cohorts of *daf-2* mutants (Figures A1, A2 & A3). However, unlike Cu, *daf-2* mutants accumulated drastically lower levels of Fe compared to wild type across all time points measured which is in agreement to previously reported measurements of Fe (95). Similarly, *daf-2* exhibited significantly lower levels of Zn and Mn. All together *daf-2* may require elevated levels of Cu, compared to wild type, from adulthood throughout lifespan to facilitate delayed ageing. How these levels of Cu are achieved and what processes require Cu or are modulated by Cu are unknown.

4.2.3 Effects of exogenous sublethal copper exposure on daf-2 mutant lifespan

A unique scenario of Cu metabolism facilitated by *cua-1* activity is believed to regulate *daf-2* mutant longevity. D*af-2* mutants were shown to have a higher resistance to short-term (24 hr) exogenous Cu(II) salts (1 – 8 mM) exposures (93). However, as this was an assay of acute toxicity using high concentrations (super -physiological levels) of Cu and exposure occurred via the liquid media. Therefore, to test if *daf-2* longevity is achieved through a unique capability of buffering or metabolising endogenous Cu *daf-2* mutant populations were exposed to a range of sublethal (greater than 50% of the population alive after 24 hr of exposure)

concentrations of Cu (II) salts and the chronic effects on lifespan were observed (Figure 4.3). At 3 days of age populations were transferred onto plates containing a range of Cu (II) concentrations (0 – 100 µM) through supplementation of Cu salts into the NGM. Median lifespan of *daf-2* mutants is significantly reduced when exposed to concentrations as low as 10 µM $CuCl_2$. Higher concentrations of Cu (50 – 100 µM) caused death events, including death events from bagging (eggs hatching inside the body of the female), very early on in *daf-2* mutants preventing completion of the assay. Wild type median survival was not affected until $CuCl_2$ concentrations reached 100 µM (Figure 4.3).

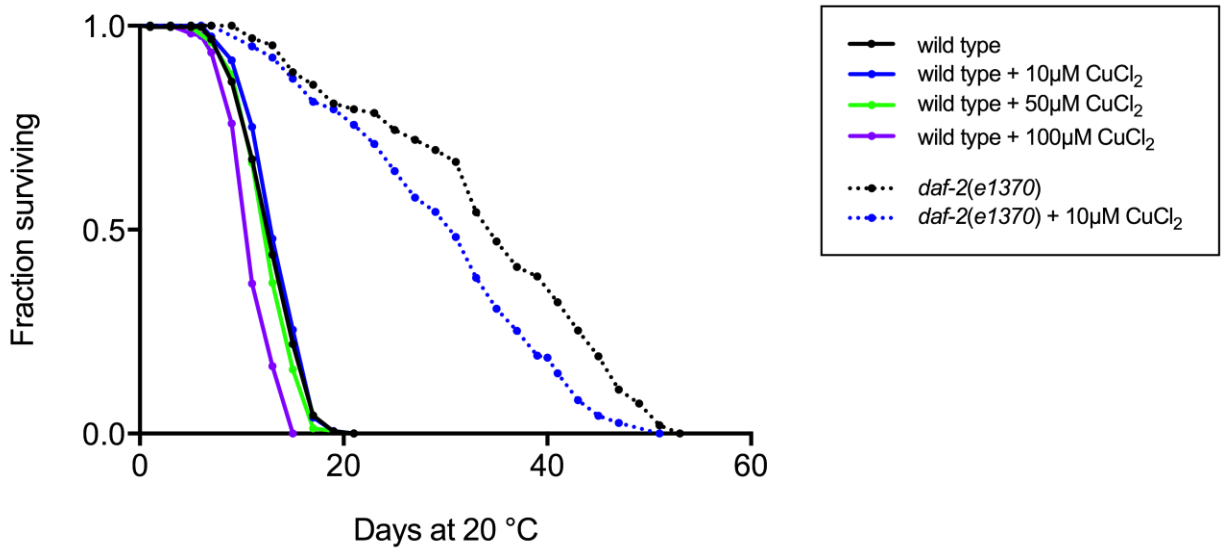

Figure 4.3 Lifespan analysis of exogenous Cu(II) salt exposure in wild type and *daf-2* mutants

Exogenous Cu exposure from adulthood (3 days of age) throughout lifespan decreases median lifespan of *daf-2* mutants at a lower concentration than wild type. Exposure of wild type populations to 10 and 50 µM $CuCl_2$ did not affect median lifespan compared to controls normal NGM (13 day median lifespan for all 3 cohorts). Wild type median lifespan was significantly decreased from exposure to 100 µM $CuCl_2$ (11 day median lifespan) ($p < 0.0001$). Exposure of *daf-2* mutants to 10 µM $CuCl_2$ significantly lowered median lifespan (32 day median lifespan) compared to controls (35 day median lifespan) ($p < 0.0001$). Data for *daf-2* exposed to 50 and 100 µM $CuCl_2$ not shown due to death events for majority of cohorts. Log-rank test, *n* (wild type) = 250 per treatment, *n* (*daf-2*(*e1370*)) = 250 per treatment, pooled data from 2 independent experiments.

The median lifespan of *daf-2* mutants is significantly shortened by long-term, low level Cu exposure (Figure 4.3). These observations could be due to a temporal effect that wild type lifespan is not long enough to experience or due to very specific homeostatic conditions

required by *daf-2* longevity that concentrations as low as 10 µM disrupt enough to modulate longevity.

In order to verify the observed effects on wild type and *daf-2* lifespan (Figure 4.3) were from excess Cu exposure and subsequent uptake, the Cu content of the NGM was measured by ICP-MS (Table 4.1). Supplementing NGM with Cu(II) salts increased mean total Cu content approximately five-fold (196.3 ng/g) compared to non-supplemented NGM (35.76 ng/g) (Table 4.1).

Table 4.1 Copper content of normal and Cu supplemented NGM. Data displayed as mean (SD)

Media	ng/g wet weight of Cu	COV (%)
NGM	35.76 (5.140)	14.37
NGM + 10 µM $CuCl_2$	196.3 (27.30) ****	13.92

**** Significantly different from control $p < 0.0001$
Student's t-test, $n = 10$ per media

Separate populations from those used to generate Figure 4.1 were used specially for metal analysis via ICP-MS (Table 4.2). Accurate analysis of elemental content requires the gut of individuals to be clear of food (251). Therefore, populations used for ICP-MS analysis were exhaustively washed to remove food from the gut and Cu-bound to the cuticle (as described in detail in Chapter 2) to ensure values from Table 4.2 are representing physiologically incorporated Cu. Supplementing NGM with Cu was successful in elevating Cu levels in both wild type and *daf-2* populations (Table 4.2). The bacterial lawn, on which *C. elegans* feed, was not supplemented with Cu. However, Cu may diffuse from the Cu-supplemented media into the lawn to facilitate Cu ingestion.

Table 4.2 Copper levels in first-day adult individuals following 24 hr of exposure to Cu(II) salts from supplemented NGM. Data displayed as mean (SD)

	pg of Cuper individual	COV (%)
wild type	5.07 (0.467)	9.21
wild type + 10 µM $CuCl_2$	33.9 (9.04) ****	26.6
daf-2	4.45 (1.10)	24.8
daf-2 + 10 µM $CuCl_2$	34.5 (7.57) ####	21.9

**** Significantly different from wild type $p < 0.0001$
Significantly different from *daf-2* $p < 0.0001$
Student's t-test, $n = 10$ replicates per treatment per genotype with $n = 25$ individuals per replicate

Excess intracellular Cu in eukaryotes cause ATP7A and ATP7B to translocate to vesicular compartments close to the plasma membrane where their primary role becomes excretion of excess Cu (211). In mammals transcriptional regulation of ATP7A and ATP7B is not well understood (252) with the majority of Cu homeostasis regulation occurring from post translational mechanisms (253). A study using *Sparus aurata*, found that exposure to excess Cu reduced ATP7A mRNA and increased ATP7B mRNA consistent with observed increased Cu excretion. Although previous studies reported a short-term tolerance to excess Cu exposure by *daf-2*, prolonged exposure appears to be detrimental to the longevity-modulating mechanisms indicating the requirement for elevated but still strictly regulated levels of Cu. The observed increased sensitivity of *daf-2* mutants to exogenous Cu could be due to changes in CUA-1 localisation in response to elevated Cu potentially altering its longevity-regulating functions in order to accommodate for the increased Cu.

4.2.4 Effect of decreased cua-1 activity via RNAi on daf-2 lifespan

Activity of *cua-1* was knocked down via RNAi through feeding in wild type and *daf-2* mutant populations (Figure 4.4) to verify the findings of the genome wide RNAi screen that identified *cua-1* activity was required for *daf-2* longevity (103). From the first day of adulthood populations were exposed to RNAi treatments and death events were scored over lifespan. Neither decreased *daf-16* or *cua-1* activity affected wild type median lifespan (11 days for all treatments). Loss of *cua-1* activity significantly reduced *daf-2* mutant median lifespan compared to controls (20 days and 39 days, respectively).

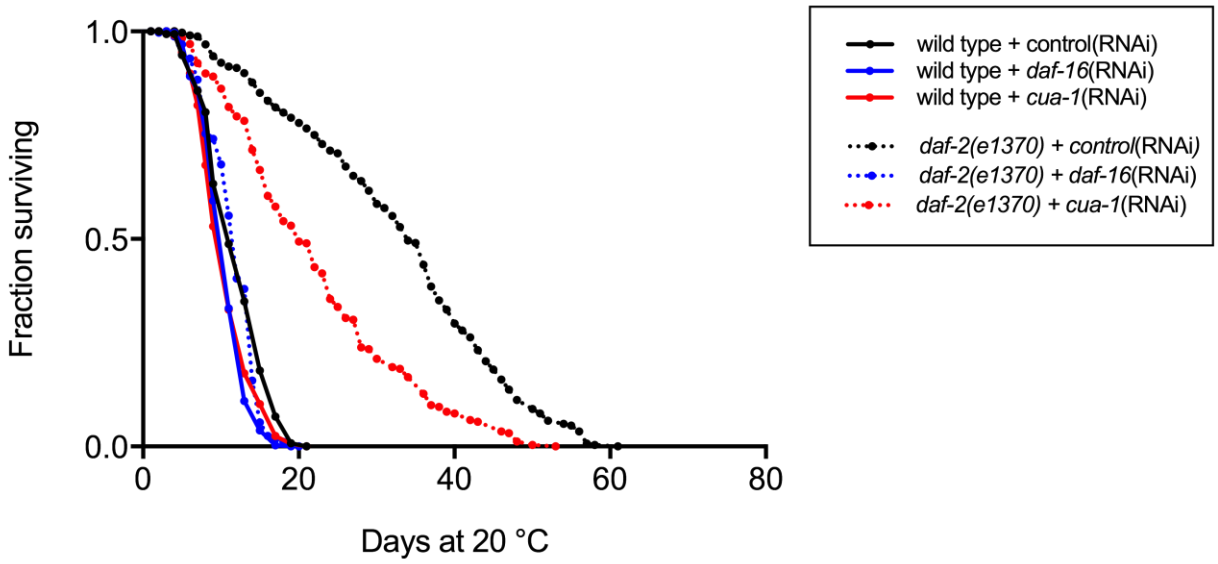

Figure 4.4 Lifespan analysis of wild type and *daf-2* mutants treated with *cua-1*(RNAi)

Wild type lifespan was not affected from decreased *daf-16* or *cua-1* activity (11 day median lifespan for all treatments). For *daf-2* mutants knockdown of *daf-16* and *cua-1* activity significantly reduced lifespan (12 and 20-day median lifespan, respectively) compared to controls (39 day median lifespan). Log-rank test, $p < 0.0001$, n (wild type) = 360 per treatment, n (*daf-2*(*e1370*)) = 360 per treatment, pooled data from 3 independent experiments.

Given that longevity of *daf-2* mutants requires the activity of *daf-16* (80) the method of gene silencing via RNAi through feeding was effective as evidence by the loss of longevity in *daf-2* + *daf-16*(RNAi) individuals (Figure 4.4). These results confirm that *cua-1* activity is necessary to confer *daf-2* mutant longevity. Furthermore, it is important to note that these results indicate *cua-1* activity is acting uniquely upon *daf-2* mutants' lifespan and not wild type. These data suggest that CUA-1 has a unique role in the delayed ageing phenotype of *daf-2* mutants, a role that is not observed in normal ageing. This activity of CUA-1 may be linked to the altered metabolism of *daf-2* mutants. Alternatively, the effects of CUA-1 may only be uncovered at extreme ages not typically reached by wild type.

4.2.5 Total copper levels in daf-2 mutant individuals treated with cua-1(RNAi)

Copper homeostasis within *C. elegans* was recently identified to be regulated by intestinal Cu trafficking by *cua-1* that is coordinated by extraintestinal Cu levels (217). Therefore, loss of *cua-1* in *daf-2* could cause an increase in total Cu that cannot be buffered potentially leading to

escalated production of ROS and subsequent damage negating longevity. Separate populations from those used in Figure 4.4 were used to analyse the elemental effects from loss of *cua-1* via ICP-MS analysis.

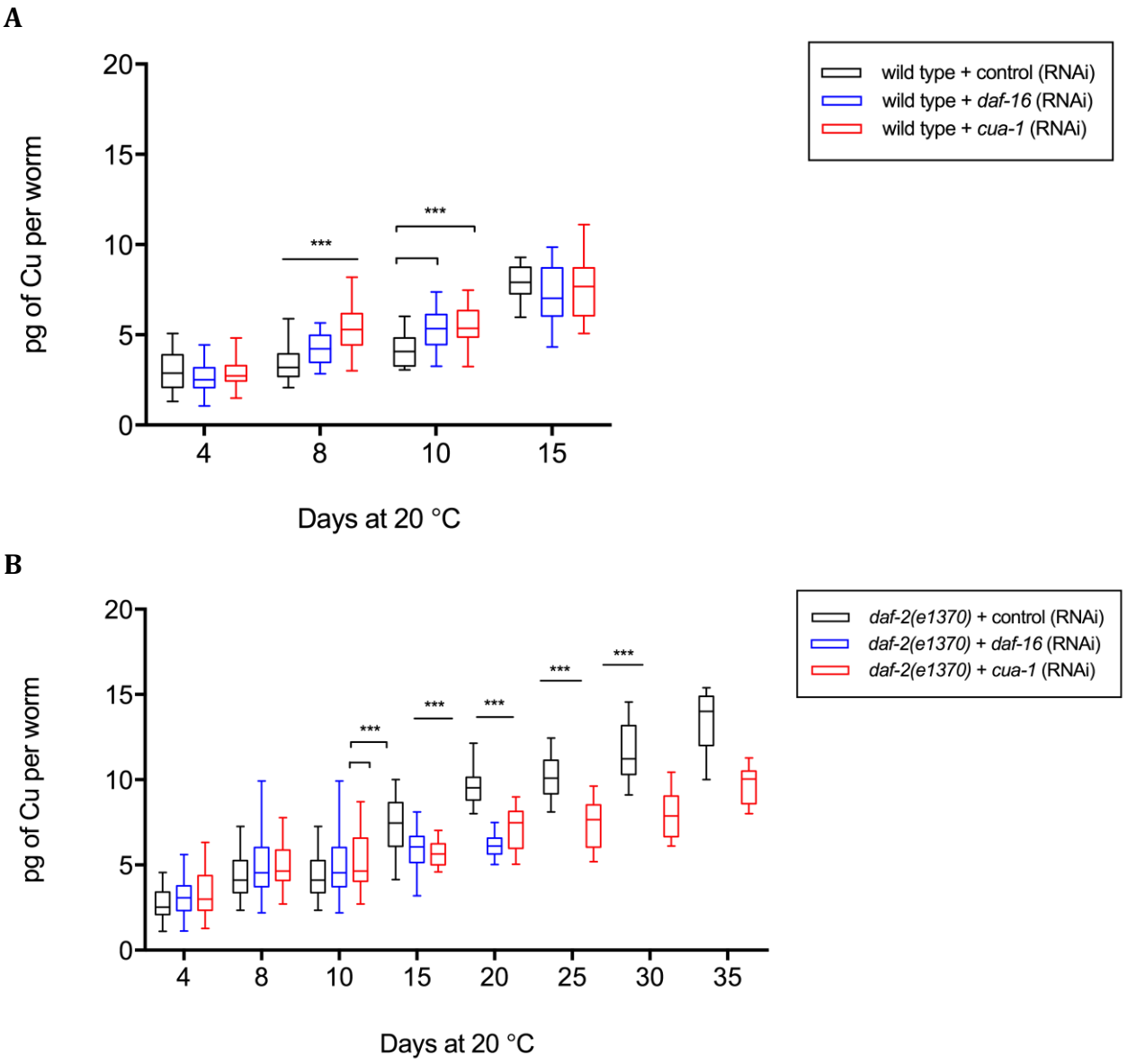

Figure 4.5. Comparison of total Cu levels in wild type and *daf-2* mutants following knockdown of *cua-1* activity via RNAi

A. 8 days of age knockdown of *daf-16* and *cua-1* significantly (*** $p < 0.001$) increased Cu levels in wild type cohorts compared to controls with wild type + *cua-1*(RNAi) individuals exhibiting the highest level of Cu. At 10 days of age Cu levels were significantly higher in wild type + *daf-16*(RNAi) and wild type + *cua-1*(RNAi) compared to controls (*** $p < 0.0001$). **B.** At 15 days of age Cu levels in *daf-2* controls were significantly higher than *daf-2* + *daf-16*(RNAi) and *daf-2* + *cua-1*(RNAi) cohorts (*** $p < 0.001$). Refer to Table A2 for exact values. One way ANOVA with Tukey's *post hoc* multiple comparisons test, *** $p < 0.001$, $n = 30$ replicates per treatment per time point with each replicate containing 25 individuals. Cohorts used for ICP-MS analysis are separate from those used for lifespan analysis in Figure 4.4.

Given the sequence similarity of CUA-1 with mammalian ATP7B (as described in further detail in Chapter 1) and increases in total Cu levels observed in wild type populations following *cua-1* knockdown (217) it is surprising that total Cu is significantly decreased in *daf-2* + *cua-1*(RNAi) individuals (Figure 4.5B, Table A4.2). Fluorescent Cu probes showed a drastic decrease in intestinal Cu following *cua-1* knockdown via RNAi in wild type backgrounds indicating CUA-1 is responsible for whole organism Cu homeostasis through intestinal trafficking (217).

Total Cu levels in the various food sources were measured via ICP-MS to help verify that the differences in individual's total Cu levels wasn't an effect of significant discrepancies between food sources with and without treatments (Table 4.3). Total Cu levels between food sources does not appear to be contributing significantly to the differences observed in total Cu between treatment groups.

Table 4.3. Total Cu levels in food sources. Data displayed as mean (SD)

Media	ng/mg wet weight of Cu
LB media	54.0 (1.23)
OP50	52.3 (2.38)
control (RNAi)	51.9 (2.39)
cua-1 (RNAi)	51.8 (2.13)

One-way ANOVA with Tukey's multiple comparisons *post hoc* test, n = 10 replicate measurements per treatment

4.2.6 Lifespan effects of copper supplementation on daf-2 mutants treated with cua-1(RNAi)

Since loss of *cua-1* activity in a *daf-2* mutant background decreases median lifespan (Figure 4.4) and Cu levels (Figure 4.5B, Table 3) then supplementing *daf-2* + *cua-1*(RNAi) populations with Cu was tested to see if it could rescue lifespan. Lifespan analysis of populations exposed to RNAi treatments and 10 µM Cu(II) salt supplementation was found to have no effect on wild type median lifespan. Median lifespan was significantly extended in *daf-2* + *cua-1*(RNAi) + 10 µM Cu(II) salt treated populations (27 days) compared to that of *daf-2* + *cua-1*(RNAi)

populations (20 days) although median lifespan was not completed restored to that of *daf-2* + control (RNAi) (37 days) populations (Table 4.4).

Table 4.4 Comparison of median lifespan following supplementation of exogenous Cu(II) to RNAi treated populations

Strain	Treatment (RNAi)	Supplemented 10 μM $CuCl_2$	Median survival (days)
wild type	control	-	11
	control	+	11
	daf-16	-	11
	daf-16	+	11
	cua-1	-	11
	cua-1	+	11
daf-2(*e1370*)	control	-	37
	control	+	33****
	daf-16	-	13
	daf-16	+	13
	cua-1	-	20
	cua-1	+	27$^{\#\#\#\#}$

**** Significantly different from *daf-2* control $p < 0.0001$

$^{\#\#\#\#}$ Significantly different from *daf-2* + *cua-1*(RNAi) $p < 0.0001$

Log-rank test, *n* (wild type) = 240 per treatment, *n* (*daf-2*(*e1370*)) = 240 per treatment, pooled data from 2 independent experiments

Loss of *cua-1* activity corresponding with a decrease in total Cu implicates a *cua-1*-mediated decrease in Cu within cells similar to Menkes disease models in which Cu-deficiency is observed due to defective ATP7A-driven transport. Loss of ATP7B function is often associated with increased total Cu levels, observed in Wilson's disease, due to the loss of cellular Cu excretion (254). Therefore, loss of *cua-1* activity could be modulating expression levels of Cu importers and/or Cu dependent enzymes.

4.2.7 Effects of decreased cua-1 activity on lifespan in additional long-lived mutant backgrounds

In order to further elucidate the role of *cua-1* activity in longevity we tested whether loss of *cua-1* activity would affect median lifespan in two other long-lived mutant *C. elegans* backgrounds, *eat-2* and *age-1*. One of the few conserved characteristics across taxa that is influenced by ageing is metabolic activity. In invertebrate and vertebrates dietary restriction

has been shown to be the most consistent way to extend lifespan (255). Increasing food supply decreases adult *C. elegans* lifespan (256). Mutations in *eat* genes cause partial starvation from disruption of the pharynx and lead to an increase of lifespan of up to 50% with *eat-2*(*ad1116*) displaying the greatest increase (99). Caloric restriction has some consistent, conserved effects including lowered circulated insulin and IGF-1 concentrations along with increased insulin sensitivity (257).

The other long-lived IIS pathway mutant, *age-1*, is located immediately downstream of *daf-2*. Like *daf-2* mutants, *age-1* mutants require the activity of *daf-16* to confer longevity (258, 259). Knocking-down *cua-1* in *age-1* mutants could give further insight into the mechanisms by which *cua-1* is acting on the IIS pathway to modulate lifespan. Populations were exposed to RNAi treatments and death events were scored following the same methods as in Figure 4.4.

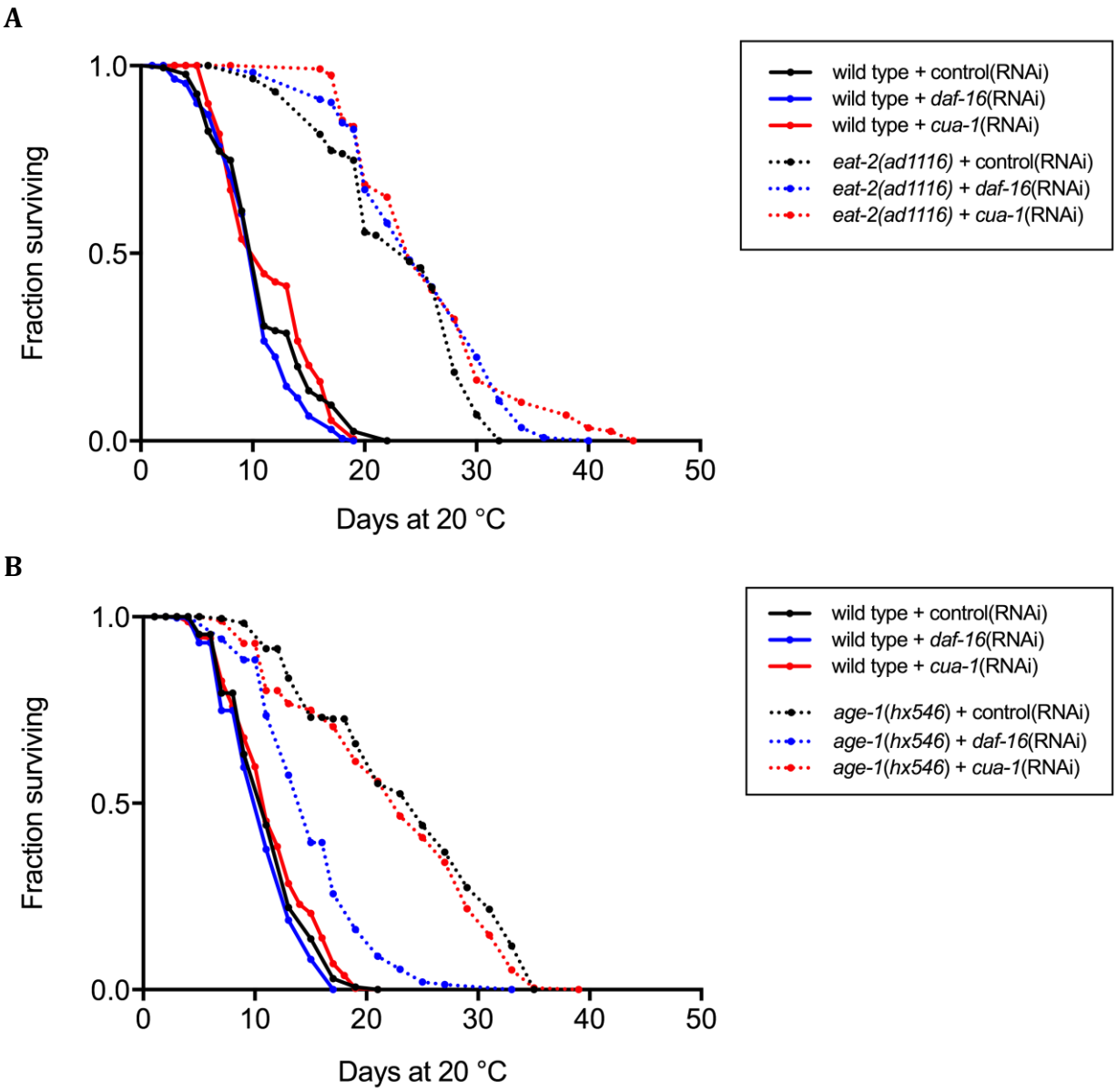

Figure 4.6 Lifespan analysis of decreased *cua-1* activity in long-lived mutant *C. elegans* backgrounds

(A) Median lifespan of wild type (11 days) and *eat-2* mutants (24 days) populations were the same across all treatments. (B) Median lifespan of wild type populations across all treatments was 11 days. Knockdown of *daf-16* significantly reduced median lifespan in *age-1* mutants (15 days) compared to *age-1* on control treatment (25 days). Knockdown of *cua-1* in *age-1* mutants did not affect median lifespan (23 days). Log-rank test, $p < 0.0001$, n (*eat-2*(*ad1116*)) = 400 replicates per treatment, n(*age-1*(*hx546*)) = 200 replicates per treatment, pooled data from 2 independent experiments.

Reduced pharyngeal function and feeding rate in *eat-2* mutants confers levels of caloric restriction by increasing lifespan up to 50% (99) (Figure 4.6A). Long-lived *eat-2* mutants do

not require the activity of *daf-16* or *cua-1* to confer longevity (Figure 4.6A). These results support previous studies showing *eat-2*; *daf-2* mutants live longer than either single mutant indicating the two pathways act distinctly to confer longevity (260). As expected knockdown of *daf-16* in an *age-1* mutant background significantly reduces median lifespan (15 days) compared to *age-1* mutants on control treatments (25 days) (Figure 4.6) while knocking-down *cua-1* activity does not significantly affect median lifespan (23 days). This suggests that *cua-1* mediated Cu-changes act downstream of *daf-2* but upstream of *age-1* to affect ageing. While Cu has been shown to act as an insulin mimetic in both mutant backgrounds, mRNA levels of Cu-binding proteins responded differently in the two mutants to elevated Cu exposure (93).

4.2.8 Effects of cua-1 activity on development

Under certain conditions *daf-2* mutants display constitutive formation of dauer larvae both of which are stress resistant and long-lived (261). Based on the finding that *cua-1*(RNAi) decreased lifespan of *daf-2*, the role of *cua-1* in *daf-2* dauer formation was investigated but found to have no effect on temperature-induced dauer formation (Table 4.5) (Chapter 2, section 2.6).

Table 4.5 Dauer formation assay following knockdown of *cua-1* via RNAi

Strain	Treatment (RNAi)	Dauers	Adults
wild type	control	0	355
	daf-16	0	316
	cua-1	0	332
daf-2(*e1370*)	control	306	0
	daf-16	0	297
	cua-1	319	0

The IIS pathway acts exclusively during adulthood throughout the reproductive period to influence lifespan (98) so it is not surprising that loss of *cua-1* activity well before adulthood does not affect dauer formation (Table 4.5). Taken together, since *cua-1* activity is necessary to confer *daf-2* longevity, these results support the hypothesis that the IIS pathways acts in separate regulatory mechanisms to regulate lifespan and dauer formation.

4.3 Chapter summary

This chapter has sought to investigate the role of *cua-1* in *daf-2* mutant longevity. Through knockdown by RNAi, *cua-1* activity was shown to be necessary for *daf-2* mutant longevity but had no effect on wild type lifespan. Therefore *cua-1* regulation of lifespan appears to be unique to daf-2 long-lived mutants. More specifically, *cua-1*'s activity is necessary for *daf-2* mutant longevity as loss of *cua-1* in two other long-lived mutant backgrounds: a non-IIS pathway mutant, *eat-2*, and another IIS pathway mutant, *age-1*, had no effect on lifespan in either mutant background. The effects of *cua-1* on longevity appear to act during adulthood as decreased *cua-1* activity did not effect dauer formation in *daf-2* mutants. Upon further analysis of Cu homeostasis in *daf-2* mutants total Cu concentrations throughout lifespan was found to be significantly elevated compared to wild type individuals. Decreased *cua-1* activity in *daf-2* mutants caused a decrease in total Cu levels from late adulthood onwards. Supplementing *daf-2* + *cua-1*(RNAi) cohorts with exogenous Cu partially rescued longevity phenotype. Taken together these observations suggest that a loss in Cu efflux, from knocking down of *cua-1*, could stimulate a decreased expression of the predicted Ctr-1 structures (Figure 1.3) resulting in decreased Cu uptake. When intestinal Cu uptake is decreased Cuproenzymes are not able to acquire their Cu cofactor(s) and thus *daf-2* mutant longevity is lost. By supplementing exogenous Cu to *daf-2* + cua-1(RNAi) cohorts expression levels of Cu-uptake proteins increase which then restores total Cu to basal levels and thus facilitating the nearly complete restoration of *daf-2* mutant longevity observed in Table 4.4. Further investigation into the effects of *cua-1* expression on the expression of Cu-uptake proteins is necessary to more comprehensively understand the mechanisms by which *cua-1* is modulating Cu metabolism in *daf-2* mutants. By determining how the supplemented exogenous Cu is being metabolised within the cell will help to further elucidate the specific mechanism(s) by which CUA-1 mediated Cu in *daf-2* regulates longevity.

Chapter 5 – Exploring the native, soluble, copper-binding profile of *daf-2* mutants to gain insight into mechanisms of longevity

5.1 Introduction

One third of all proteins encoded by the human genome require at least one metal ion for structural and functional purposes (262, 263). Despite the size of this 'metalloproteome', the precise mechanisms by which metal cofactor(s) participate in fundamental cellular processes and senescence remains unknown for many metal-binding proteins. Recent advances in atomic spectrometry have facilitated characterisation of metalloproteins into proteomics workflows, though it remains an analytical challenge to observe metalloproteins in their native, unadulterated state. Ensuring that relatively weak metal-protein intermolecular forces are preserved throughout sample preparation and until completion of metalloproteomic analysis is critical for understanding the functional roles metals cofactors play in biochemical processes.

Maintaining the native metal-protein interactions is not trivial. More traditional analytical approaches for measuring proteins require denaturing conditions and enzymatic digestion, both of which disturb metal-protein bonds. Impaired protein or enzymatic function as a direct result of a loss of metal binding therefore cannot be assessed using traditional proteomic approaches. Spurious results can also be obtained: once the metalloprotein is stripped of its native metal ion, a range of non-native metal species can be readily incorporated (264).

The metalloproteome of *daf-2* mutants has been largely unexplored. As presented in Chapter 4, *daf-2* metabolism of Cu may play a key role in the delayed ageing phenotype of this mutant organism. While quantitative whole-organism metal analysis can provide sensitive and accurate information about changes in total metal levels, additional analytical techniques are required to assess the molecular distribution of biometals. Size exclusion chromatography-inductively couple plasma-mass spectrometry (SEC-ICP-MS) provides complementary information regarding soluble Cu-binding proteins, measured using physiological conditions that preserve the weak ligands of metal-protein complexes.

Here, SEC-ICP-MS of soluble cuproproteins in near-physiological conditions was used to investigate which Cu-binding biomolecule(s) account for the observed changes in total Cu levels in *daf-2* mutants. In accordance with the overarching hypothesis that *daf-2* mutants confer longevity through altered Cu metabolism, it is crucial that the Cu-binding species involved in regulating Cu levels be identified.

5.2 Results and discussion

Size exclusion separates molecules on the basis of molecular size, which is subsequently used as a proxy for molecular mass. The mass range of the SEC-ICP-MS column (see Chapter 2, Section 2.9.2) was determined by on-line detection of heteroatoms in a mixed standard containing five biomolecules covering a mass range of 12-450 kDa (Figure A5.1(A and B)). The $\log_{10}$ of each molecular weight was plotted against retention volume, and linear regression analysis ($R^2 = 0.985$) was used to estimate molecular weights of identified Cu-binding proteins (Figure A5.1C).

5.2.1 Unique soluble copper metalloproteome of long-lived daf-2 mutants

SEC-ICP-MS was used to investigate the specific protein fraction that could be attributed to the trend of increased total Cu levels in *daf-2* mutants compared to wild type (see Chapter 4 Figure 4.2). Although it has relatively poor resolution, SEC uses biologically inert conditions (pH 7.5, ammonium nitrate buffer) to retain metals natively bound to proteins, which are detected on-line using an ICP-MS can be associated with a specific molecular mass (265). This technique was used to identify the potential differences in the Cu proteome of age-matched (7 day old) wild type and *daf-2* mutant populations (Figure 5.1).

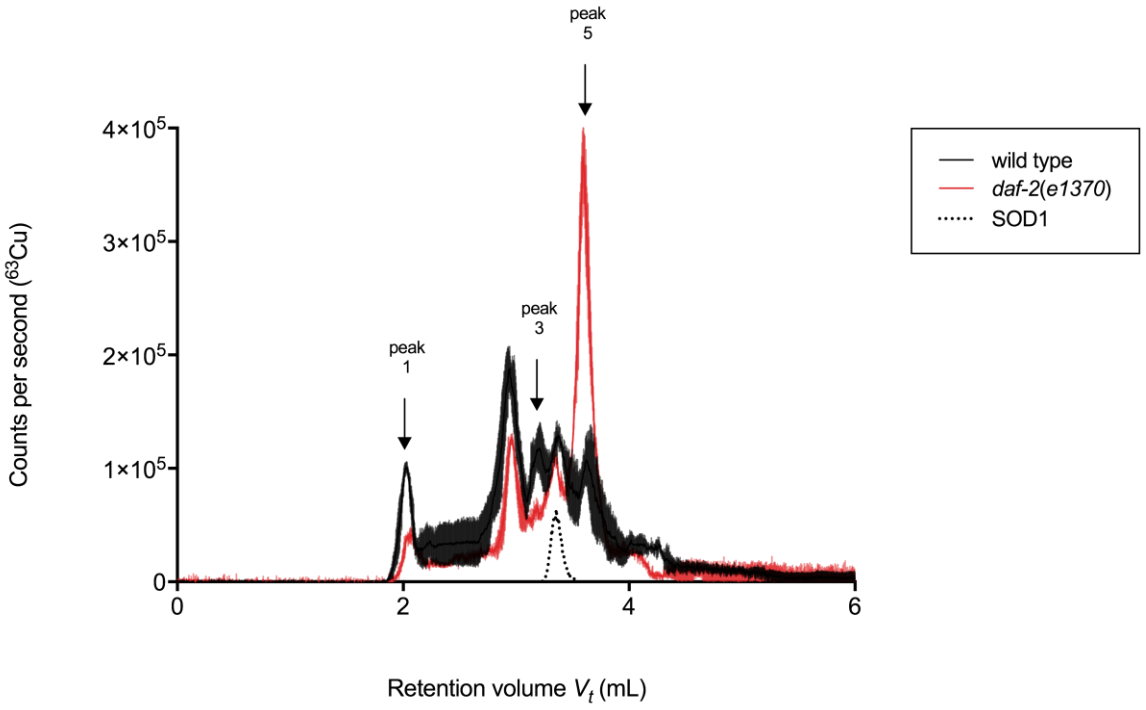

Figure 5.1 Copper proteome of adult *daf-2* mutants

SEC-ICP-MS chromatogram of Cu-63 signal shows varying levels of Cu associated to high, mid and low molecular weight soluble, Cu-binding molecules between 7-day old age-matched adult wild type and *daf-2* mutant populations. In wild type populations peaks 1-4 showed significantly elevated levels of Cu binding (p < 0.0001) compared to those of *daf-2* mutants. Inclusion of bovine Cu, Zn-SOD (SOD1) molecular weight standard (~MW = 32 kDa) shows peak 4 with a similar retention volume (V_t = 3.36 mL) and ~ MW of 44 kDa. Peak 5 (V_t = 3. 59 mL, ~MW = 22 kDa) displays significantly elevated levels of Cu-bound in *daf-2* mutant populations compared to wild type (p < 0.001); Student's t-test; traces represent the mean of 3 independent samples ± 95% confidence interval.

Several soluble Cu-binding biomolecules showed significant decreases in its levels in *daf-2* mutants compared to wild types (Figure 5.1, Figure A5.2). However, only one Cu-binding peak with a retention volume (V_t) of 3.59 mL and ~ molecular weight (MW) of 22 kDa shows a significant elevation of Cu in *daf-2* mutant populations (p < 0.001). Given that *C. elegans* MTLs are low molecular weight proteins (~6.5 – 8 kDa) have a cysteine content similar to mammalian metallothioneins (266, 267) and are therefore predicted to bind Cu with similar affinity to mammalian metallothioneins, we hypothesised the unknown peak with a V_t of 3.59 mL and ~MW of 22 kDa to be MTL.

Metallothioneins are saturated with metal ions following expression in ribosomes in accordance with the specific isoform or the ambient concentrations of available metals (268). The exact function of metallothionein remains unresolved despite over 50 years of research since first described in 1957 (269). Evidence continues to grow indicating metallothionein is a multifaceted protein due to its role in a number of physiological processes including metal ion homeostasis (189), heavy metal detoxification (though this is more likely an antecedent effect of high sulfur content) (270), protection against oxidative stress and chaperoning for protein folding (271, 272). The cysteine rich content of metallothionein and its high affinity for Cu support the theory that its primary function in mammals is sequestration of Cu and subsequent protection from oxidative stress. Free Cu rarely exists in the cytoplasm as cellular uptake involves high affinity transporters to prevent formation of ROS from labile Cu ions. For example, metallothionein readily binds Cu (II) ions to facilitate its storage and transport. Oxidative stress is known to induce metallothionein expression (273), with their thiol groups acting as reducing agents to protect against ROS-mediate damage (274). Therefore, metallothionein could be considered a candidate for lifespan regulation by mitigating age-related oxidative damage.

Most of the structural information gathered to date is from NMR spectroscopy, X-ray absorption or diffraction studies (275, 276) whereas information on metal coordination, ligand identification and oxidation states of residues is achieved *via* Raman or circular dichroism spectroscopy or emission studies (277-279) with the later providing useful information on the dynamic structural and thus functional nature of metallothionein.

5.2.2 Using metal-binding affinities to identify metallothioneins

Two distinct metallothionein peptides were first isolated in *C. elegans* (MTL-1 and MTL-2, approx. monomeric MW of 8 and 6.5 kDa, respectively) by upregulating *expression via* Cd exposure (280); a finding that was later confirmed from a genome-wide screen (281). Double MTL knockout mutants are viable, indicating MTLs are not essential for wild type survival or metal homeostasis (225). Under basal conditions MTL-1 expression levels were found to be elevated in young adult (3 days of age cultured at 20 °C) *daf-2* mutants compared to wild types (93) and suggested MTL expression is DAF-16-regulated. This same study found that exposure

to sub-lethal concentrations of Cu(II) salts in liquid medium did not have an effect on MTL expression in either background. However, older *daf-2* mutant adults exhibited increased expression of antioxidant Cu-binding proteins under physiological conditions (78, 81) suggesting age may influence basal expression levels.

The *in vitro* metal binding affinities of the two *C. elegans* MTL isoforms have been previously investigated using electrospray ionization mass spectrometry with MTL-1 showing a bias towards Zn(II) and MTL-2 biased towards Cd (II) binding (279). This same study found that in vitro exogenous Cu exposure to recombinant wild type MTL failed to yield Cu-thionein features characteristic of those observed in mammalian metallothionein. *In vivo* exposure to equimolar Cd and Zn revealed Cd-induced MTL-1 expression with a larger percentage of Cd associated to MTL-2 and MTL-1 biased towards Zn (II) binding (282). It has been suggested that previously reported structural information may have been obtained from less common forms of metallothionein due to the *ex vivo* modification during sample preparation; competition for binding sites exists between different metals as well as competition for metals with other metalloenzymes (282). Furthermore, metallothionein metal binding has been suggested to be transient given their ability to rapidly release bound metals (282-284). Like mammalian MT, MTL-1 and MTL-2 have a high cysteine content supporting the inference that both isoforms are likely to have a high affinity for Cu. However, to date, *in vivo* Cu-MTL interactions have only been investigated to show exogenous Cu exposure does not induce *mtl* mRNA levels.

Metallothionein dimerisation can occur through several different mechanisms including covalent cysteine bridges, sharing of ions in conditions of metal excess or as an artefact of the ionization process for mass spectrometry analysis (285). MT dimerization has been observed in mammalian models following Cd supplementation (286). If the observed peak with retention volume of 3.59 mL and ~MW of 22 kDa (Figure 5.1) is one of the two MTL isoforms it represents either a 6% MW error for the MTL-1 dimer or a 9% MW error for the MTL-2 dimer. Both calculated errors MWs were within the acceptable range of the 95% confidence interval of MW calibration curve.

These data provide support for our hypothesis that the unknown Cu-binding molecule with elevated metal levels in *daf-2* mutant populations (Figure 5.1) is MTL. Wild type populations were supplemented with low, sub-lethal concentrations of Cd and Zn salts (282) and subsequent SEC-ICP-MS analysis was used to exploit the binding affinity of both *C. elegans* MTLs for Cd (II) and Zn (II) (Figure 5.2). Metallothioneins are a unique cuproenzyme in their ability to bind Cd therefore MT can be distinguished from other possible low MW Cu-binding proteins via SEC-ICP-MS following Cd supplementation as most other Cu-binding proteins are not known to bind Cd with similar affinity. By identifying the unknown Cu-binding protein further advances in our understanding of the underlying mechanisms by which *daf-2* mutants metabolise Cu to regulate longevity can be made.

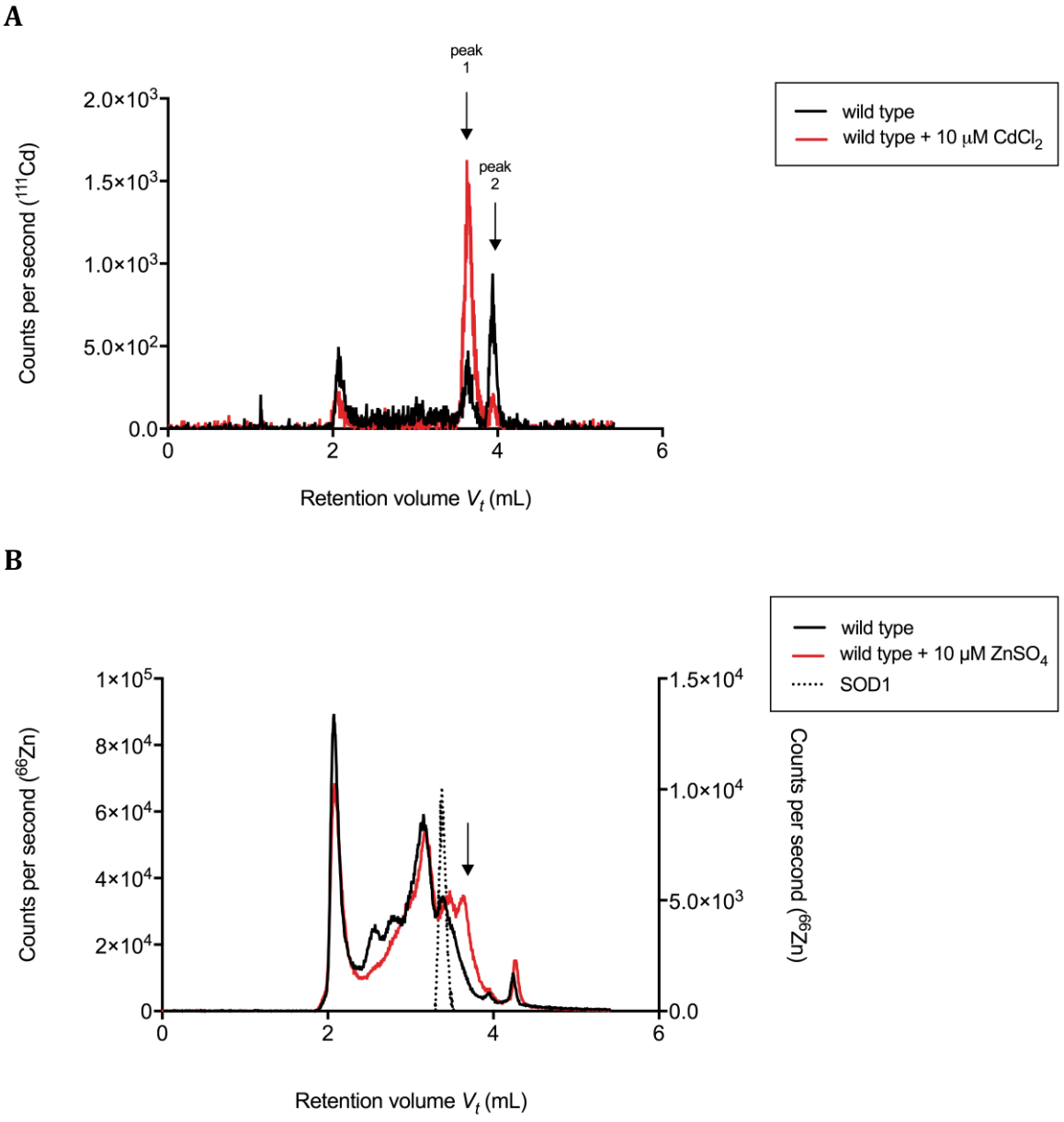

Figure 5.2 Effect of exogenous sub-toxic Cd and Zn salt exposure on soluble metalloproteome

Exogenous, sub-lethal supplementation of (A) 10 μM $CdCl_2$ and (B) $ZnSO_4$ in wild type populations. (A) A significant increase in Cd-binding in peak 1 (V_t = 3.63 mL; ~MW = 20 kDa) following Cd supplementation ($p < 0.0001$). Peak 2 (V_t = 3.94 mL; ~MW = 8 kDa) displays a significant decrease in Cd-binding following Cd supplementation ($p < 0.0001$) compared to controls. (B) Appearance of unique Zn-binding peak (denoted by black arrow) (V_t = 3.66 mL; ~ MW = 18 kDa) following Zn salt supplementation ($p < 0.0001$); student's t-test.

Supplementation of 10 μM Cd salt in NGM resulted in a significant increase in Cd-bound to a molecule (peak 1, Figure 5.2A) with a retention volume of 3.63 mL and ~MW of 20 kDa. Given

this biomolecule's affinity for Cd(II) and previous studies showing MTL-2's bias for Cd (II)-binding it is predicted to be an MTL-2 dimer (MW = 13 kDa). However, based off retention volume and approximate MW the peak is closer to that of a MTL-1 dimer (MW = 16 kDa). Displacement of naturally bound Zn ions to MT by Cd has been shown to occur following Cd (II) supplementation (287), a feature that is to the credit of the ability of MT to counter a range of potential cellular insults. Supplementation of NGM with 10 μM Zn salt yielded a unique peak at V_t = 3.66 and ~MW of 18 kDa that is not observed in control populations (Figure 5.2B). This peak is predicted to be the same MTL isoform as peak 1 in Figure 5.2A as it has a V_t that is < 1 % greater than that of peak 1 (Figure 5.2A). Additionally, the molecular weight of peak 1 (Figure 5.2B) is only 10% higher than that of peak 1 in Figure 5.2A. Given the similarities in V_t (3.63 mL and 3.66 mL) and MW (~20 kDa and ~18 kDa) in conjunction with Cd's ability to displace natively bound Zn-MTL-1 the unique peak from Figure 5.2B and peak 1 from Figure 5.2A are predicted to be MTL-1.

5.2.3 Investigating the soluble copper-binding profiles of multiple mutant backgrounds

The soluble Cu-binding profile of three viable *mtl* mutants *mtl-1*(*tm1770*), *mtl-2*(*gk125*) and *mtl-(tm1770)1*;*mtl-2*(*gk125;*) were analysed by SEC-ICP-MS in order to distinguish the MTL isoform seen by the unique peak seen at retention volume ~ 3.6 mL and ~MW of 20 kDa (Figure 5.1 and 5.2).

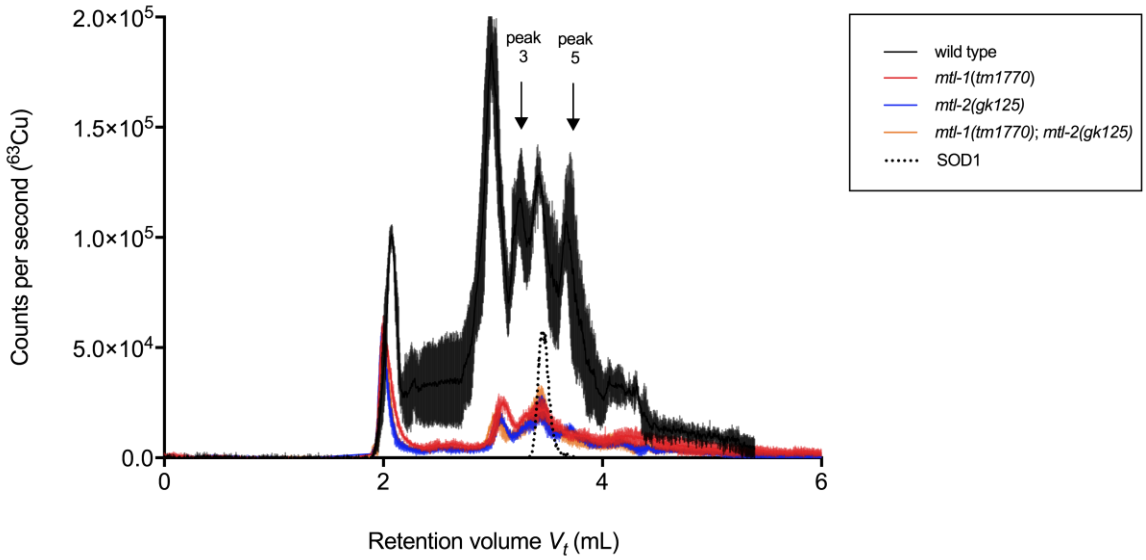

Figure 5.3 Effect of MTL deletion mutants on soluble Cu-binding proteome

SEC-ICP-MS chromatogram of soluble Cu-binding proteins of age-matched 5-day old MTL mutants. Decrease Cu levels observed across all soluble Cu-binding proteins for all three MTL mutants. Peaks 1 and 2 have significantly decreased Cu-bound for all MTL mutants compared to wild type ($p < 0.0001$). Obliteration of Cu-binding is observed for all mutants in peaks 3 and 5 (V_t = 3.502 mL; ~MW = 29 kDa and V_t = 3.67 mL; ~MW = 18 kDa, respectively); student's t-test; traces represent the mean of 3 independent samples with vertical lines showing the standard deviation.

Deletion of MTL-1, MTL-2 and the double deletion mutant resulted in significantly ($p < 0.0001$, $p < 0.01$ and $p < 0.05$, respectively) decreased levels of Cu across all observable soluble Cu-binding proteins (Figure 5.3) and total Cu levels (Table A5.1). Specifically Cu-binding to peak 3 (V_t = 3.502 mL; ~MW = 29 kDa) and peak 5 (V_t = 3.67 mL; ~MW = 18 kDa) were obliterated in all 3 *mtl* mutants. Peak 5 (Figure 5.3) has a 2.23 % greater retention volume and a 22% increase in the predicted molecular weight than those of the unique peak in Figure 5.1. Peak 5 has a < 1% increase in retention volume and the same approx. MW as the predicted MTL-1 peaks from Figure 5.2) As all *mtl* mutants resulted in the elimination of Cu-bound to peak 5 in Figure 5.3, a more definitive conclusion as to which MTL isoform is present in the unique peak can't be made from these results.

The requirement of *daf-16* activity for *daf-2* mutant longevity is well established (80) as is the ability of DAF-16 to regulate expression levels of genes whose activities is required for *daf-2*

longevity. Specifically a DNA microarray analysis of *daf-2* mutants found that *mtl-1* expression was upregulated and *mtl-2* expression down regulated by DAF-16 (288). Therefore, if the unknown peak in *daf-2* mutants displaying elevated Cu (Figure 5.1) predicted to be MTL is a requirement for *daf-2* longevity, we might expect to see an effect on Cu association to this peak upon decreased or lost *daf-16* activity. The soluble Cu-binding profile of the double loss-of-function *daf-2*; *daf-16* mutant was investigated using SEC-ICP-MS (Figure 5.4). We hypothesised that changes in the proposed MTL peak ($V_t \sim 3.60$ mL; ~MW 20 kDa) are unique to *daf-2* mutants and loss of *daf-16* activity should cause a decrease in Cu-bound as these double mutants display and overall decrease in total Cu content (Table A5.1).

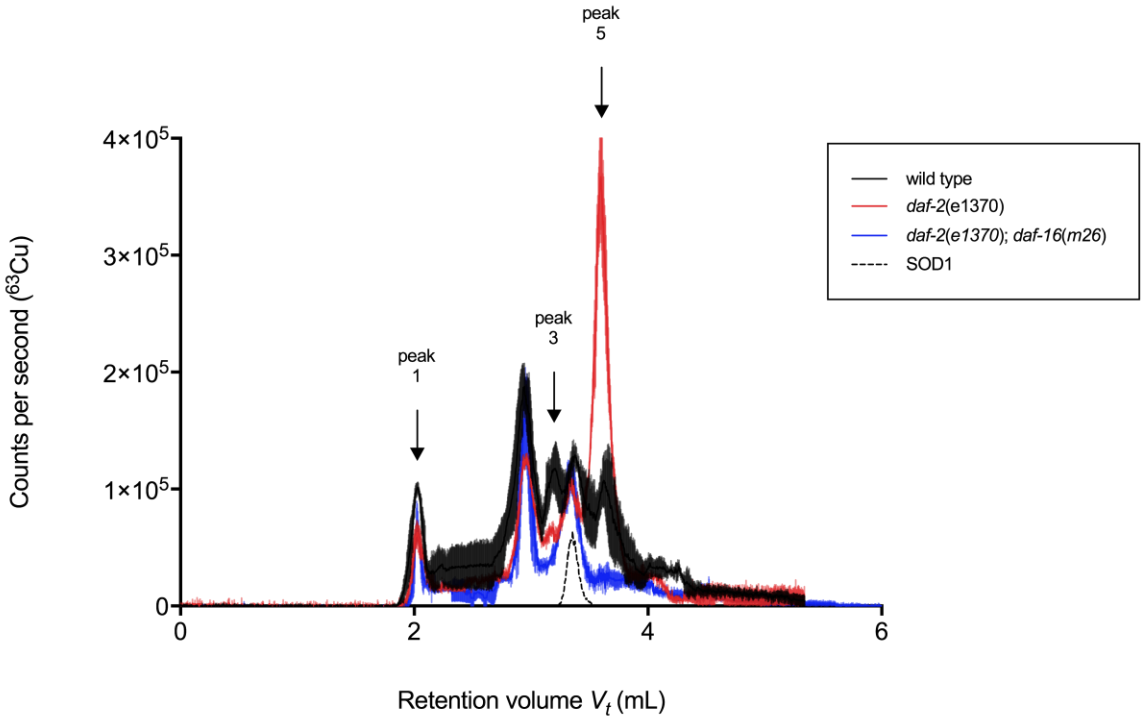

Figure 5.4 Effect of *daf-16* activity on the *daf-2* mutant soluble Cu-binding proteome

SEC-ICP-MS chromatogram shows varying levels of Cu-bound to mid and low molecular weight peaks between 7-day old age-matched adult wild type, *daf-2* and *daf-2*; *daf-16* mutant populations. Peak 1 has significantly higher Cu-bound in wild type populations compared to *daf-2* and *daf-2*; *daf-16* mutants ($p < 0.05$). Similarly, peak 2 has significantly higher Cu-bound in wild type compared to *daf-2* mutants ($p < 0.01$). Peak 3 (V_t = 3.23 mL; ~ MW = 66 kDa) and peak 5 (V_t = 3.61 mL; ~MW = 20 kDa) Cu-binding is obliterated in *daf-2*; *daf-16* mutants. Copper-bound to peak 3 is significantly decreased in *daf-2* mutants compared to wild type ($p < 0.0001$). Peak 5 has significantly elevate Cu-bound in *daf-2* mutants compared to wild type and *daf-2*; *daf-16* mutants ($p < 0.0001$); student's t-test; traces represent the mean of 3 independent samples with vertical lines showing the standard deviation.

Loss of *daf-16* in a *daf-2* mutant background resulted in an overall significant decrease in total Cu levels (Table A5.1) and obliterated Cu-bound to peak 5 (V_t = 3.61 mL; ~MW of 20 kDa). Taken with the findings of Murphy *et al*. (288) and data from Figures 5.1-5.3, these results suggest that peak 5 (Figure 5.4) is likely MTL-1.

5.2.4 Effects of cua-1 activity on the soluble Cu-binding profile of daf-2 mutants

Daf-2 mutants have shown to be dependent on *cua-1* activity to confer longevity ((103), Figure 4.4). Analysis of the soluble Cu-binding profile of *daf-2* mutants with knock-down of *cua-1*

activity was analysed using SEC-ICP-MS (Figure 5.5). We hypothesised that loss of *cua-1* activity in a *daf-2* background is modulating longevity through a mechanism of Cu metabolism involving MTL.

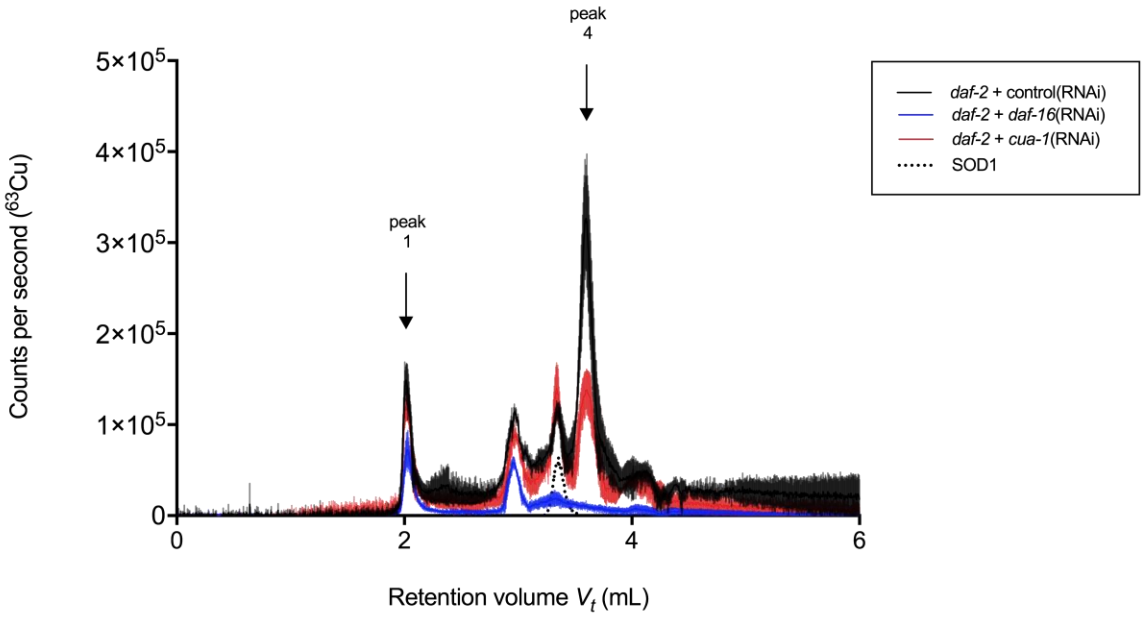

Figure 5.5 Changes in soluble Cu-binding proteome from decreased *cua-1* activity in *daf-2* mutants

SEC-ICP-MS chromatogram shows varying concentration of Cu in mid and low MW peaks in 7-day-old *daf-2* mutant populations following RNAi treatment. Decreased *daf-16* activity significantly decreased Cu levels ($p < 0.01$) in peak 1 (V_t = 2.02 mL) as did decreased *cua-1* activity ($p < 0.05$). Similarly, following knock-down of *daf-16* and *cua-1* activity, peak 2 (V_t = 2.96 mL) had significantly lower Cu levels ($p < 0.01$ and $p < 0.05$, respectively). Peak 3 that has a very similar retention volume (V_t = 3.34 mL) to the bovine Cu, Zn–SOD MW standard and has significantly increased Cu levels ($p < 0.05$) following knock-down of *cua-1* ($p < 0.05$) and while knock-down of *daf-16* activity significantly decreased Cu levels ($p < 0.0001$). Peak 4 (V_t = 3.59 mL; ~MW = 22 kDa) has significantly lower Cu in *daf-2* + *cua-1*(RNAi) compared to controls ($p < 0.001$). A low-abundance peak 5 (V_t = 4.04 mL; ~MW = 6 kDa) shows a significant loss of Cu-bound upon knock-down of *daf-16* activity via RNAi ($p < 0.0001$); student's t-test; traces represent the mean of 3 independent samples with vertical lines showing the standard deviation.

Copper-binding was obliterated in the predicted MTL-1 peak, peak 4, V_t = 3.59 mL, following *daf-2* + *daf-16*(RNAi) (Figure 5.5) as well as in the *daf-2*; *daf-16* mutant (Figure 5.3). Decreased *cua-1* activity resulted in a significant decrease ($p < 0.01$) in Cu-bound to the same peak

(Figure 5.5). The difference in retention volume from this peak and the obliterated Cu-binding peak in Figure 5.4 is < 1% and the predicted MW difference between the two peaks is 10% both within acceptable range to infer they are the same Cu-binding species. In conjunction with the results presented in chapter 4, decreased *cua-1* in *daf-2* mutants causes a whole-organism decrease in Cu that is manifesting most significantly as a loss of Cu-bound to MTL-1. These results suggest that the mechanism by which *cua-1* activity is functioning to modulate *daf-2* longevity is through Cu-storage by MTL-1.

5.3 Chapter summary

Data presented in this chapter in conjunction with evidence from the literature that builds upon data from the previous chapter support the hypothesis that metallothionein is involved in Cu metabolism in *daf-2* mutants. However, to definitively determine if the Cu-binding peak is metallothionein experiments such as high resolution mass spectrometry would need to be conducted to identify the molecule(s) that comprise the peak of interest. Positive identification of the peak as metallothionein would reveal a unique requirement of the protein as a Cu storage protein necessary for *daf-2* longevity.

Chapter 6 – Commentary and future directions

The following chapter serves to provide commentary regarding the significance of the results I have presented in the previous chapters of this thesis by putting them into the context of my understanding of the landscape of the importance of Cu homeostasis in ageing.

Ageing is a complex process defined as the accumulation of damage from the molecular level up to organ level is the increased vulnerability to disease and death. Mutations that extend lifespan can protect from these age-related vulnerabilities. Identification of mutations capable of extending lifespan were first identified using *C. elegans* and they have since continued to serve as an ideal organism for ageing studies. Specifically, long-lived insulin-like signalling *C. elegans* mutants exhibit increased resistance to oxidative stress (289, 290) and reduced oxidative damage (291, 292). A role for Cu in the generation of reactive oxygen species is well established (293), extensive investigation has gone into resolving its role in age-associated diseases (294-296). *C. elegans* is an ideal whole model organism for studying the relationship between Cu metabolism and ageing, in part, because many of the mammalian cellular Cu trafficking mechanisms are conserved in *C. elegans* (Figure 1.4). Resolving the underlying mechanisms by which insulin-like signalling mutants are capable of delaying ageing is of great interest. Given that resistance to oxidative stress and reduced oxidative damage is a key feature of such mutants, Cu homeostasis could provide key insight into how ageing is regulated.

Prior to the commencement of this thesis, using an RNAi library a genome wide screen found that *cua-1* activity was required for *daf-2*(*e1370*) longevity (103). The aim of this thesis was to further explore these observations to continue to understand the underlying subcellular mechanisms responsible for modulating *daf-2* longevity. This chapter will bring together and discuss the main results from this thesis and outline their significance in the context of the wider field of the potential role of Cu in regulating ageing.

6.1 Conclusions

The results published in Chapter 3 established the analytical methods that set the foundation for many of the assays employed in the following chapters. In order to facilitate quantitative

analysis of biometals in populations of ageing cohorts exposed to various treatments it was imperative to develop a method that allowed for the fewest number of individuals possible. Establishing such a method would greatly increase the ease of conducting treatment assays in which cohorts of many hundreds of individuals are exposed to a variety of treatments and metal analysis occurs at multiple time points throughout lifespan. The potential of introducing variation in quantitative analysis increases with increasing numbers used for analysis due to the complex sample preparation techniques. It was demonstrated that as few as 10 individuals could be used to accurately and precisely quantify Mn, Fe, Cu and Zn via ICP-MS.

Data presented in Chapter 4 utilised the analytical methods established in Chapter 3 to determine the potential difference in physiological changes that occur to total Cu levels between *daf-2* mutants and wild type with age. This data was necessary to collect to establish baseline values for total Cu in *daf-2* as these values haven't been previously reported. It was found that throughout lifespan, *daf-2* was found to have elevated total Cu levels for each time point measured. As well, the findings of Samuelson (103) were supported by using RNAi to show *cua-1* activity is necessary for *daf-2* longevity as knocking-down *cua-1*(RNAi) drastically decreased median lifespan in *daf-2* mutants. Furthermore, the activity of *cua-1* was shown to be unique to *daf-2* mutants as knocking-down *cua-1* in wild type, another insulin signalling pathway mutant (*age-1*(*hx546*)) and a non-insulin signalling, long-lived mutant (*eat-2*(*ad1116*)) had no effect on median lifespan. Recently, CUA-1 was shown to function similarly to ATP7A/B in maintaining Cu homeostasis in the gut and liver of mammals. Specifically, under basal and Cu-limited conditions CUA-1 localises to basolateral membranes and the Golgi and under conditions of Cu excess redistributes to lysosome-like organelles, gut granules (217). Knocking down *cua-1* mRNA via RNAi in *daf-2* mutants resulted in significantly decreased total Cu levels compared to controls across all time points measured supporting the hypothesised role of CUA-1 in Cu delivery to peripheral tissues when localised to the basolateral membrane (217). Disruption of CUA-1 activity may inhibit Cu delivery to Cu-requiring proteins. Supplementing *daf-2* mutants, treated with *cua-1*(RNAi), with exogenous Cu (II) salts in efforts to restore levels closer to normal physiology was predicted to rescue *daf-2* mutant longevity. A partial rescue of lifespan was observed following supplementation of sub-lethal concentrations of Cu. From these results we predicted loss of *cua-1* activity was preventing Cu delivery to

cuproenzyme(s) and together this is modulating *daf-2* longevity. Further investigation into how *cua-1* activity is affecting Cu homeostasis and in turn *daf-2* mutant longevity is required to further resolve this lifespan-modulating relationship.

Data presented in Chapter 5 worked to further elucidate the mechanisms responsible for the unique Cu metabolism seen in *daf-2* mutants from data in chapter 4. To do this, size-exclusion chromatography-inductively coupled plasma mass-spectrometry (SEC-ICP-MS) was applied as native metal-protein bonds are preserved while online detection of metal status associated with biomolecules with specific molecular weights (265). Using this technique, *daf-2* mutants displayed a unique soluble, Cu-binding profile compared to age-matched wild types. In particular, a significant increase in Cu-bound to a relatively low molecular weight protein (retention volume, V_t = 3.59 mL; ~ MW 22 kDa) was observed in *daf-2* mutants. Given what is known about cellular Cu trafficking in *C. elegans* this protein was predicted to be one of two possible metallothioneins (MTL-1 and MTL-2). There are a number of functions proposed for MTs, with the most common including metal detoxification, metal ion homeostasis, metal chaperoning and protection from oxidative stress (297). Following analysis of several mutant strains, Cu, Zn-SOD1 and exploitation of the known metal-binding affinities of metallothioneins, our prediction was supported as two, single loss of function and one double loss of function *mtl* deletion mutants showed that this peak (V_t = 3.59 mL) was obliterated from Cu-binding. Expression of *mtl-1* is known to be up-regulated by DAF-16 which could be due to an insulin response sequence within the *mtl-1* promoter (64). The same peak obliteration was observed upon analysis of *daf-2*; *daf-16* double mutants via SEC-ICP-MS. Furthermore, supplementation of wild type populations with Cd yielded a significant increase in Cd-bound to peak 1 (V_t = 3.63 mL; ~ MW = 20 kDa) with another lower molecular weight protein (peak 2) displaying no increase in Cd-binding (V_t = 3.94 mL; ~ MW = 8 kDa)(Figure 5.2A). From this peak 1 could be (1) a dimer of MTL-1 with Zn-binding displaced by the supplemented Cd (287) or (2) a MTL-2 dimer. Zinc supplementation of wild type populations resulted in a unique Zn-binding peak (V_t = 3.66 mL; ~ MW = 18 kDa) (Figure 5.2B) predicted to be an MTL-1 dimer. This Zn-binding peak has a closer retention volume and MW to peak 1 from Figure 5.2A further supporting our prediction that it is MTL-1. Finally, knocking-down *cua-1* in *daf-2* mutants (Figure 5.5) leads to the obliteration of Cu-binding by a peak with a

retention volume (3.59 mL) and approximate MW (22 kDa) similar to the previously observed predicted MTL-1 peaks. From this we conclude that CUA-1 and MTL-1 are facilitating a unique scenario of Cu metabolism within *daf-2* mutants that is responsible for modulating longevity.

Copper bound to MT is thought to occur for storage and transport needs as Cu ions are rapidly transferred to MT in order to safely store and transport to other Cu-requiring proteins. While the function of MTs are traditionally considered to be prevention of Cu-toxicity by binding excess Cu, the data presented in this thesis is suggesting MT plays a more elegant role in Cu metabolism. Under basal conditions *mtl-1* expression levels are higher in *daf-2* mutants compared to wild types (93). In conjunction, *daf-2* mutants contain higher levels of Cu throughout most of their lifespan than wild types and this Cu is largely associated with MTL-1 through mechanisms involving CUA-1. Despite these observations it remains unknown if copper-association to MTL-1 is required for *daf-2* mutant longevity. In long-lived *daf-2* mutants MTL may serve to transport Cu to other Cu-requiring proteins including CUA-1 for transport to cuproenzymes.

6.2 Future directions

Moving forward, additional techniques to identify the Cu-binding peak that is predicted to be MTL-1 is the first step towards resolving the pathway by which CUA-1 and MTL regulate Cu metabolism to confer *daf-2* longevity. While the SEC-ICP-MS results indicate that the unique Cu-binding peak in *daf-2* mutants is closer to the MW of MTL-1 this is based off the column calibration that may not be able to distinguish between these two low molecular weight isoforms. Additional MS/MS techniques could be employed to further characterise the unknown peak including but not limited to two-dimensional LC-ICP-MS which may reveal the peak of interest is more than one Cu-binding protein. High-resolution mass spectrometry methods can be used to characterise Cu-binding proteins within peaks separated by LC-MS. It is worth considering that the sample preparation for SEC-ICP-MS involved lyophilising tissue that may cause natively bound metals to become liberated from their endogenous ligands and associated with other copper binding ligands. If this were the case, the Cu-binding peak that is predicted to be MTL may be an artefact of sample preparation. In conjunction with identifying

the unknown peak, single and double *mtl* knockout mutants can be used to generate *daf-2*; *mtl* double mutants. These double mutants could determine if the loss of *mtl-1* would have an effect on longevity. Furthermore, LC-ICP-MS analysis of this mutant would be predicted to have a decrease in Cu-bound to the unknown peak predicted to be MTL-1 and could reveal any other potential soluble Cu-binding proteins involved in the Cu metabolism mechanisms regulating *daf-2* mutant lifespan.

Identifying the Cu-binding peak predicted to be MTL-1 will work to elucidate a mechanism of Cu metabolism that facilitates delayed ageing. Changes in Cu homeostasis have long been implicated in ageing and diseases of ageing this mechanism would, for the first time, reveal the subcellular mechanisms responsible for Cu homeostasis in a mutant background that has delayed ageing. As many studies of ageing and disease often observe or characterise the artefacts of disease this Cu-metabolism pathway represents a fundamental process within the *daf-2* model of longevity. The findings presented here could be used to better understand the complex molecular mechanisms of longevity in other model organisms that still remain unresolved as the components of the *C. elegans*' insulin signalling and Cu metabolism pathways are evolutionarily conserved.

References

1. Kenyon CJ (2010) The genetics of ageing. in *Nature* (Nature Publishing Group), pp 504-512.
2. Christensen K, Johnson TE, & Vaupel JW (2006) The quest for genetic determinants of human longevity: challenges and insights. *Nature reviews. Genetics* 7(6):436.
3. Hayflick L (2007) Biological aging is no longer an unsolved problem. *Annals of the New York Academy of Sciences* 1100(1):1-13.
4. Harman D (1955) Aging: a theory based on free radical and radiation chemistry.
5. Raha S & Robinson BH (2000) Mitochondria, oxygen free radicals, disease and ageing. in *Trends in biochemical sciences* (Elsevier), pp 502-508.
6. Villalba JM*, et al.* (1995) Coenzyme Q reductase from liver plasma membrane: purification and role in trans-plasma-membrane electron transport. in *Proceedings of the National Academy of Sciences* (National Acad Sciences), pp 4887-4891.
7. Borges F, Fernandes E, & Roleira F (2002) Progress towards the discovery of xanthine oxidase inhibitors. in *Current medicinal chemistry* (Bentham Science Publishers), pp 195-217.
8. Kamata H & Hirata H (1999) Redox regulation of cellular signalling. in *Cellular signalling* (Elsevier), pp 1-14.
9. Loh K*, et al.* (2009) Reactive oxygen species enhance insulin sensitivity. in *Cell metabolism* (Elsevier), pp 260-272.
10. Halliwell B & Gutteridge J (1984) Oxygen toxicity, oxygen radicals, transition metals and disease. in *Biochemical journal* (Portland Press Ltd), p 1.
11. Haber F & Weiss J (1934) The catalytic decomposition of hydrogen peroxide by iron salts. in *Proceedings of the Royal Society of London A: Mathematical, Physical and Engineering Sciences* (The Royal Society), pp 332-351.
12. Liochev SI (1998) The mechanism of" Fenton-like" reactions and their importance for biological systems. A biologist's view. *Metal ions in biological systems* 36:1-39.
13. Chance B, Sies H, & Boveris A (1979) Hydroperoxide metabolism in mammalian organs. in *Physiological reviews* (Am Physiological Soc), pp 527-605.
14. McCord JM & Fridovich I (1969) Superoxide dismutase an enzymic function for erythrocuprein (hemocuprein). in *Journal of Biological chemistry* (ASBMB), pp 6049-6055.
15. Freeman B, Jackson R, Matalon S, & Harding S (1988) Biochemical and functional aspects of oxygen-mediated injury to vascular endothelium. *Endothelial cells* 3:13-31.
16. Fenton H (1894) LXXIII.—Oxidation of tartaric acid in presence of iron. *Journal of the Chemical Society, Transactions* 65:899-910.
17. Nathan C & Xie Q (1994) Regulation of biosynthesis of nitric oxide. *Journal of Biological Chemistry* 269(19):13725-13728.
18. Drew B & Leeuwenburgh C (2002) Aging and the role of reactive nitrogen species. *Annals of the New York Academy of Sciences* 959(1):66-81.
19. Beckman JS, Beckman TW, Chen J, Marshall PA, & Freeman BA (1990) Apparent hydroxyl radical production by peroxynitrite: implications for endothelial injury from nitric oxide and superoxide. *Proceedings of the National Academy of Sciences* 87(4):1620-1624.

20. Bohr VA & Anson RM (1995) DNA damage, mutation and fine structure DNA repair in aging. in *Mutation Research/DNAging* (Elsevier), pp 25-34.
21. Warner HR (1994) Superoxide dismutase, aging, and degenerative disease. in *Free radical biology and medicine* (Elsevier), pp 249-258.
22. Levine RL & Stadtman ER (2001) Oxidative modification of proteins during aging. in *Experimental gerontology* (Elsevier), pp 1495-1502.
23. Sohal RS & Orr WC (2012) The redox stress hypothesis of aging. *Free Radical Biology and Medicine* 52(3):539-555.
24. Gaggelli E, Kozlowski H, Valensin D, & Valensin G (2006) Copper homeostasis and neurodegenerative disorders (Alzheimer's, prion, and Parkinson's diseases and amyotrophic lateral sclerosis). in *Chem. Rev.* (ACS Publications), pp 1995-2044.
25. Wood ZA, Poole LB, & Karplus PA (2003) Peroxiredoxin evolution and the regulation of hydrogen peroxide signaling. *Science* 300(5619):650-653.
26. Maher P (2006) Redox control of neural function: background, mechanisms, and significance. *Antioxidants & redox signaling* 8(11-12):1941-1970.
27. Jones DP (2008) Radical-free biology of oxidative stress. *American Journal of Physiology-Cell Physiology* 295(4):C849-C868.
28. Jackson MJ & McArdle A (2011) Age‐related changes in skeletal muscle reactive oxygen species generation and adaptive responses to reactive oxygen species. *The Journal of physiology* 589(9):2139-2145.
29. Gems D & Doonan R (2009) Antioxidant defense and aging in C. elegans: is the oxidative damage theory of aging wrong? *Cell Cycle* 8(11):1681-1687.
30. Mockett RJ, Sohal BH, & Sohal RS (2010) Expression of multiple copies of mitochondrially targeted catalase or genomic Mn superoxide dismutase transgenes does not extend the life span of Drosophila melanogaster. *Free Radical Biology and Medicine* 49(12):2028-2031.
31. Brenner S (1974) The genetics of Caenorhabditis elegans. *Genetics* 77(1):71-94.
32. Hope IA (1999) *C. elegans: a practical approach* (OUP Oxford).
33. Benedetto A, Au C, & Aschner M (2009) Manganese-induced dopaminergic neurodegeneration: insights into mechanisms and genetics shared with Parkinson's disease. *Chemical reviews* 109(10):4862-4884.
34. Leung MC*, et al.* (2008) Caenorhabditis elegans: an emerging model in biomedical and environmental toxicology. *Toxicological sciences* 106(1):5-28.
35. Kaletta T & Hengartner MO (2006) Finding function in novel targets: C. elegans as a model organism. *Nature Reviews Drug Discovery* 5(5):387-399.
36. Jorgensen EM & Mango SE (2002) The art and design of genetic screens: Caenorhabditis elegans. *Nature reviews. Genetics* 3(5):356.
37. Ni Z & Lee SS (2010) RNAi screens to identify components of gene networks that modulate aging in Caenorhabditis elegans. *Briefings in functional genomics* 9(1):53-64.
38. Timmons L & Fire A (1998) Specific interference by ingested dsRNA. *Nature* 395(6705):854-854.
39. Roh HC, Collier S, Guthrie J, Robertson JD, & Kornfeld K (2012) Lysosome-related organelles in intestinal cells are a zinc storage site in C. elegans. *Cell metabolism* 15(1):88-99.

40. Ackerman D & Gems D (2012) Insulin/IGF-1 and hypoxia signaling act in concert to regulate iron homeostasis in Caenorhabditis elegans. *PLoS Genet* 8(3):e1002498.
41. Panowski SH, Wolff S, Aguilaniu H, Durieux J, & Dillin A (2007) PHA-4/Foxa mediates diet-restriction-induced longevity of C. elegans. *Nature* 447(7144):550-555.
42. Kirkwood TB (2005) Understanding the odd science of aging. *Cell* 120(4):437-447.
43. Masoro EJ (2005) Overview of caloric restriction and ageing. in *Mechanisms of ageing and development* (Elsevier), pp 913-922.
44. Partridge L (2010) The new biology of ageing. *Philosophical Transactions of the Royal Society of London B: Biological Sciences* 365(1537):147-154.
45. Kenyon C (2005) The plasticity of aging: insights from long-lived mutants. *Cell* 120(4):449-460.
46. Partridge L & Gems D (2007) Benchmarks for ageing studies. in *Nature* (Nature Publishing Group), pp 165-167.
47. Vijg J & Campisi J (2008) Puzzles, promises and a cure for ageing. in *Nature* (NIH Public Access), p 1065.
48. Fontana L, Partridge L, & Longo VD (2010) Extending healthy life span—from yeast to humans. in *Science* (American Association for the Advancement of Science), pp 321-326.
49. Greer EL & Brunet A (2009) Different dietary restriction regimens extend lifespan by both independent and overlapping genetic pathways in C. elegans. in *Aging cell* (Wiley Online Library), pp 113-127.
50. Tatar M, Bartke A, & Antebi A (2003) The endocrine regulation of aging by insulin-like signals. in *Science* (American Association for the Advancement of Science), pp 1346-1351.
51. Bonafè M*, et al.* (2003) Polymorphic variants of insulin-like growth factor I (IGF-I) receptor and phosphoinositide 3-kinase genes affect IGF-I plasma levels and human longevity: cues for an evolutionarily conserved mechanism of life span control. *The Journal of Clinical Endocrinology & Metabolism* 88(7):3299-3304.
52. Pinkston JM, Garigan D, Hansen M, & Kenyon C (2006) Mutations that increase the life span of C. elegans inhibit tumor growth. in *Science* (American Association for the Advancement of Science), pp 971-975.
53. Wu Y, Yakar S, Zhao L, Hennighausen L, & LeRoith D (2002) Circulating insulin-like growth factor-I levels regulate colon cancer growth and metastasis. *Cancer research* 62(4):1030-1035.
54. Morley JF, Brignull HR, Weyers JJ, & Morimoto RI (2002) The threshold for polyglutamine-expansion protein aggregation and cellular toxicity is dynamic and influenced by aging in Caenorhabditis elegans. *Proceedings of the National Academy of Sciences* 99(16):10417-10422.
55. Cohen E, Bieschke J, Perciavalle RM, Kelly JW, & Dillin A (2006) Opposing activities protect against age-onset proteotoxicity. *Science* 313(5793):1604-1610.
56. Killick R*, et al.* (2009) Deletion of Irs2 reduces amyloid deposition and rescues behavioural deficits in APP transgenic mice. *Biochemical and biophysical research communications* 386(1):257-262.
57. Freude S*, et al.* (2009) Neuronal IGF-1 resistance reduces Aβ accumulation and protects against premature death in a model of Alzheimer's disease. *The FASEB Journal* 23(10):3315-3324.

58. Cohen E, *et al.* (2009) Reduced IGF-1 signaling delays age-associated proteotoxicity in mice. *Cell* 139(6):1157-1169.
59. Selman C & Withers DJ (2011) Mammalian models of extended healthy lifespan. *Philosophical Transactions of the Royal Society of London B: Biological Sciences* 366(1561):99-107.
60. Pinkston JM, Garigan D, Hansen M, & Kenyon C (2006) Mutations that increase the life span of C. elegans inhibit tumor growth. *Science* 313(5789):971-975.
61. McElwee JJ, *et al.* (2007) Evolutionary conservation of regulated longevity assurance mechanisms. *Genome biology* 8(7):R132.
62. Blakesley VA, Butler AA, Koval AP, Okubo Y, & LeRoith D (1999) IGF-I receptor function. *The IGF system*, (Springer), pp 143-163.
63. Vowels JJ & Thomas JH (1992) Genetic analysis of chemosensory control of dauer formation in Caenorhabditis elegans. *Genetics* 130(1):105-123.
64. Murphy CT, *et al.* (2003) Genes that act downstream of DAF-16 to influence the lifespan of Caenorhabditis elegans. *Nature* 424(6946):277-283.
65. Giannakou ME, *et al.* (2004) Long-lived Drosophila with overexpressed dFOXO in adult fat body. *Science* 305(5682):361-361.
66. Hwangbo DS, Gersham B, Tu M-P, Palmer M, & Tatar M (2004) Drosophila dFOXO controls lifespan and regulates insulin signalling in brain and fat body. *Nature* 429(6991):562-566.
67. Suh Y, *et al.* (2008) Functionally significant insulin-like growth factor I receptor mutations in centenarians. *Proceedings of the National Academy of Sciences* 105(9):3438-3442.
68. Klass MR (1983) A method for the isolation of longevity mutants in the nematode Caenorhabditis elegans and initial results. *Mechanisms of ageing and development* 22(3):279-286.
69. Friedman DB & Johnson TE (1988) A mutation in the age-1 gene in Caenorhabditis elegans lengthens life and reduces hermaphrodite fertility. *Genetics* 118(1):75-86.
70. Kenyon C, Chang J, Gensch E, Rudner A, & Tabtiang R (1993) A C. elegans mutant that lives twice as long as wild type. *Nature* 366(6454):4.
71. Kimura KD, Tissenbaum HA, Liu Y, & Ruvkun G (1997) daf-2, an insulin receptor-like gene that regulates longevity and diapause in Caenorhabditis elegans. *Science* 277(5328):942-946.
72. Finch CE & Ruvkun G (2001) The genetics of aging. *Annual review of genomics and human genetics* 2(1):435-462.
73. Ebina Y, *et al.* (1985) Expression of a functional human insulin receptor from a cloned cDNA in Chinese hamster ovary cells. *Proceedings of the National Academy of Sciences* 82(23):8014-8018.
74. Hekimi S, Lakowski B, Barnes TM, & Ewbank JJ (1998) Molecular genetics of life span in C. elegans: how much does it teach us? *Trends in Genetics* 14(1):14-20.
75. Van Voorhies WA & Ward S (1999) Genetic and environmental conditions that increase longevity in Caenorhabditis elegans decrease metabolic rate. *Proceedings of the National Academy of Sciences* 96(20):11399-11403.
76. Paradis S & Ruvkun G (1998) Caenorhabditis elegans Akt/PKB transduces insulin receptor-like signals from AGE-1 PI3 kinase to the DAF-16 transcription factor. *Genes & development* 12(16):2488-2498.

77. Morris JZ, Tissenbaum HA, & Ruvkun G (1996) A phosphatidylinositol-3-OH kinase family member regulating longevity and diapause in Caenorhabditis elegans. *Nature* 382(6591):536.
78. Larsen PL (1993) Aging and resistance to oxidative damage in Caenorhabditis elegans. *Proceedings of the National Academy of Sciences* 90(19):8905-8909.
79. Ogg S*, et al.* (1997) The Fork head transcription factor DAF-16 transduces insulin-like metabolic and longevity signals in C. elegans. *Nature* 389(6654):994-999.
80. Lin K, Dorman JB, Rodan A, & Kenyon C (1997) daf-16: An HNF-3/forkhead family member that can function to double the life-span of Caenorhabditis elegans. *Science* 278(5341):1319-1322.
81. Vanfleteren JR (1993) Oxidative stress and ageing in Caenorhabditis elegans. *Biochemical Journal* 292(2):605-608.
82. Honda Y & Honda S (1999) The daf-2 gene network for longevity regulates oxidative stress resistance and Mn-superoxide dismutase gene expression in Caenorhabditis elegans. in *The FASEB Journal* (FASEB), pp 1385-1393.
83. Honda Y & Honda S (2002) Oxidative stress and life span determination in the nematode Caenorhabditis elegans. in *Annals of the New York Academy of Sciences* (Wiley Online Library), pp 466-474.
84. Murakami S & Johnson TE (1996) A genetic pathway conferring life extension and resistance to UV stress in Caenorhabditis elegans. *Genetics* 143(3):1207-1218.
85. Murakami S & Johnson TE (1998) Life extension and stress resistance in Caenorhabditis elegans. modulated by the tkr-1 gene. *Current biology* 8(19):1091-S1094.
86. Samet JM*, et al.* (1998) Activation of MAPKs in human bronchial epithelial cells exposed to metals. *American Journal of Physiology-Lung Cellular and Molecular Physiology* 275(3):L551-L558.
87. Walter PL*, et al.* (2006) Modulation of FoxO signaling in human hepatoma cells by exposure to copper or zinc ions. *Archives of biochemistry and biophysics* 454(2):107-113.
88. Tolbert ME, Kamalu JA, & Draper GD (1981) Effects of cadmium, zinc, copper and manganese on hepatic parenchymal cell gluconeogenesis. *Journal of Environmental Science & Health Part B* 16(5):575-585.
89. Rutman JZ, Meltzer LE, Kitchell JR, Rutman RJ, & George P (1965) Effect of metal ions on in vitro gluconeogenesis in rat kidney cortex slices. *American Journal of Physiology--Legacy Content* 208(5):841-846.
90. Rana S, Prakash R, Kumar A, & Sharma C (1985) A study of glycogen in the liver of metal-fed rats. *Toxicology letters* 29(1):1-4.
91. Barthel A, Ostrakhovitch EA, Walter PL, Kampkötter A, & Klotz L-O (2007) Stimulation of phosphoinositide 3-kinase/Akt signaling by copper and zinc ions: mechanisms and consequences. *Archives of biochemistry and biophysics* 463(2):175-182.
92. Eckers A & Klotz L-O (2009) Heavy metal ion-induced insulin-mimetic signaling. *Redox Report* 14(4):141-146.
93. Barsyte D, Lovejoy DA, & LITHGOW GJ (2001) Longevity and heavy metal resistance in daf-2 and age-1 long-lived mutants of Caenorhabditis elegans. *The FASEB Journal* 15(3):627-634.
94. Longo VD & Finch CE (2003) Evolutionary medicine: from dwarf model systems to healthy centenarians? *Science* 299(5611):1342-1346.

95. James SA*, et al.* (2015) Direct in vivo imaging of ferrous iron dyshomeostasis in ageing Caenorhabditis elegans. *Chemical Science* 6(5):2952-2962.
96. Senoo-Matsuda N*, et al.* (2001) A defect in the cytochrome b large subunit in complex II causes both superoxide anion overproduction and abnormal energy metabolism in Caenorhabditis elegans. *Journal of Biological Chemistry* 276(45):41553-41558.
97. Duhon SA, Murakami S, & Johnson TE (1996) Direct isolation of longevity mutants in the nematode Caenorhabditis elegans. *genesis* 18(2):144-153.
98. Dillin A, Crawford DK, & Kenyon C (2002) Timing requirements for insulin/IGF-1 signaling in C. elegans. *Science* 298(5594):830-834.
99. Lakowski B & Hekimi S (1998) The genetics of caloric restriction in Caenorhabditis elegans. *Proceedings of the National Academy of Sciences* 95(22):13091-13096.
100. Montgomery MK & Fire A (1998) Double-stranded RNA as a mediator in sequence-specific genetic silencing and co-suppression. *Trends in Genetics* 14(7):255-258.
101. Kenyon C, Chang J, Gensch E, Rudner A, & Tabtiang R (1993) A C. elegans mutant that lives twice as long as wild type. *Nature* 366(6454):461-464.
102. Patti GJ*, et al.* (2014) Meta-analysis of global metabolomic data identifies metabolites associated with life-span extension. *Metabolomics* 10(4):0.
103. Samuelson AV, Carr CE, & Ruvkun G (2007) Gene activities that mediate increased life span of C. elegans insulin-like signaling mutants. *Genes & development* 21(22):2976-2994.
104. Waldron KJ, Rutherford JC, Ford D, & Robinson NJ (2009) Metalloproteins and metal sensing. in *Nature* (Nature Publishing Group), pp 823-830.
105. Turski ML & Thiele DJ (2009) New roles for copper metabolism in cell proliferation, signaling, and disease. *Journal of Biological Chemistry* 284(2):717-721.
106. Jansen J, Karges W, & Rink L (2009) Zinc and diabetes—clinical links and molecular mechanisms. *The Journal of nutritional biochemistry* 20(6):399-417.
107. McRae R, Bagchi P, Sumalekshmy S, & Fahrni CJ (2009) In situ imaging of metals in cells and tissues. *Chemical reviews* 109(10):4780-4827.
108. Valko M, Morris H, & Cronin M (2005) Metals, toxicity and oxidative stress. *Current medicinal chemistry* 12(10):1161-1208.
109. Finney L, Vogt S, Fukai T, & Glesne D (2009) Copper and angiogenesis: unravelling a relationship key to cancer progression. *Clinical and Experimental Pharmacology and Physiology* 36(1):88-94.
110. Bush AI (2000) Metals and neuroscience. *Current opinion in chemical biology* 4(2):184-191.
111. Que EL, Domaille DW, & Chang CJ (2008) Metals in neurobiology: probing their chemistry and biology with molecular imaging. *Chemical Reviews* 108(5):1517-1549.
112. Burdette SC & Lippard SJ (2003) Meeting of the minds: metalloneurochemistry. *Proceedings of the National Academy of Sciences* 100(7):3605-3610.
113. Bourassa MW & Miller LM (2012) Metal imaging in neurodegenerative diseases. in *Metallomics* (Royal Society of Chemistry), pp 721-738.
114. Lovell MA, Robertson JD, Teesdale WJ, Campbell JL, & Markesbery WR (1998) Copper, iron and zinc in Alzheimer's disease senile plaques. in *Journal of the neurological sciences* (Elsevier), pp 47-52.

115. Aguirre N, Flint Beal M, Matson WR, & Bogdanov MB (2005) Increased oxidative damage to DNA in an animal model of amyotrophic lateral sclerosis. *Free radical research* 39(4):383-388.
116. Roos PM, Vesterberg O, Syversen T, Flaten TP, & Nordberg M (2013) Metal concentrations in cerebrospinal fluid and blood plasma from patients with amyotrophic lateral sclerosis. *Biological trace element research* 151(2):159-170.
117. Markesbery WR*, et al.* (1995) Neutron activation analysis of trace elements in motor neuron disease spinal cord. *Neurodegeneration* 4(4):383-390.
118. Tokuda E, Okawa E, Watanabe S, Ono S-i, & Marklund SL (2013) Dysregulation of intracellular copper homeostasis is common to transgenic mice expressing human mutant superoxide dismutase-1s regardless of their copper-binding abilities. *Neurobiology of disease* 54:308-319.
119. Sian J*, et al.* (1994) Alterations in glutathione levels in Parkinson's disease and other neurodegenerative disorders affecting basal ganglia. *Annals of neurology* 36(3):348-355.
120. Dexter D*, et al.* (1989) Increased nigral iron content and alterations in other metal ions occurring in brain in Parkinson's disease. *Journal of neurochemistry* 52(6):1830-1836.
121. Davies KM*, et al.* (2014) Copper pathology in vulnerable brain regions in Parkinson's disease. *Neurobiology of aging* 35(4):858-866.
122. Davies KMM, Julian FB; Chen, Nicholas; Double, Kay L (2016) Copper dyshomeostasis in Parkinson's disease: implications for pathogenesis and indications for novel therapeutics. *Clinical Science* 130(8):9.
123. Yamasaki S*, et al.* (2007) Zinc is a novel intracellular second messenger. *The Journal of cell biology* 177(4):637-645.
124. Bleackley MR & MacGillivray RT (2011) Transition metal homeostasis: from yeast to human disease. *Biometals* 24(5):785-809.
125. Davies KM*, et al.* (2013) Localization of copper and copper transporters in the human brain. in *Metallomics* (Royal Society of Chemistry), pp 43-51.
126. Linder MC & Hazegh-Azam M (1996) Copper biochemistry and molecular biology. *The American journal of clinical nutrition* 63(5):797S-811S.
127. Brewer G*, et al.* (2006) Normal copper metabolism and lowering copper to subnormal levels for therapeutic purposes. *Textbook of Hepatology: From basic science to clinical practice. Oxford, England: Blackwell Publishing, Expected publication*.
128. Huffman DL & O'Halloran TV (2001) Function, structure, and mechanism of intracellular copper trafficking proteins. *Annual review of biochemistry* 70(1):677-701.
129. Vulpe CD & Packman S (1995) Cellular copper transport. *Annual review of nutrition* 15(1):293-322.
130. Peña MM, Lee J, & Thiele DJ (1999) A delicate balance: homeostatic control of copper uptake and distribution. *The Journal of nutrition* 129(7):1251-1260.
131. Rosenzweig AC (2001) Copper delivery by metallochaperone proteins. *Accounts of Chemical Research* 34(2):119-128.
132. Barnham KJ & Bush AI (2014) Biological metals and metal-targeting compounds in major neurodegenerative diseases. *Chemical Society Reviews* 43(19):6727-6749.
133. Mercer JF*, et al.* (1993) Isolation of a partial candidate gene for Menkes disease by positional cloning. *Nature genetics* 3(1):20-25.

134. Gouider-Khouja N (2009) Wilson's disease. *Parkinsonism & related disorders* 15:S126-S129.
135. Wilson SK (1912) Progressive lenticular degeneration: a familial nervous disease associated with cirrhosis of the liver. *The Lancet* 179(4626):1115-1119.
136. Bull PC, Thomas GR, Rommens JM, Forbes JR, & Cox DW (1993) The Wilson disease gene is a putative copper transporting P–type ATPase similar to the Menkes gene. *Nature genetics* 5(4):327-337.
137. DM D (1995) *Disorders of Copper Transport* (McGraw-Hill, New York) 7 Ed p 24.
138. Kodama H & Murata Y (1999) Molecular genetics and pathophysiology of Menkes disease. *Pediatrics international* 41(4):430-435.
139. Camakaris J*, et al.* (1980) Altered copper metabolism in cultured cells from human Menkes' syndrome and mottled mouse mutants. *Biochemical genetics* 18(1):117-131.
140. Fox PL (2003) The copper-iron chronicles: the story of an intimate relationship. *Biometals* 16(1):9-40.
141. Hart E, Steenbock H, Elvehjem C, & Waddell J (1925) Iron in nutrition. I. Nutritional anemia on whole milk diets and the utilization of inorganic iron in hemoglobin building. *The Journal of biological chemistry* 65(1):13.
142. Hart EB SH, Waddell J, et al. (1928) Copper as a supplement to iron for haemoglobin building in the rat. *Journal of Biological Chemistry* 77:15.
143. Askwith C & Kaplan J (1998) Iron and copper transport in yeast and its relevance to human disease. *Trends in biochemical sciences* 23(4):135-138.
144. Crichton R & Pierre J-L (2001) Old iron, young copper: from Mars to Venus. *Biometals* 14(2):99-112.
145. Harris ED (1995) The iron-copper connection: the link to ceruloplasmin grows stronger. *Nutrition reviews* 53(6):170-173.
146. Lei P*, et al.* (2012) Tau deficiency induces parkinsonism with dementia by impairing APP-mediated iron export. *Nature medicine* 18(2):291-295.
147. Oshiro S, Morioka MS, & Kikuchi M (2011) Dysregulation of iron metabolism in Alzheimer's disease, Parkinson's disease, and amyotrophic lateral sclerosis. *Advances in pharmacological sciences* 2011.
148. Roijers RB*, et al.* (2011) Microcalcifications in early intimal lesions of atherosclerotic human coronary arteries. *The American journal of pathology* 178(6):2879-2887.
149. Sullivan JL (2009) Iron in arterial plaque: A modifiable risk factor for atherosclerosis. *Biochimica et Biophysica Acta (BBA)-General Subjects* 1790(7):718-723.
150. Tajima S*, et al.* (2012) Iron reduction by deferoxamine leads to amelioration of adiposity via the regulation of oxidative stress and inflammation in obese and type 2 diabetes KKAy mice. *American Journal of Physiology-Endocrinology and Metabolism* 302(1):E77-E86.
151. Torti SV & Torti FM (2011) Ironing out cancer. *Cancer research* 71(5):1511-1514.
152. Toyokuni S (2009) Role of iron in carcinogenesis: cancer as a ferrotoxic disease. *Cancer science* 100(1):9-16.
153. Bilgic B, Pfefferbaum A, Rohlfing T, Sullivan EV, & Adalsteinsson E (2012) MRI estimates of brain iron concentration in normal aging using quantitative susceptibility mapping. *Neuroimage* 59(3):2625-2635.

154. Zecca L*, et al.* (2001) Iron, neuromelanin and ferritin content in the substantia nigra of normal subjects at different ages: consequences for iron storage and neurodegenerative processes. *Journal of neurochemistry* 76(6):1766-1773.
155. Hellman NE & Gitlin JD (2002) Ceruloplasmin metabolism and function. *Annual review of nutrition* 22(1):439-458.
156. Gubler C, Cartwright G, & Wintrobe M (1957) Studies on copper metabolism. 20. Enzyme activities and iron metabolism in copper and iron deficiencies. *Journal of Biological Chemistry* 224:533-546.
157. MC L (1991) *Biochemistry of copper* (Plenum Press, New York).
158. Halliwell B & Gutteridge JM (1990) [1] Role of free radicals and catalytic metal ions in human disease: an overview. *Methods in enzymology* 186:1-85.
159. Kim B-E, Nevitt T, & Thiele DJ (2008) Mechanisms for copper acquisition, distribution and regulation. *Nature chemical biology* 4(3):176-185.
160. Maryon EB, Molloy SA, Zimnicka AM, & Kaplan JH (2007) Copper entry into human cells: progress and unanswered questions. *Biometals* 20(3-4):355.
161. Dancis A, Haile D, Yuan DS, & Klausner RD (1994) The Saccharomyces cerevisiae copper transport protein (Ctr1p). Biochemical characterization, regulation by copper, and physiologic role in copper uptake. *Journal of Biological Chemistry* 269(41):25660-25667.
162. Nose Y*, et al.* (2010) Ctr1 is an apical copper transporter in mammalian intestinal epithelial cells in vivo that is controlled at the level of protein stability. *Journal of Biological Chemistry* 285(42):32385-32392.
163. Ohgami RS, Campagna DR, McDonald A, & Fleming MD (2006) The Steap proteins are metalloreductases. in *Blood* (Am Soc Hematology), pp 1388-1394.
164. Dancis A*, et al.* (1994) Molecular characterization of a copper transport protein in S. cerevisiae: an unexpected role for copper in iron transport. *Cell* 76(2):393-402.
165. Jensen LT & Winge DR (1998) Identification of a copper‐induced intramolecular interaction in the transcription factor Mac1 from Saccharomyces cerevisiae. *The EMBO Journal* 17(18):5400-5408.
166. Song I-S*, et al.* (2008) Transcription factor Sp1 plays an important role in the regulation of copper homeostasis in mammalian cells. *Molecular pharmacology* 74(3):705-713.
167. Molloy SA & Kaplan JH (2009) Copper-dependent recycling of hCTR1, the human high affinity copper transporter. *Journal of Biological Chemistry* 284(43):29704-29713.
168. Lee J, Prohaska JR, Dagenais SL, Glover TW, & Thiele DJ (2000) Isolation of a murine copper transporter gene, tissue specific expression and functional complementation of a yeast copper transport mutant. *Gene* 254(1):87-96.
169. Nose Y, Rees EM, & Thiele DJ (2006) Structure of the Ctr1 copper trans 'PORE'ter reveals novel architecture. *Trends in biochemical sciences* 31(11):604-607.
170. Lee J, Peña MMO, Nose Y, & Thiele DJ (2002) Biochemical characterization of the human copper transporter Ctr1. *Journal of Biological Chemistry* 277(6):4380-4387.
171. Garrick MD*, et al.* (2006) DMT1: which metals does it transport? *Biological research* 39(1):79-85.
172. Arredondo M, Muñoz P, Mura CV, & Núñez MT (2003) DMT1, a physiologically relevant apical Cu 1+ transporter of intestinal cells. *American Journal of Physiology-Cell Physiology* 284(6):C1525-C1530.

173. Harrison MD, Jones CE, Solioz M, & Dameron CT (2000) Intracellular copper routing: the role of copper chaperones. *Trends in biochemical sciences* 25(1):29-32.
174. Rosenzweig AC & O'Halloran TV (2000) Structure and chemistry of the copper chaperone proteins. *Current opinion in chemical biology* 4(2):140-147.
175. Pufahl R*, et al.* (1997) Metal ion chaperone function of the soluble Cu (I) receptor Atx1. *Science* 278(5339):853-856.
176. Hasan NM & Lutsenko S (2012) Regulation of copper transporters in human cells. *Curr. Top. Membr* 69:137-161.
177. Lin S-J, Pufahl RA, Dancis A, O'Halloran TV, & Culotta VC (1997) A role for the Saccharomyces cerevisiae ATX1 gene in copper trafficking and iron transport. *Journal of Biological Chemistry* 272(14):9215-9220.
178. Hamza I, Schaefer M, Klomp LW, & Gitlin JD (1999) Interaction of the copper chaperone HAH1 with the Wilson disease protein is essential for copper homeostasis. *Proceedings of the National Academy of Sciences* 96(23):13363-13368.
179. Lutsenko S, Petrukhin K, Cooper MJ, Gilliam CT, & Kaplan JH (1997) N-terminal domains of human copper-transporting adenosine triphosphatases (the Wilson's and Menkes disease proteins) bind copper selectively in vivo and in vitro with stoichiometry of one copper per metal-binding repeat. *Journal of Biological Chemistry* 272(30):18939-18944.
180. DiDonato M, Narindrasorasak S, Forbes JR, Cox DW, & Sarkar B (1997) Expression, purification, and metal binding properties of the N-terminal domain from the Wilson disease putative copper-transporting ATPase (ATP7B). *Journal of Biological Chemistry* 272(52):33279-33282.
181. Petris M*, et al.* (1996) Ligand-regulated transport of the Menkes copper P-type ATPase efflux pump from the Golgi apparatus to the plasma membrane: a novel mechanism of regulated trafficking. *The EMBO journal* 15(22):6084.
182. Petris MJ & Mercer JF (1999) The Menkes protein (ATP7A; MNK) cycles via the plasma membrane both in basal and elevated extracellular copper using a C-terminal di-leucine endocytic signal. *Human molecular genetics* 8(11):2107-2115.
183. Schaefer M, Hopkins RG, Failla ML, & Gitlin JD (1999) Hepatocyte-specific localization and copper-dependent trafficking of the Wilson's disease protein in the liver. *American Journal of Physiology-Gastrointestinal and Liver Physiology* 276(3):G639-G646.
184. Weisiger RA & Fridovich I (1973) Mitochondrial superoxide dismutase site of synthesis and intramitochondrial localization. *Journal of Biological Chemistry* 248(13):4793-4796.
185. Chang L-Y, Slot JW, Geuze HJ, & Crapo JD (1988) Molecular immunocytochemistry of the CuZn superoxide dismutase in rat hepatocytes. *The Journal of cell biology* 107(6):2169-2179.
186. Sturtz LA, Diekert K, Jensen LT, Lill R, & Culotta VC (2001) A fraction of yeast cu, zn-superoxide dismutase and its metallochaperone, ccs, localize to the intermembrane space of mitochondria a physiological role for sod1 in guarding against mitochondrial oxidative damage. *Journal of Biological Chemistry* 276(41):38084-38089.
187. Hayward LJ*, et al.* (2002) Decreased metallation and activity in subsets of mutant superoxide dismutases associated with familial amyotrophic lateral sclerosis. *Journal of Biological Chemistry* 277(18):15923-15931.
188. Coyle P, Philcox J, Carey L, & Rofe A (2002) Metallothionein: the multipurpose protein. *Cellular and Molecular Life Sciences CmLS* 59(4):627-647.

189. Klaassen CD, Liu J, & Choudhuri S (1999) Metallothionein: an intracellular protein to protect against cadmium toxicity. *Annual review of pharmacology and toxicology* 39(1):267-294.
190. Maret W (2008) Metallothionein redox biology in the cytoprotective and cytotoxic functions of zinc. *Experimental gerontology* 43(5):363-369.
191. West A*, et al.* (1990) Human metallothionein genes: structure of the functional locus at 16q13. *Genomics* 8(3):513-518.
192. Carrasco J*, et al.* (2006) Metallothionein-I and-III expression in animal models of Alzheimer disease. *Neuroscience* 143(4):911-922.
193. Manso Y, Adlard PA, Carrasco J, Vašák M, & Hidalgo J (2011) Metallothionein and brain inflammation. *JBIC Journal of Biological Inorganic Chemistry* 16(7):1103-1113.
194. Masters BA, Kelly EJ, Quaife CJ, Brinster RL, & Palmiter RD (1994) Targeted disruption of metallothionein I and II genes increases sensitivity to cadmium. *Proceedings of the National Academy of Sciences* 91(2):584-588.
195. Li Y, Du J, Zhang P, & Ding J (2010) Crystal structure of human copper homeostasis protein CutC reveals a potential copper-binding site. *Journal of structural biology* 169(3):399-405.
196. Doonan R*, et al.* (2008) Against the oxidative damage theory of aging: superoxide dismutases protect against oxidative stress but have little or no effect on life span in Caenorhabditis elegans. *Genes & development* 22(23):3236-3241.
197. Hunter T, Bannister WH, & Hunter GJ (1997) Cloning, expression, and characterization of two manganese superoxide dismutases from Caenorhabditis elegans. *Journal of Biological Chemistry* 272(45):28652-28659.
198. Fujii M, Ishii N, Joguchi A, Yasuda K, & Ayusawa D (1998) A novel superoxide dismutase gene encoding membrane-bound and extracellular isoforms by alternative splicing in Caenorhabditis elegans. *DNA Research* 5(1):25-30.
199. Jensen LT & Culotta VC (2005) Activation of CuZn superoxide dismutases from Caenorhabditis elegans does not require the copper chaperone CCS. *Journal of Biological Chemistry* 280(50):41373-41379.
200. Van Raamsdonk JM & Hekimi S (2009) Deletion of the mitochondrial superoxide dismutase sod-2 extends lifespan in Caenorhabditis elegans. *PLoS Genet* 5(2):e1000361.
201. Wakabayashi T*, et al.* (1998) Identification of the copper chaperone, CUC‐1, in Caenorhabditis elegans: tissue specific co‐expression with the copper transporting ATPase, CUA‐1. *FEBS letters* 440(1-2):141-146.
202. Freedman JH, Slice LW, Dixon D, Fire A, & Rubin CS (1993) The novel metallothionein genes of Caenorhabditis elegans. Structural organization and inducible, cell-specific expression. *Journal of Biological Chemistry* 268(4):2554-2564.
203. Bofill R*, et al.* (2009) Caenorhabditis elegans metallothionein isoform specificity–metal binding abilities and the role of histidine in CeMT1 and CeMT2. *FEBS journal* 276(23):7040-7056.
204. Calafato S, Swain S, Hughes S, Kille P, & Stürzenbaum SR (2008) Knock down of Caenorhabditis elegans cutc-1 exacerbates the sensitivity toward high levels of copper. *Toxicological sciences* 106(2):384-391.
205. Finney LA & O'halloran TV (2003) Transition metal speciation in the cell: insights from the chemistry of metal ion receptors. *Science* 300(5621):931-936.

206. Mercer JF & Llanos RM (2003) Molecular and cellular aspects of copper transport in developing mammals. *The Journal of nutrition* 133(5):1481S-1484S.
207. Veldhuis NA, *et al.* (2009) Phosphorylation regulates copper-responsive trafficking of the Menkes copper transporting P-type ATPase. *The international journal of biochemistry & cell biology* 41(12):2403-2412.
208. Petrukhin K, *et al.* (1994) Characterization of the Wilson disease gene encoding a P-type copper transporting ATPase: genomic organization, alternative splicing, and structure/function predictions. *Human Molecular Genetics* 3(9):1647-1656.
209. Lutsenko S, Barnes NL, Bartee MY, & Dmitriev OY (2007) Function and regulation of human copper-transporting ATPases. *Physiological reviews* 87(3):1011-1046.
210. Veldhuis NA, Gaeth AP, Pearson RB, Gabriel K, & Camakaris J (2009) The multi-layered regulation of copper translocating P-type ATPases. *Biometals* 22(1):177-190.
211. La Fontaine S & Mercer JF (2007) Trafficking of the copper-ATPases, ATP7A and ATP7B: role in copper homeostasis. *Archives of biochemistry and biophysics* 463(2):149-167.
212. Vanderwerf SM, Cooper MJ, Stetsenko IV, & Lutsenko S (2001) Copper specifically regulates intracellular phosphorylation of the Wilson's disease protein, a human copper-transporting ATPase. *Journal of Biological Chemistry* 276(39):36289-36294.
213. Yatsunyk LA & Rosenzweig AC (2007) Cu (I) binding and transfer by the N terminus of the Wilson disease protein. *Journal of Biological Chemistry* 282(12):8622-8631.
214. Sievers F, *et al.* (2011) Fast, scalable generation of high‐quality protein multiple sequence alignments using Clustal Omega. *Molecular systems biology* 7(1):539.
215. Lye JC, *et al.* (2011) Detection of genetically altered copper levels in Drosophila tissues by synchrotron X-ray fluorescence microscopy. *PloS one* 6(10):e26867.
216. Sambongi Y, *et al.* (1997) Caenorhabditis elegans cDNA for a Menkes/Wilson disease gene homologue and its function in a yeast CCC2 gene deletion mutant. *The Journal of Biochemistry* 121(6):1169-1175.
217. Chun H, *et al.* (2017) The Intestinal Copper Exporter CUA-1 Is Required for Systemic Copper Homeostasis in Caenorhabditis elegans. *Journal of Biological Chemistry* 292(1):1-14.
218. Beauchemin D (2010) Inductively coupled plasma mass spectrometry. *Analytical chemistry* 82(12):4786-4810.
219. Hare DJ, *et al.* (2016) High-resolution complementary chemical imaging of bio-elements in Caenorhabditis elegans. *Metallomics* 8(2):156-160.
220. McColl G, *et al.* (2008) Pharmacogenetic analysis of lithium-induced delayed aging in Caenorhabditis elegans. *Journal of Biological Chemistry* 283(1):350-357.
221. Klang IM, *et al.* (2014) Iron promotes protein insolubility and aging in C. elegans. *Aging (Albany NY)* 6(11):975.
222. Lin Y-T, *et al.* (2006) Manganous ion supplementation accelerates wild type development, enhances stress resistance, and rescues the life span of a short–lived Caenorhabditis elegans mutant. *Free radical biology and medicine* 40(7):1185-1193.
223. Bensaddek D, *et al.* (2016) Micro‐proteomics with iterative data analysis: Proteome analysis in C. elegans at the single worm level. *Proteomics* 16(3):381-392.
224. Ganio K, James SA, Hare DJ, Roberts BR, & McColl G (2016) Accurate biometal quantification per individual Caenorhabditis elegans. *Analyst* 141(4):1434-1439.

225. Hughes S & Stürzenbaum SR (2007) Single and double metallothionein knockout in the nematode C. elegans reveals cadmium dependent and independent toxic effects on life history traits. *Environmental Pollution* 145(2):395-400.
226. Lin K, Hsin H, Libina N, & Kenyon C (2001) Regulation of the Caenorhabditis elegans longevity protein DAF-16 by insulin/IGF-1 and germline signaling. *Nature genetics* 28(2):139-145.
227. Byerly L, Cassada R, & Russell R (1976) The life cycle of the nematode Caenorhabditis elegans: I. Wild-type growth and reproduction. *Developmental biology* 51(1):23-33.
228. Sulston J & Hodgkin J (1988) *The Nematode Caenorhabditis elegans* (Cold Spring Harbor Press, New York) p 29.
229. Bianchi L & Driscoll M (2006) Culture of embryonic C. elegans cells for electrophysiological and pharmacological analyses (September 30, 2006), WormBook, ed. The C. elegans Research Community, WormBook, doi/10.1895/wormbook. 1.122. 1.
230. Kamath RS & Ahringer J (2003) Genome-wide RNAi screening in Caenorhabditis elegans. *Methods* 30(4):313-321.
231. Kamath RS, Martinez-Campos M, Zipperlen P, Fraser AG, & Ahringer J (2000) Effectiveness of specific RNA-mediated interference through ingested double-stranded RNA in Caenorhabditis elegans. *Genome biology* 2(1):1.
232. Klang IM*, et al.* (2014) Iron promotes protein insolubility and aging in C. elegans. *Aging* 6(11):975-991.
233. Paunesku T, Vogt S, Maser J, Lai B, & Woloschak G (2006) X‐ray fluorescence microprobe imaging in biology and medicine. *Journal of cellular biochemistry* 99(6):1489-1502.
234. Henderson ST & Johnson TE (2001) daf-16 integrates developmental and environmental inputs to mediate aging in the nematode Caenorhabditis elegans. *Current Biology* 11(24):1975-1980.
235. Murphy CT*, et al.* (2003) Genes that act downstream of DAF-16 to influence C. elegans lifespan. *International Worm Meeting*.
236. Southon A, Burke R, Norgate M, Batterham P, & Camakaris J (2004) Copper homoeostasis in Drosophila melanogaster S2 cells. *Biochemical Journal* 383(2):303-309.
237. Ostrakhovitch EA, Lordnejad MR, Schliess F, Sies H, & Klotz L-O (2002) Copper ions strongly activate the phosphoinositide-3-kinase/Akt pathway independent of the generation of reactive oxygen species. *Archives of biochemistry and biophysics* 397(2):232-239.
238. Ostrakhovitch E & Cherian M (2004) Differential regulation of signal transduction pathways in wild type and mutated p53 breast cancer epithelial cells by copper and zinc. *Archives of biochemistry and biophysics* 423(2):351-361.
239. Tatar M, Bartke A, & Antebi A (2003) The endocrine regulation of aging by insulin-like signals. *Science* 299(5611):1346-1351.
240. Ebina Y*, et al.* (1985) The human insulin receptor cDNA: the structural basis for hormone-activated transmembrane signalling. *Cell* 40(4):747-758.
241. Ullrich A*, et al.* (1985) Human insulin receptor and its relationship to the tyrosine kinase family of oncogenes. *Nature* 313(6005):756-761.
242. Shier P & Watt VM (1989) Primary structure of a putative receptor for a ligand of the insulin family. *Journal of Biological Chemistry* 264(25):14605-14608.

243. Tornqvist H, *et al.* (1988) Identification of the insulin receptor tyrosine residues undergoing insulin-stimulated phosphorylation in intact rat hepatoma cells. *Journal of Biological Chemistry* 263(1):350-359.
244. Chou C, *et al.* (1987) Human insulin receptors mutated at the ATP-binding site lack protein tyrosine kinase activity and fail to mediate postreceptor effects of insulin. *Journal of Biological Chemistry* 262(4):1842-1847.
245. Halaschek-Wiener J, *et al.* (2005) Analysis of long-lived C. elegans daf-2 mutants using serial analysis of gene expression. *Genome research* 15(5):603-615.
246. Hsin H & Kenyon C (1999) Signals from the reproductive system regulate the lifespan of C. elegans. *Nature* 399(6734):362.
247. Gems D, *et al.* (1998) Two pleiotropic classes of daf-2 mutation affect larval arrest, adult behavior, reproduction and longevity in Caenorhabditis elegans. *Genetics* 150(1):129-155.
248. Liu J-P, Baker J, Perkins AS, Robertson EJ, & Efstratiadis A (1993) Mice carrying null mutations of the genes encoding insulin-like growth factor I (Igf-1) and type 1 IGF receptor (Igf1r). *Cell* 75(1):59-72.
249. Sutter NB, *et al.* (2007) A single IGF1 allele is a major determinant of small size in dogs. *Science* 316(5821):112-115.
250. Vanfleteren JR & De Vreese A (1995) The gerontogenes age-1 and daf-2 determine metabolic rate potential in aging Caenorhabditis elegans. *The FASEB Journal* 9(13):1355-1361.
251. Sávoly Z, Nagy P, Havancsák K, & Záray G (2012) Microanalytical investigation of nematodes. *Microchemical Journal* 105:83-87.
252. Lenartowicz M, Moos T, Ogórek M, Jensen TG, & Møller LB (2016) Metal-dependent regulation of ATP7A and ATP7B in fibroblast cultures. *Frontiers in molecular neuroscience* 9.
253. van den Berghe PV & Klomp LW (2010) Posttranslational regulation of copper transporters. *JBIC Journal of Biological Inorganic Chemistry* 15(1):37.
254. Das SK & Ray K (2006) Wilson's disease: an update. *Nature clinical practice Neurology* 2(9):482-493.
255. Finch CE (1994) *Longevity, senescence, and the genome* (University of Chicago Press).
256. Klass MR (1977) Aging in the nematode Caenorhabditis elegans: major biological and environmental factors influencing life span. *Mechanisms of ageing and development* 6:413-429.
257. Heilbronn LK & Ravussin E (2003) Calorie restriction and aging: review of the literature and implications for studies in humans. *The American journal of clinical nutrition* 78(3):361-369.
258. Guarente L & Kenyon C (2000) Genetic pathways that regulate ageing in model organisms. *Nature* 408(6809):255-262.
259. Kenyon C (2001) A conserved regulatory system for aging. *Cell* 105(2):165-168.
260. Braeckman BP, Houthoofd K, & Vanfleteren JR (2001) Insulin-like signaling, metabolism, stress resistance and aging in Caenorhabditis elegans. *Mechanisms of ageing and development* 122(7):673-693.
261. Hu PJ (2007) Dauer. *WormBook: the online review of C. elegans biology*:1-19.
262. Waldron KJ, Rutherford JC, Ford D, & Robinson NJ (2009) Metalloproteins and metal sensing. *Nature* 460(7257):823-830.

263. Andreini C, Bertini I, Cavallaro G, Holliday GL, & Thornton JM (2008) Metal ions in biological catalysis: from enzyme databases to general principles. *JBIC Journal of Biological Inorganic Chemistry* 13(8):1205-1218.
264. Cvetkovic A*, et al.* (2010) Microbial metalloproteomes are largely uncharacterized. *Nature* 466(7307):779.
265. Lothian A & Roberts BR (2016) Standards for quantitative metalloproteomic analysis using size exclusion ICP-MS. *Journal of visualized experiments: JoVE* (110).
266. Kaegi JH & Kojima Y (1987) Chemistry and biochemistry of metallothionein. *Metallothionein II*, (Springer), pp 25-61.
267. Rupp H & Weser U (1978) Circular dichroism of metallothioneins: a structural approach. *Biochimica et Biophysica Acta (BBA)-Protein Structure* 533(1):209-226.
268. Carpenè E, Andreani G, & Isani G (2007) Metallothionein functions and structural characteristics. *Journal of Trace Elements in Medicine and Biology* 21:35-39.
269. Margoshes M & Vallee BL (1957) A cadmium protein from equine kidney cortex. *Journal of the American Chemical Society* 79(17):4813-4814.
270. Beattie JH*, et al.* (2005) Metallothionein overexpression and resistance to toxic stress. *Toxicology letters* 157(1):69-78.
271. Colangelo D, Mahboobi H, Viarengo A, & Osella D (2004) Protective effect of metallothioneins against oxidative stress evaluated on wild type and MT-null cell lines by means of flow cytometry. *Biometals* 17(4):365-370.
272. Palmiter RD (1998) The elusive function of metallothioneins. *Proceedings of the National Academy of Sciences* 95(15):8428-8430.
273. Andrews GK (2000) Regulation of metallothionein gene expression by oxidative stress and metal ions. *Biochemical pharmacology* 59(1):95-104.
274. Chiaverini N & De Ley M (2010) Protective effect of metallothionein on oxidative stress-induced DNA damage. *Free radical research* 44(6):605-613.
275. Vašák M & Hasler DW (2000) Metallothioneins: new functional and structural insights. *Current opinion in chemical biology* 4(2):177-183.
276. Arseniev A*, et al.* (1988) Three-dimensional structure of rabbit liver [Cd7] metallothionein-2a in aqueous solution determined by nuclear magnetic resonance. *Journal of molecular biology* 201(3):637-657.
277. Torreggiani A & Tinti A (2010) Raman spectroscopy a promising technique for investigations of metallothioneins. *Metallomics* 2(4):246-260.
278. Romero-Isart N & Vašák M (2002) Advances in the structure and chemistry of metallothioneins. *Journal of inorganic biochemistry* 88(3):388-396.
279. Bofill R*, et al.* (2009) Caenorhabditis elegans metallothionein isoform specificity–metal binding abilities and the role of histidine in CeMT1 and CeMT2. *The FEBS journal* 276(23):7040-7056.
280. Maruyama K, Hori R, Tsutomo N, & Kondo M (1986) Isolation and characterization of metallothionein from nematode (Caenorhabditis elegans). *Eisei kagaku* 32(1):22-27.
281. Consortium TCeS (1998) Genome sequence of the nematode C. elegans: a platform for investigating biology. *Science*:2012-2018.
282. Zeitoun‐Ghandour S*, et al.* (2010) The two Caenorhabditis elegans metallothioneins (CeMT‐1 and CeMT‐2) discriminate between essential zinc and toxic cadmium. *The FEBS journal* 277(11):2531-2542.

283. Martinez-Finley EJ & Aschner M (2011) Revelations from the nematode Caenorhabditis elegans on the complex interplay of metal toxicological mechanisms. *Journal of toxicology* 2011.
284. Vallee BL (1995) The function of metallothionein. *Neurochemistry international* 27(1):23-33.
285. Afonso C, Hathout Y, & Fenselau C (2004) Evidence for zinc ion sharing in metallothionein dimers provided by collision-induced dissociation. *International Journal of Mass Spectrometry* 231(2):207-211.
286. Palumaa P, Mackay EA, & Vasak M (1992) Nonoxidative cadmium-dependent dimerization of Cd7-metallothionein from rabbit liver. *Biochemistry* 31(7):2181-2186.
287. Zhang B, *et al.* (2003) Activity of metal-responsive transcription factor 1 by toxic heavy metals and H2O2 in vitro is modulated by metallothionein. *Molecular and cellular biology* 23(23):8471-8485.
288. Murphy CT, McCarroll SA, Bargmann CI, & Fraser A (2003) Genes that act downstream of DAF-16 to influence the lifespan of Caenorhabditis elegans. *Nature* 424(6946):277.
289. Lithgow GJ, White TM, Melov S, & Johnson TE (1995) Thermotolerance and extended life-span conferred by single-gene mutations and induced by thermal stress. *Proceedings of the National Academy of Sciences* 92(16):7540-7544.
290. Honda Y & Honda S (1999) The daf-2 gene network for longevity regulates oxidative stress resistance and Mn-superoxide dismutase gene expression in Caenorhabditis elegans. *The FASEB Journal* 13(11):1385-1393.
291. Ishii N, Goto S, & Hartman PS (2002) Protein oxidation during aging of the nematode Caenorhabditis elegans. *Free Radical Biology and Medicine* 33(8):1021-1025.
292. Yasuda K, Adachi H, Fujiwara Y, & Ishii N (1999) Protein carbonyl accumulation in aging dauer formation—defective (daf) mutants of Caenorhabditis elegans. *Journals of Gerontology Series A: Biomedical Sciences and Medical Sciences* 54(2):B47-B51.
293. Brewer GJ (2007) Iron and copper toxicity in diseases of aging, particularly atherosclerosis and Alzheimer's disease. *Experimental Biology and Medicine* 232(2):323-335.
294. Poon HF, Calabrese V, Scapagnini G, & Butterfield DA (2004) Free radicals: key to brain aging and heme oxygenase as a cellular response to oxidative stress. *The Journals of Gerontology Series A: Biological Sciences and Medical Sciences* 59(5):M478-M493.
295. Hung YH, Bush AI, & Cherny RA (2010) Copper in the brain and Alzheimer's disease. *JBIC Journal of Biological Inorganic Chemistry* 15(1):61-76.
296. Barnham KJ & Bush AI (2008) Metals in Alzheimer's and Parkinson's diseases. *Current opinion in chemical biology* 12(2):222-228.
297. Sutherland DE & Stillman MJ (2011) The "magic numbers" of metallothionein. *Metallomics* 3(5):444-463.

Appendix I – Additional results for chapters 4 and 5

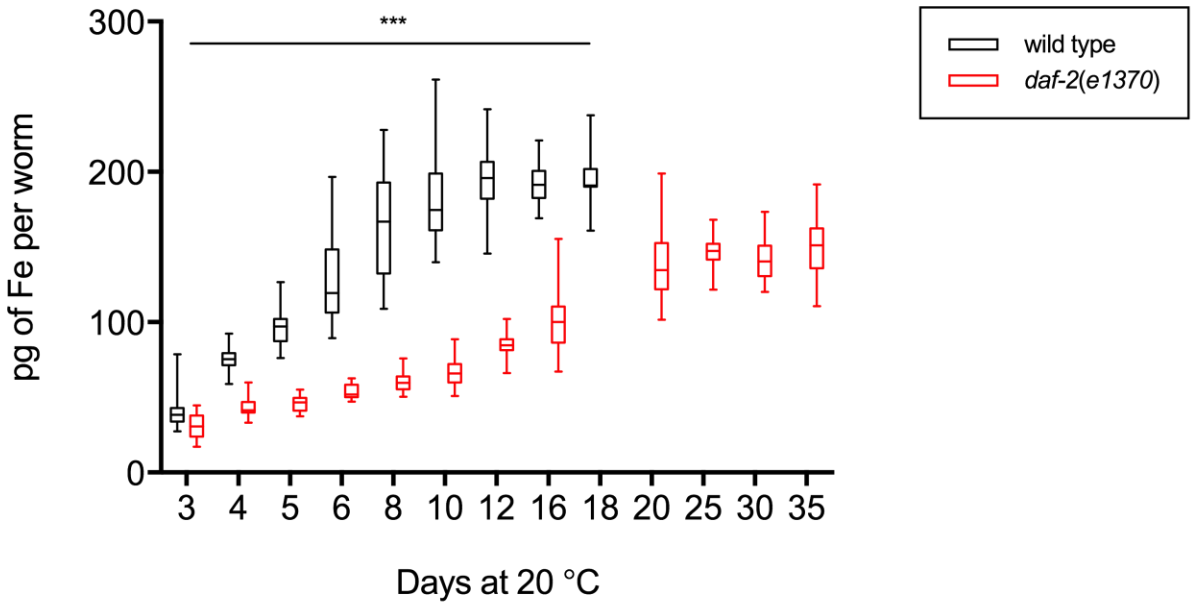

Figure A4.1 Comparison of total Fe levels in individual wild type and *daf-2* mutant *C. elegans* at intervals across lifespan

Wild type and *daf-2* exhibit an overall increase in total iron over their lifespan with wild types displaying a significant increase in total iron compared to *daf-2* throughout lifespan. Two-tailed unpaired Student's t-test; *** $p < 0.001$; box and whiskers plot with 5-95 percentiles displayed, *n* individuals per measurement per genotype = 25; *n* replicate measurements per time-point per genotype = 10.

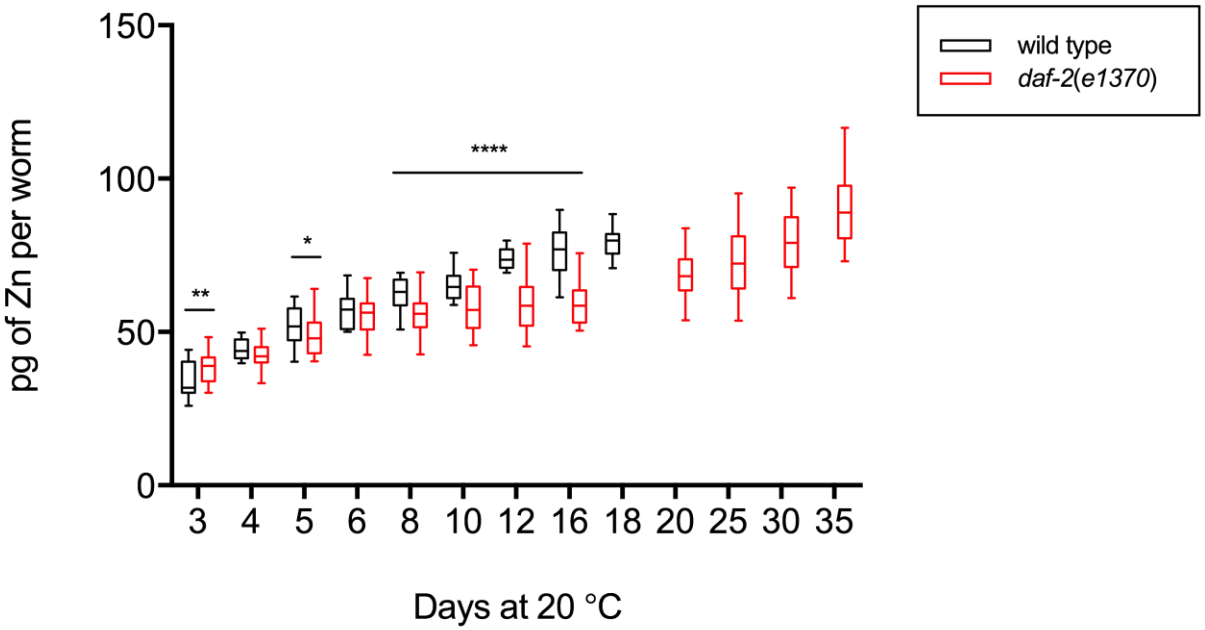

Figure A4.2 Comparison of total Zn levels in individual wild type and *daf-2* mutant *C. elegans* at intervals across lifespan

An increase in total zinc is observed for wild type and *daf-2* throughout lifespan. Zinc levels in wild type were significantly higher for all age-matched individuals except 4-day old individuals compared to *daf-2*. Two-tailed unpaired Student's t-test; * $p < 0.05$, ** $p < 0.01$ and *** $p < 0.001$; box and whiskers plot with 5-95 percentiles displayed; *n* individuals per measurement per genotype = 25; *n* replicate measurements per time-point per genotype = 10.

Table A4.1 Quantification of total Cu content in individual wild type and *daf-2* mutants at intervals across lifespan. Data displayed as mean (SD)

Strain	Days at 20 °C	pg of copper per individual	COV (%)
wild type	3	1.69 (0.617)	36.5
	4	2.60 (0.908)	34.9
	5	2.89 (0.574)	19.9
	6	3.54 (0.657)	18.5
	8	4.26 (0.946)	22.2
	10	4.79 (0.783)	16.4
	12	5.01 (0.629)	12.6
	16	6.38 (1.19)	18.6
	18	7.55 (1.13)	14.9
daf-2(*e1370*)	3	1.99 (1.16)	58.5
	4	2.73 (1.18)	43.2
	5	3.89 (1.36) ***	35.1
	6	3.91 (0.656) *	16.8
	8	4.66 (0.834 **	17.9
	10	5.46 (1.54) **	28.3
	12	5.92 (1.53) *	25.9
	16	6.74 (1.82)	27.02
	20	8.94 (2.49) #	27.9
	25	10.3 (3.02) @	29.4
	30	10.4 (2.67)	25.6
	35	10.2 (2.56)	25.2

* Significantly different from age-matched wild types $p < 0.05$

** Significantly different from age-matched wild types $p < 0.01$

**** Significantly different from age-matched wild types $p < 0.0001$

Significantly different from 16-day old *daf-2* mutants $p < 0.05$

@ Significantly different from 20-day old *daf-2* mutants $p < 0.05$

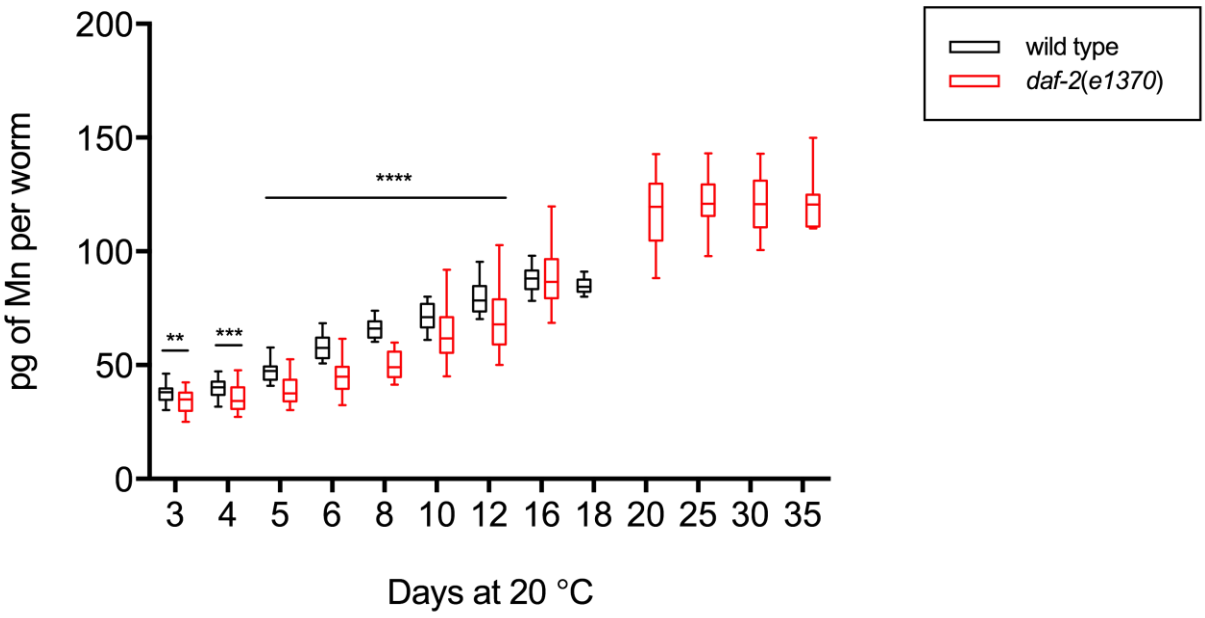

Figure A4.3 Comparison of total Mn levels in individual wild type and *daf-2* mutant *C. elegans* at intervals across lifespan

An increase in total Mn is observed for wild type and *daf-2* throughout lifespan. Wild type have significantly higher Mn levels in 3, 4 and 5-12 day old age matched individuals compared to *daf-2* mutants. From 20-25 days of age changes in Mn levels plateau in *daf-2*. Two-tailed unpaired Student's t-test; ** $p < 0.01$, *** $p < 0.001$ and **** $p < 0.0001$; box and whiskers plot with 5-95 percentiles displayed; *n* individuals per measurement per genotype = 25; *n* replicate measurements per time-point per genotype = 10.

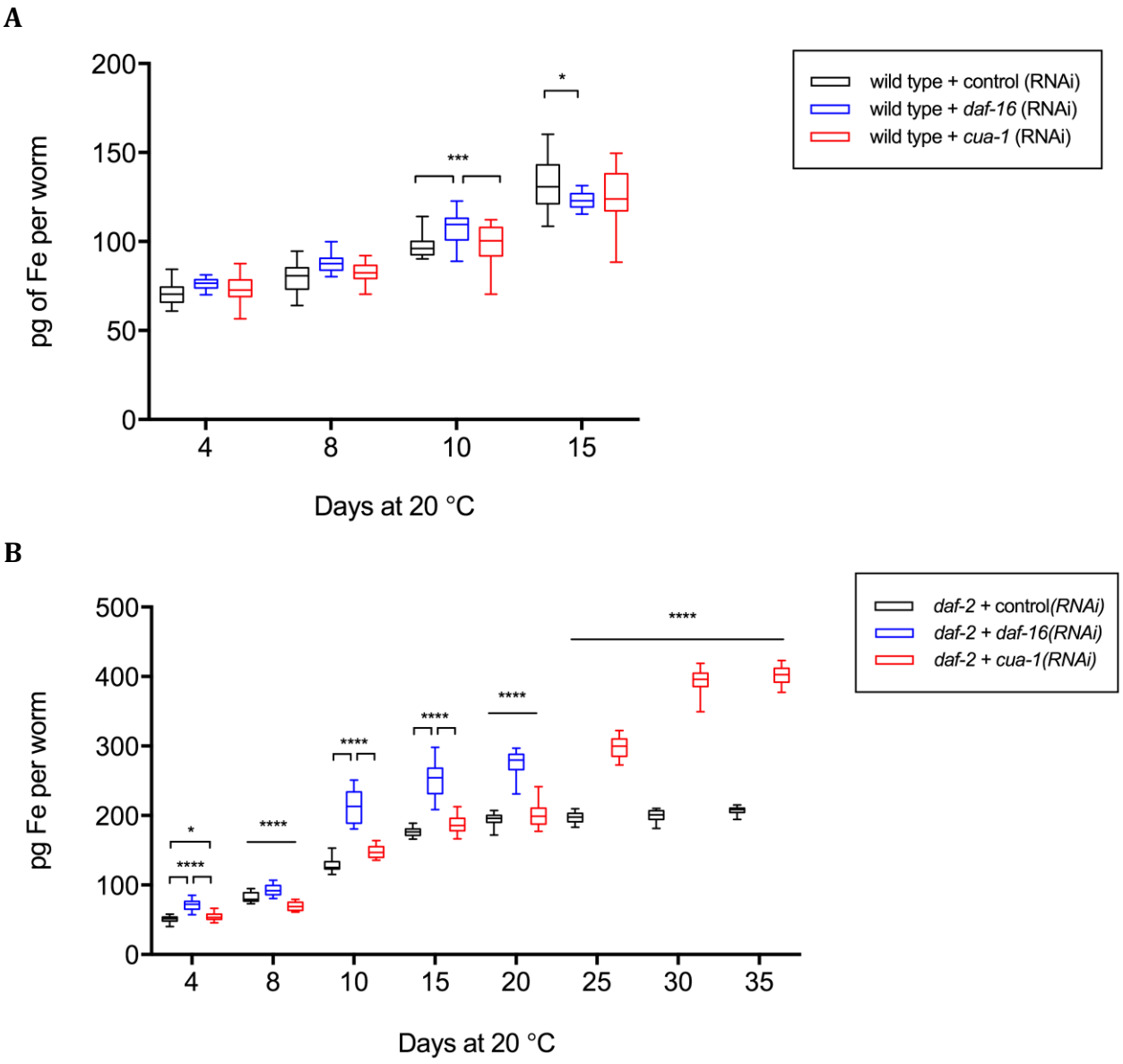

Figure A4.4 Comparison of total Fe in individual RNAi treated wild type and *daf-2* mutant *C. elegans* at intervals across lifespan

Iron levels in wild type + *daf-16*(RNAi) are elevated compared to controls and wild type + *cua-1*(RNAi) at 10 days of age ($p < 0.001$). At 15 days of age iron levels in wild type controls are elevated compared to both treatments ($p < 0.05$). A similar elevation in iron levels was exhibited in *daf-2* + *daf-16*(RNAi) at each time point sampled from 4 to 20 days of age ($p < 0.0001$). At 4 days of age, knock-down of *cua-1* in *daf-2*s results in higher iron levels ($p < 0.05$) and then at 25, 30 and 35 days of age ($p < 0.0001$). One way ANOVA with Tukey's *post hoc* multiple comparisons test, * $p < 0.05$, ** $p < 0.01$, *** $p < 0.001$ and **** $p < 0.0001$; box and whiskers plot with 5-95 percentiles displayed; $n = 30$ replicates per treatment per time point with each replicate containing 25 individuals. Cohorts used for ICP-MS analysis are separate from those used for lifespan analyses.

A

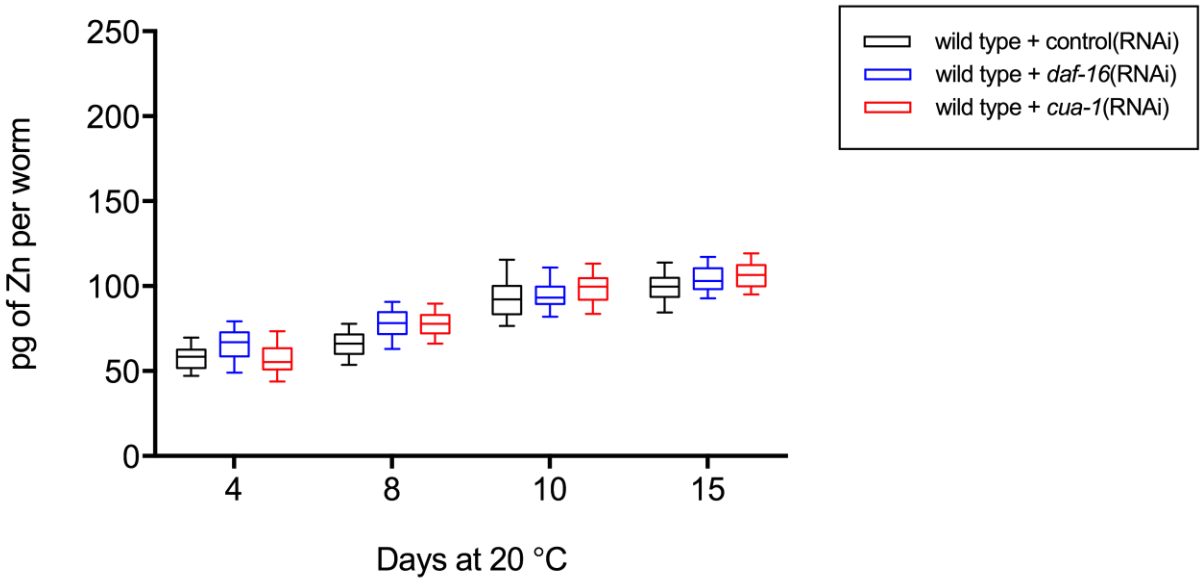

B

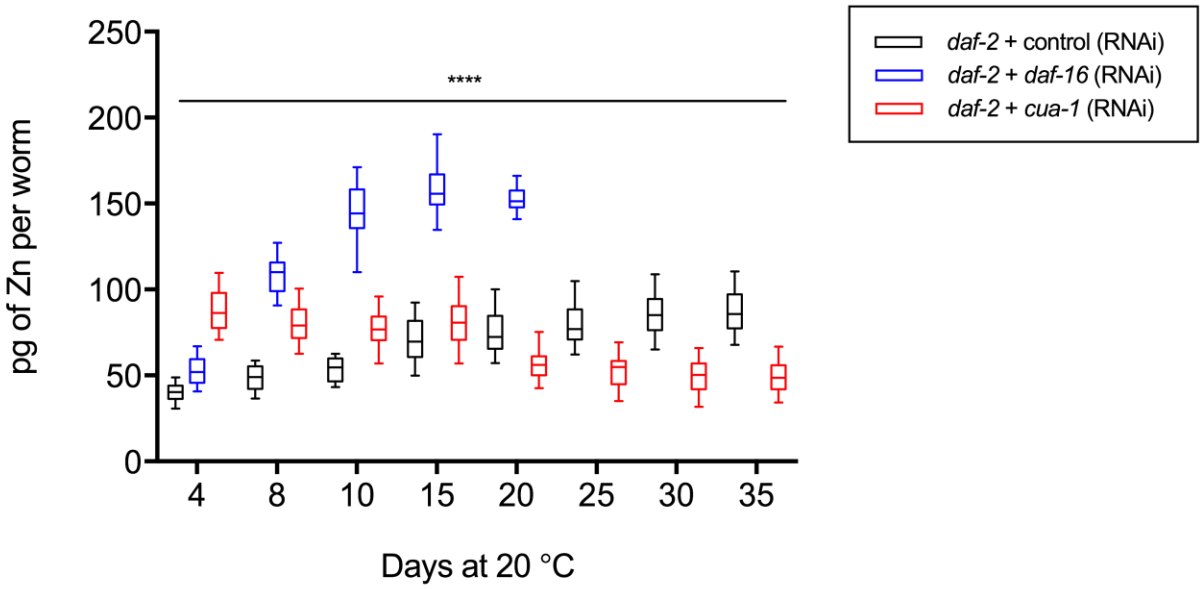

Figure A4.5 Comparison of total Zn in individual RNAi treated wild type and *daf-2* mutant *C. elegans* at intervals across lifespan

Zinc levels in wild type populations were not significantly affected by RNAi treatments. Knockdown of *daf-16* in *daf-2* mutants caused a significant increase in zinc throughout lifespan ($p < 0.0001$). At 4, 8, 10 and 15 days of age *daf-2* + *cua-1*(RNAi) had significantly higher zinc levels compared to controls ($p < 0.0001$). From 20 days of age until 35 days of age *daf-2* + *cua-1*(RNAi) had significantly lower zinc levels compared to controls. One way ANOVA with Tukey's *post hoc* multiple comparisons test, **** $p < 0.0001$; box and whiskers plot with 5-95 percentiles displayed; $n = 30$ replicates per treatment per time point with each replicate containing 25 individuals. Cohorts used for ICP-MS analysis are separate from those used for lifespan analyses.

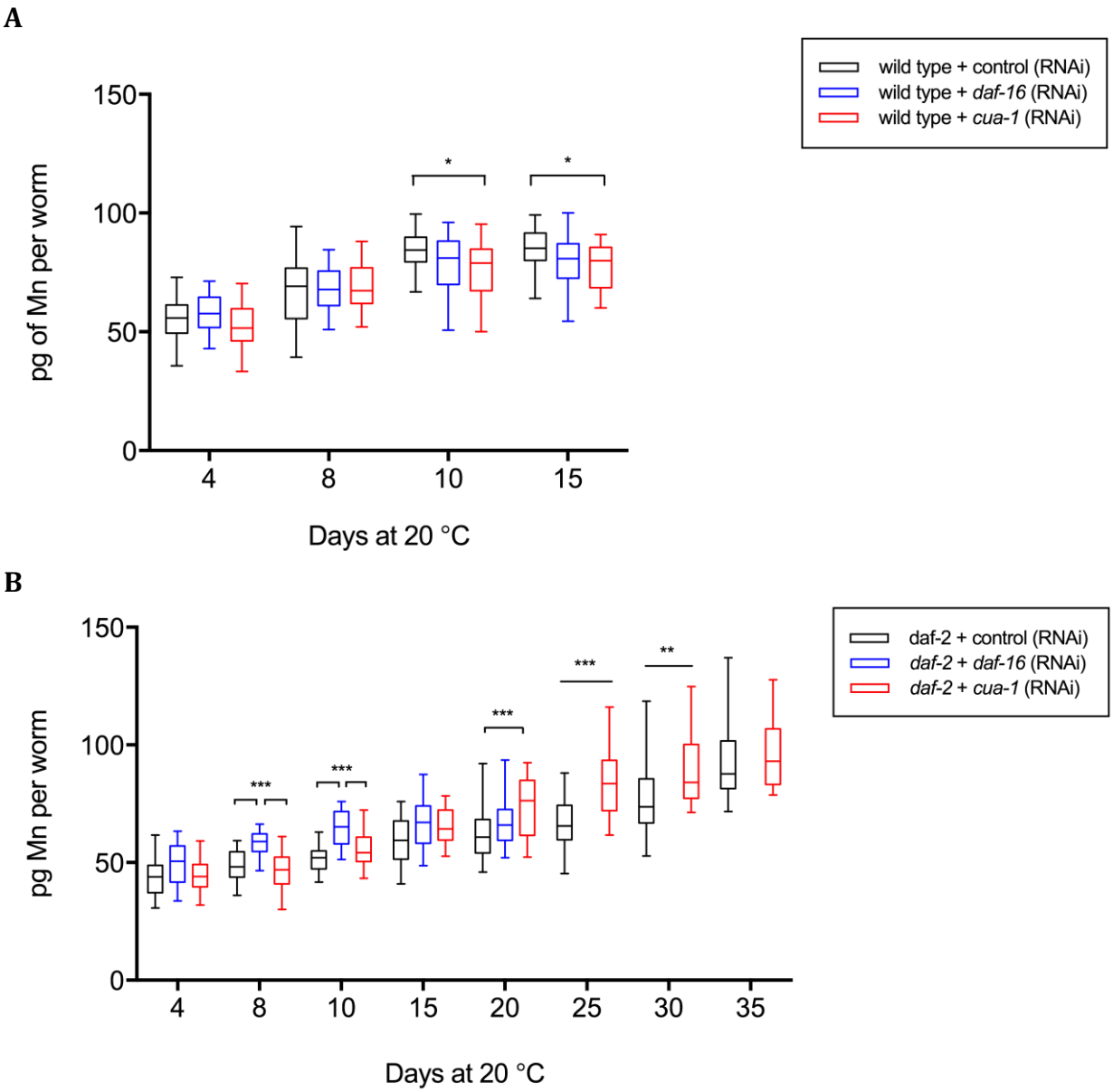

Figure A4.6 Comparison of total Mn in individual RNAi treated wild type and *daf-2* mutant *C. elegans* at intervals across lifespan

(A) Total Mn levels in wild type + *cua-1*(RNAi) individuals were significantly lower compared to controls at 10 and 15 days of age. (B) Knockdown of *daf-16* in *daf-2* mutants caused a significant increase in Mn at 8 and 10 days of age compared to controls and *cua-1* knockdown populations. At 20, 25 and 30 days of age *daf-2* + *cua-1*(RNAi) had significantly higher Mn levels compared to controls. One way ANOVA with Tukey's *post hoc* multiple comparisons test,** $p < 0.01$ and *** $p < 0.001$; box and whiskers plot with 5-95 percentiles displayed; $n = 30$ replicates per treatment per time point with each replicate containing 25 individuals. Cohorts used for ICP-MS analysis are separate from those used for lifespan analyses.

Table A4.2 Quantification of total Cu content in individual wild type and *daf-2* mutants following knockdown of *cua-1* activity by RNAi at intervals across lifespan. Data displayed as means (SD)

Strain	Days at 20 °C	Treatment (RNAi)	pg of copper per individual	COV (%)
wild type	4	control	3.01 (1.04)	34.5
		daf-16	2.61 (0.851)	32.7
		cua-1	2.88 (0.824)	28.6
	8	control	3.56 (1.26)	35.4
		daf-16	4.22 (0.856) ***	20.3
		cua-1	5.37 (1.06) ***	19.6
	10	control	4.18 (0.939)	22.5
		daf-16	5.38 (1.05) ***	19.6
		cua-1	5.61 (0.981) ***	17.5
	15	control	7.66 (0.944)	23.3
		daf-16	7.17 (1.73)	24.2
		cua-1	7.61 (1.77)	23.3
daf-2(*e1370*)	4	control	2.73 (0.815)	29.8
		daf-16	3.13 (1.04)	33.4
		cua-1	3.23 (1.26)	38.9
	8	control	4.34 (1.19)	27.4
		daf-16	4.43 (1.21)	27.3
		cua-1	4.94 (1.30)	26.2
	10	control	4.74 (1.29)	27.3
		daf-16	4.93 (1.73)	35.2
		cua-1	5.27 (1.73)	32.8
	15	control	7.35 (1.495)	20.3
		daf-16	5.93 (1.11)	18.7
		cua-1	5.66 (0.719)	12.7
	20	control	9.62 (1.03)	10.7
		daf-16	6.11 (0.643) ###	10.5
		cua-1	7.16 (1.22) ###	17.0
	25	control	10.2 (1.17)	11.5
		cua-1	7.46 (1.34) ###	17.91
	30	control	11.6 (1.67)	14.4
		cua-1	7.94 (1.28) ###	16.2
	35	control	13.4 (1.78)	13.3
		cua-1###	9.68 (1.056)	10.9

*** Significantly different compared to wild type controls $p < 0.001$

Significantly different compared to *daf-2* controls $p < 0.001$

Table A5.1 Quantification of total Cu content in individual 5-day old wild type, *daf-2*, *daf-2*; *daf-16*, *mtl-1*, *mtl-2* and *mtl-1*; *mtl-2* mutants by ICP-MS. Data displayed as mean (SD)

Strain	pg of copper per individual	COV (%)
wild type	2.86 (0.558)	19.4
daf-2(*e1370*)	4.03 (0.464) *	11.5
daf-2(*e1370*); *daf-16*(*m26*)	1.83 (0.657) ####	35.9
mtl-1(*tm1770*)	0.540 (0.131) ****	24.3
mtl-2(*gk125*)	1.37 (0.344) **	24.9
mtl-1; *mtl-2*(*zs1*)	1.69 (0.943) *	55.8

* Significantly different from age-matched wild types $p < 0.05$

** Significantly different from age-matched wild types $p < 0.01$

**** Significantly different from age-matched wild types $p < 0.0001$

Significantly different from age-matched *daf-2* mutants $p < 0.0001$

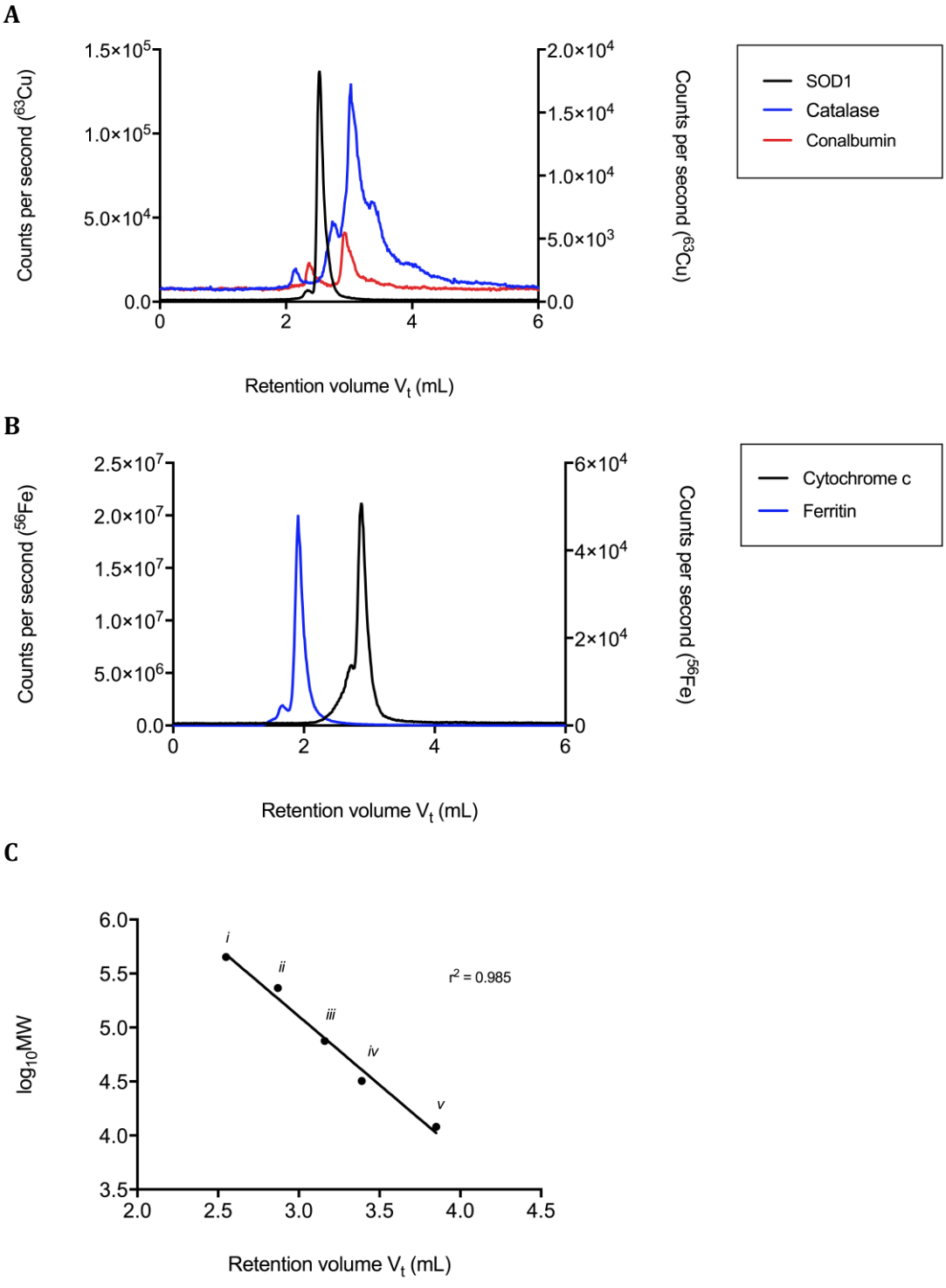

Figure A5.1 (A-C) Column calibration by SEC-ICP-MS

SEC column was calibrated using (A) bovine Cu, Zn - SOD1 (*iv*; MW = 32 k Da) catalase (*ii*; MW = 232 k Da) cobalamin (*iii*; MW = 75 kDa) (B) cytochrome complex (*v*; MW = 12 kDa) and horse spleen holo-ferritin (*i*; MW = 450 kDa) and (C) linear regression analysis was done against the retention volume.

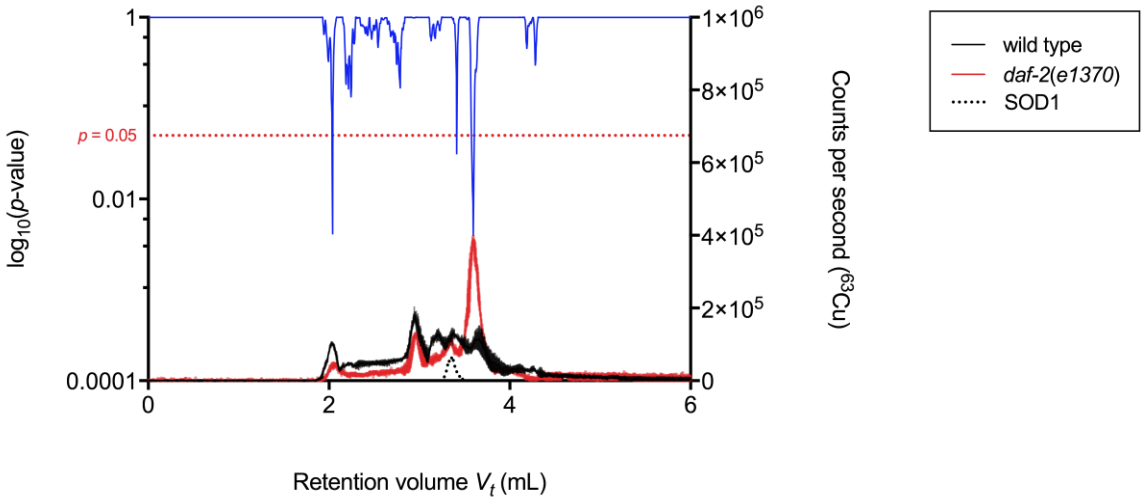

Figure A5.2 Student's *t* test of each data point collected by SEC-ICP-MS of soluble, Cu-binding profile of *daf-2* mutants

Student's *t*-test of each data point collected by SEC-ICP-MS reveals a significant difference in Cu-bound to peak 1 ($p < 0.01$), peak 4 ($V_t = 3.36$ mL; ~ MW = 44 k Da; $p < 0.05$) and peak 5 ($V_t = 3.59$ mL; ~ MW = 22 k Da; $p < 0.001$). Traces represent the mean of 3 independent samples ± 95% confidence interval.

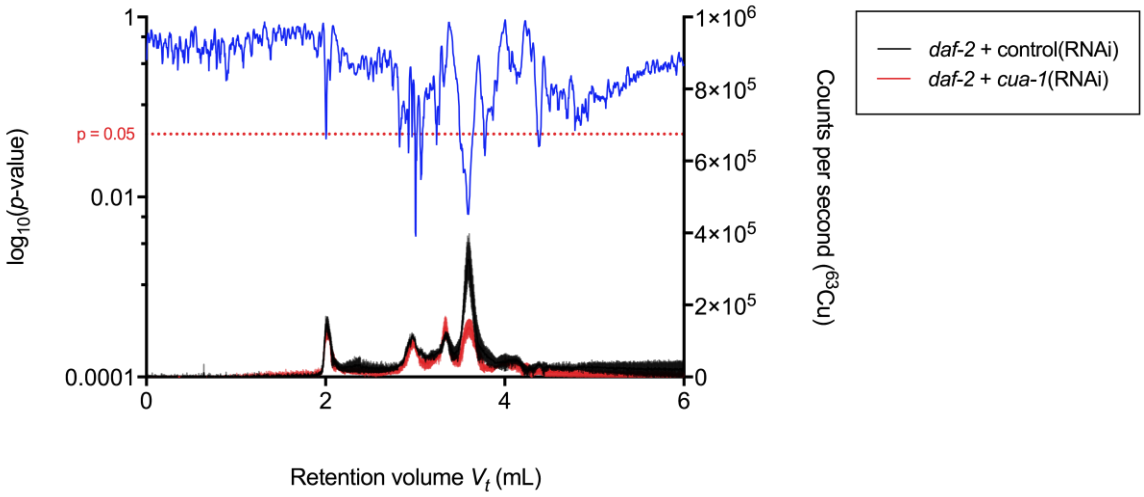

Figure A5.3 Student's *t* test of each data point collected by SEC-ICP-MS of comparison of soluble, Cu-binding profile in *daf-2* mutants following knockdown of *cua-1* activity

Student's *t*-test of each data point collected by SEC-ICP-MS reveals a significant difference in Cu-bound to peak 1 ($p < 0.05$), peak 2 ($p < 0.01$) and peak 4 (V_t = 3.59 mL; ~MW = 22 k Da; $p < 0.01$). Traces represent the mean of 3 independent samples ± 95% confidence interval.